Universität Rostock Traditio et Innovatio

Respiration of sandy Baltic Sea sediments

Dissertation
zur
Erlangung des akademischen Grades
doctor rerum naturalium (Dr. rer. nat.)
der Mathematisch-Naturwissenschaftlichen Fakultät
der Universität Rostock

vorgelegt von Hanna Schade,
geb. am 30.11.1985 in Langenhagen
aus Rostock
Datum der Einreichung: 09.04.2019
Datum der Verteidigung: 14.06.2019

Rostock, 5. Juli 2019

https://doi.org/10.18453/rosdok_id00002498

“In every outthrust headland, in every curving beach, in every grain of sand there is the story of the earth.”

— Rachel Carson

Gutachter

Dr. Markus Huettel
Department of Earth, Ocean and Atmospheric Science
Florida State University
117 N Woodward Av., Tallahasee
Florids 32306-4320, USA

Dr. Stefan Forster
Institut für Biowissenschaften - Meeresbiologie
Universität Rostock
Albert-Einstein-Straße 3, 18059 Rostock

List of Figures

List of Tables

List of Abbreviations

AFDW	ash free dry weight
ANOVA	analysis of variance
C	carbon
C. glaucum	*Cerastoderma glaucum* (Bruguière, 1789)
chl	chlorophyll
Dp	differential pressure
DW	dry weight
FTExp	flow-through experiment
H. diversicolor	*Hediste diversicolor* (O.F. Müller, 1776)
k	permeability
LOI	loss on ignition
n	number of replicates
N	nitrogen
$Na_2S_2O_4$	sodium dithiosulfate
NH_4^+	ammonium
NMDS	non-metric multidimensional scaling
NO_2^-	nitrite
NO_3^-	nitrate
M. arenaria	*Mya arenaria* (Linnaeus, 1758)
Marenzelleria spp.	*Marenzelleria viridis* (Verrill, 1873)/ *Marenzelleria neglecta* (Sikorski & Bick, 2004)
Mytilus spp.	*Mytilus edulis* (Linnaeus, 1758)/ *Mytilus trossulus* (Gould, 1850)
PO_4^{3-}	phosphate
rpm	rounds per minute
SD	standard deviation
SFDW	shell free dry weight
SiO_2	silicate
St	station
TOU	total oxygen uptake
WW	wet weight

List of formula symbols

dp	[Pa]	differential pressure
R	[µmol l^{-1} h^{-1}]	volumetric oxygen consumption
Δ_{O_2}	[µmol l^{-1}]	delta between outflow and inflow of each flow-through core
Vol_{Sed}	[l]	sediment volume
A_{Sed}	[cm^2]	sediment area
Φ		sediment porosity
C_{tot}	[µmol h^{-1}]	total oxygen uptake
C_{Start}	[µmol l^{-1}]	start oxygen concentration on the cores for *M. arenaria* respiration rate measurements
C_{End}	[µmol l^{-1}]	end oxygen concentration on the cores for *M. arenaria* respiration rate measurements
$C_{Control}$	[µmol h^{-1}]	oxygen uptake of the control cores
V_C	[l]	core volume
t	[h]	time
rr	[mmol d^{-1} g^{-1}_{SFDW}]	respiration rate of *M. arenaria*

Contents

Explanation

Macrofauna respiration was dealt with the same way as published in Schade et al. (2019). Data for the original manuscript was collected by M.P and N.A; Data was analysed by H.S.; N.A.; M.P. and S.F.; the manuscript was written by H.S. and edited by M.P. and S.F. Each paragraph taken from the original manuscript is marked by ””; chapters in which published information is included are indicated by a footnote.

Summary

Within the framework of this study we analysed different processes taking place in sandy sediments and their influence on the total oxygen uptake (TOU).

We investigated the influence of current-driven advection in contrast to concentration-driven diffusion with benthic chambers in the laboratory and in situ close to Warnemünde in front of the Hütelmoor. As these two processes are dependent on the occurring sediment parameters, we characterized the study area as one of the main objectives in this study. Therefore the organic content of the sediments, grain size distribution, permeability, chlorophyll a content and the distribution of macrofaunal organisms were analysed.

TOU is affected by current- and concentration-driven processes, but additionally by the occurrence of macrofauna which respire and indirectly influence the TOU by additional oxygen input to the sediment due to e.g. bioturbation. To estimate the share of macrofauna of the TOU, we developed a reliable respiration rate formula for the most abundant infauna species in the study area, *Mya arenaria*. With this formula, a respiration rate and therefore the contribution to the TOU can be calculated for the *M. arenaria* population, based on their abundance and individual size distribution. *M. arenaria* contributes with less than 16% only a minor fraction to the TOU. The indirect contribution to TOU by *M. arenaria* was not determined in this study.

The TOU measured at the field stations ranged from -10 to -28 mmol O_2 m^{-2} d^{-1}. The assumption of the greatest part of the study area to be permeable and thus subject to potential advective processes was not met in our study. An effect of advective influence on oxygen uptake was only shown for one in situ station. For this in situ station we found an increase in TOU at a factor of 2.

Laboratory results show that oxygen transport in permeable sediments is not necessarily associated with an increase in TOU, but that oxygen uptake needs to be fuelled additionally. Laboratory flow-through experiments showed that increasing porewater flow increased volumetric oxygen uptake rates and that the rate of this increase was in turn higher when properly fuelled with e.g. dissolved organic carbon sources.

When wanting to analyse potential advective influence on the TOU of an area, the definition of a threshold for permeability is crucial. For this purpose it is important to differentiate between possible effects on porewater advection and the affected TOU (total oxygen uptake). We argue for an increase of this threshold.

The originally defined threshold for permeable sediments of $2.5*10^{-12}$ m^2 (which led to the assumption of most of the area to be permeable) was based on studies using tracers.

In our study, oxygen uptake of sediments with a permeability of $<7.5*10^{-12}$ m^2 was not affected by advective influence. Therefore the permeability threshold has to be set higher. Regarding results of our study and literature data, we argue the threshold to be increased to at least to $7.5*10^{-12}$ m^2 or even to $2*10^{-11}$ m^2. The permeability in the analysed study area was therefore not as decisive as originally estimated and less parts of the area were subjective to an advective influence on TOU.

With this threshold a permeability effect on TOU can be assumed for 47 - 80% of the study area.

As the advective influence in the field depends on bottom velocity in the study area, a wave spectrum was assessed. As a rough estimation less than 70% of the occurring waves would reach the sea floor in the study area further reducing the occurence of advective effects. Summing up the permeable part of the investigated area and the times when waves would induce advection in the sediments, the possibility of oxygen uptake to be influenced by advective porewater flow would be reduced to 33 - 56%.

Zusammenfassung

Im Zuge dieser Arbeit wurden unterschiedliche, im sandigen Sediment stattfindende Prozesse und deren Einfluss auf die Sauerstoffzehrung untersucht. Hierfür wurde im Labor und in situ in der Nähe von Warnemünde, vor dem Hütelmoor, mit benthischen Kammern der Einfluss von strömungsgetriebener Advektion im Gegensatz zur konzentrationsgetriebenen Diffusion untersucht.

Da diese Prozesse von den vorhandenen Sedimenteigenschaften im Feld abhängig sind, wurde als ein Schwerpunkt der Arbeit das Studiengebiet charakterisiert. Hierfür wurde der Gehalt an organischem Material der Sedimente, die Korngrößenverteilung, die Permeabilität, Chlorophyll-a-Gehalte und die Verteilung der vorkommenden Makrofauna bestimmt.

Die Sauerstoffzehrung wird durch strömungs- oder konzentrationsgetriebene Prozesse beeinflusst, aber auch durch die Anwesenheit der Makrofauna, welche atmen und zusätzlich durch Sauerstoffeintrag ins Sediment einen indirekten Einfluss auf die gesamte Sauerstoffzehrung der Sedimente haben. Um abschätzen zu können, wieviel Anteil die Makrofauna an der gesamten Sauerstoffzehrung im Studiengebiet hat, wurde eine Atmungsformel für die häufigste Infauna Art im Studiengebiet, *Mya arenaria*, entwickelt. Anhand dieser Formel konnten wir, basierend auf der Abundanz und der Größenverteilung der Individuen, den Anteil an der gesamten Sauerstoffzehrung für diese Population bestimmen. Mit bis zu 16% macht *M. arenaria* nur einen geringen Teil der Sauerstoffatmung im Sediment aus. Der indirekte Anteil an der Sauerstoffzehrung wurde für diese Art in dieser Arbeit nicht bestimmt.

Die gesamte im Feld gemessene Sauerstoffzehrung reichte von -10 bis -28 mmol O_2 m^{-2} d^{-1}. Die Annahme, dass der größte Teil des Studiengebietes permeabel ist und damit ein advektiv induzierter Porenwasserfluss die Sauerstoffzehrungsrate steigert, konnte nicht gezeigt werden. Während der in situ Inkubationen wurde die Sauerstoffzehrungsrate nur bei einem Standort durch advektiven Einfluss erhöht. An diesem Standort wurde die Sauerstoffzehrungsrate allerdings um den Faktor 2 gesteigert.

Die Laborergebnisse haben gezeigt, dass Sauerstofftransport in permeablen sandigen Sedimenten nicht unbedingt zu einer Steigerung der Sauerstoffzehrung führt. Zusätzlich zur Sauerstoffzufuhr muss eine Nährstoffquelle gegeben sein. Durchflussexperimente haben außerdem gezeigt, dass volumetrische Sauerstoffzehrungsraten durch einen Anstieg der Porenwassergeschwindigkeit gesteigert werden können. Die Rate dieser Steigerung wurde zusätzlich durch Zugabe von z.B. gelößten organischen Kohlenstoffquellen erhöht.

Um analysieren zu können, welcher Anteil eines Gebietes potentiell von einer Steigerung der Sauerstoffzehrungsrate durch advektiven Einfluss betroffen ist, ist die Definition eines

Grenzwertes ausschlaggebend. Wichtig hierbei ist es zwischen advektivem Einfluss auf den Porenwasseraustauch und messbarem advektivem Einfluss auf die Sauerstoffzehrungsrate zu differenzieren. In unserer Studie argumentieren wir für eine Anhebung des Grenzwertes.

Der ursprünglich angenommene Permeabilitätsgrenzwert von $2.5*10^{-12}$ m^2 (welcher zu der Annahme führte, das fast das gesamte Studiengebiet permeabel sei) basiert auf Studien, welche als Indikatoren z.B. Farbe nutzten. In unserer Studie wurde die Sauerstoffzehrungsrate von Sedimenten mit einer Permeabilität von $7.5*10^{-12}$ m^2 nicht beeinflusst. Der Permeabilitätsgrenzwert muss also höher gesetzt werden als ursprünglich angenommen. Nach unseren Ergebnissen und Literaturdaten, sollte der Grenzwert auf mindestens $7.5*10^{-12}$ m^2 oder sogar auf $2*10^{-11}$ m^2 angehoben werden. Die Permeabilität des gesamten Studiengebietes ist somit weniger ausschlaggebend, als ursprünglich gedacht. Mit den potentiellen Grenzwerten für advektiven Einfluss auf die Sauerstoffzehrung können 47 - 80% als permeabel betrachtet werden.

Advektiver Einfluss ist immer abhängig von der Bodenströmung im jeweiligen Gebiet. Aus diesem Grund wurde ein Wellenspektrum im Studiengebiet aufgenommen. Weniger als 70% der aufgezeichneten Wellen erreichen den Seeboden. Wenn wir jetzt den permeablen Teil des untersuchten Gebietes und die Zeiten, wann Wellen den Porenwasserfluss steigern können zusammenfassen, reduziert sich die Wahrscheinlichkeit, dass die Sauerstoffzehrungsrate durch advektiven Porenwasserfluss beeinflusst wird auf 33 - 56%.

1 Introduction

71% of the world's surface are covered by oceans. Of these marine waters, more than 7% are continental shelf seas (depth <200 m) (Hall 2002; Winogradow and Pempkowiak 2014). Shelf seas are the areas connecting terrestrial, oceanic and atmospheric environments (Gattuso et al. 1998). Even though shelf seas only cover a small part of the whole ocean, they are highly important in terms of biogeochemical cycling and belong to the most biologically active areas mineralizing organic matter. The recycling of organic carbon occurs in the water column and in the benthic zone. Benthic processes are highly important and 90% of organic matter mineralization of the oceans takes place in the shelf seas (Gattuso et al. 1998). The shelves thus play a crucial role in the global cycling of carbon and nutrients. Generally benthic habitats can supply up to half of the nutrients for primary production in coastal seas (Lohrer et al. 2004). As these ecosystems are highly productive, they are important for the whole ocean and are highly valuable also for the earth. Coastal seas are subject to extreme pressures due to strong societal use, such as transportation, recreational use and fisheries. Despite their strong usage, some aspects of shelf sediments are astonishingly little understood, such as the processes in sandy sediments.

An important inner continental shelf area (water depth <65 m) is the Baltic Sea with an average depth of 52 m. More than 45% of the inner continental shelf areas are covered by sandy sediments (Hall 2002). Sand in temperate regions is usually formed of different particles; e.g. quartz particles and shell fragments. Quartz particles vary in size and all particles within the sediment range from silt <63 μm to coarse sand grains >1000 μm. In contrast to muddy sediments, sandy sediments have low organic carbon contents, generally lower abundance of microbes (Rusch et al. 2003) and have been considered as sites of low biogeochemical cycling for a long time (Boudreau et al. 2001). However, due to advective porewater flow coupled with strong biogeochemical reactions in sandy sediments, high mineralization rates can be encountered (Huettel and Webster 2001; Santos et al. 2012; Huettel et al. 2014) and thus sandy sediments may play a more important role in nutrient cycling than originally thought (Huettel et al. 2014). The role of sediments in the recycling of organic matter and the processes involved differ between areas and are influenced by marine sediment properties like permeability.

About 20% of the German Baltic Sea sediments consist of medium and coarser rest sediments (defined as coarse to medium sediment) (BmBF-Projekt: „SECOS“ (The Service of Sediments in German Coastal Seas)). In sandy sediments the relatively large pore spaces allow for an interstitial flow which is referred to as porewater advection (Huettel et al. 2014). Advective transport of material contained in the water flows, leads to an acceleration of material exchange across the sediment water interface. Generally the rates of solute exchange due

to porewater advection are higher than compared to molecular diffusion (Huettel et al. 1996, 1998; Aller et al. 2001). During molecular diffusion, the exchange between the porewater in the sediments and the overlaying water is solely driven by the concentration gradient. The magnitude of an advective flow however, depends on sediment characteristics as well as the underlying hydrodynamic forces.

Processes in the ocean's sediment depend on the sediment properties of any given area. Sediment properties differ between sites and can be quite variable. One fundamental property influencing the interstitial flow of overlaying water into the sediment is its permeability (k). Permeability depends on the compaction, fractionation and sorting of particles. Mostly sediments are defined in two categories, permeable and impermeable, despite the fact that there exists a continuous spectrum of permeability. Focussing on these two categories only, sediment was originally estimated as impermeable if k $<2.5*10^{-12}$ m^2 (Forster et al. 1996; Huettel and Gust 1992a; Glud et al. 1996) and as permeable if the permeability is above this threshold. Permeable sediments allow advective movement of porewater into the sediment, while impermeable sediments allow only for diffusive input. Generally sediments are defined permeable if porewater flushing can alter the biogeochemical cycling (Huettel et al. 1998; Jahnke et al. 2000; Reimers et al. 2004). In the Baltic Sea, 82% of the area is considered to be permeable (calculated for 52% of the Baltic Sea; Forster et al. 2003) and is thus possibly subject to advective processes assuming a threshold of k = $2.5*10^{-12}$ m^2. However, a threshold between permeable and impermeable is debatable. One study define a third category of moderate permeability (Neumann et al. 2017a). Further investigations are needed to determine the definition of a permeability range (Forster et al. (1996) also suggest necessary investigation for areas of intermediate permeability of 2.5 - $5*10^{-12}$ m^2).

Oxygen entering the sediment via a diffusive process typically has a penetration depth of 2 - 5 mm in coastal sediments (Ziebis et al. 1996). The accelerated porewater exchange due to advection leads to an increased oxygen penetration depth (Shum 1993; Ziebis et al. 1996; Marchant et al. 2014). Oxygen is highly important for the metabolism of microbial communities, as heterotrophic communities gain energy from the oxidation of organic carbon. Oxygen is the most favourable final electron acceptor as it is the most efficient energetic pathway for organic matter degradation. The availability of oxygen shapes the metabolism and also the composition of microbial communities (Forster et al. 1996; Glud 2008). Oxygen uptake by microbial communities follows a zero order kinetic and the uptake rate is basically independent of the oxygen concentration (Doran 1995). All oxygen reaching the sediment thus stimulates the microbial community and is consumed immediately.

Available oxygen determines the composition and metabolism of invertebrate and microbial communities (Forster et al. 1996; Glud 2008), therefore the oxygen penetration depth

has a strong influence on the organic matter mineralization within the sediment (Huettel et al. 1996; Forster and Zettler 2004; Jahnke et al. 2005; Janssen et al. 2005a). With increased oxygen penetration depth, oxygen reaches a larger surface area of sediment grains which harbour bacteria and can metabolise oxygen. As a result, active sites of biogeochemical reactions are increased and extended to greater sediment depths (Forster et al. 1999; Huettel et al. 2014). With increased oxygen availability, the metabolic activity and remineralization within the sediment (Kristensen et al. 1995; Aller et al. 2001) will be enhanced. Therefore the deeper oxygen penetration is expected to have a strong influence on the organic matter mineralization in the sediment (Huettel et al. 1996; Forster and Zettler 2004; Jahnke et al. 2005; Janssen et al. 2005a).

Oxygen is a good indicator for organic matter mineralization. To estimate organic matter mineralization and activity of sediments, one common measure is the total oxygen uptake (TOU). The TOU includes all processes involving bacterial and animal oxygen uptake (Jahnke et al. 2000; Woulds et al. 2007; Glud et al. 2016), photosynthetic processes during the day, oxygen uptake by phytoplankton and potential increased oxygen uptake due to advective processes. TOU as used in this study always refers to the total uptake rate including all processes/ organisms within the sediment.

The transport of oxygen into the sediment depends on its permeability. However, this transport in permeable sediments is dependant not only on permeability, but also on current velocity in the overlaying water at the sediment surface. Especially the interaction with the topography of the sediment surface has a strong influence on the porewater exchange (Precht and Huettel 2003b; Santos et al. 2012). Advective, physically driven transport across the sediment-water interface is caused by the pressure gradients which result from the interaction of currents with the seafloor topography. Physical structures, such as ripples, influence advective transport and matter exchange across the sediment-water interface through interactions with currents and waves (Rusch and Huettel 2000; Huettel and Webster 2001). Ripples, for example, interact with the overlaying currents, resulting in a pressure gradient as the dynamic pressure is high in the ripple troughs and low on the crests (Huettel and Gust 1992a,b). These pressure gradients lead to the pumping of water through the sediment pores supplying oxygen to the microbial communities (Boudreau et al. 2001) at the high pressure sites and on the other hand removing reduced material such as dissolved nutrients where the pressure is low. High turbulence, currents and near-bottom oscillatory wave motions are thus the major drivers of O_2 exchange in permeable sands (Huettel et al. 1996, 1998; Precht et al. 2004; Janssen et al. 2005a,b).

Advective and diffusive conditions can be artificially induced using specific benthic chambers. Several benthic chamber designs exist, but to induce a porewater flow similar to porewater flow paths occurring in connection with ripples, a chamber needs to be equipped with

a specific stirring disc as originally introduced by Huettel and Gust (1992a) (Janssen et al. 2005b). Porewater flows simulated in these chambers imitate either diffusive or advective porewater flow pathways.

Advection may also transport particulate organic matter into the sediment and make it available to benthic microbial communities (Huettel et al. 1996). As heterotrophic microbial communities gain energy by the oxidation of organic carbon, the metabolism is not solely changed by the availability of oxygen as most favourable final electron acceptor, but is also strongly dependent on the availability of organic carbon. Labile C is the most important source for bacterial respiration (Eyre and Ferguson 2005). If enough organic carbon is available in the sediment, bacterial respiration increases with increased oxygen supply. Sediments in the Baltic Sea are quite variable in their organic content and values range from 0.1 - 16% dry weight (Premuzic et al. 1982; Leipe et al. 2011). Deep muddy basins have higher contents of organic carbon compared to shallow sandy sites (Leipe et al. 2011).

Generally sandy sediments are located in regions of strong hydrodynamic forcing where limited settling of organic matter takes place. The advective process driven by hydrodynamic forcing is thus important for the supply of oxygen and nutrient rich water to the microbial communities in sediment which is naturally deprived of sedimenting organics. Metabolic activity of the microbes is thus elevated. Microbes in the sediment mainly live attached to sand grains and only a few percent live in the porewater (Rusch et al. 2003). Sand is under strong hydrodynamic forcing, subject to frequent movement and all flat surfaces are subject to mechanical abrasion (Miller 1989). Therefore, microbes in the sand mainly live in the micro environments of cracks and depressions of sand grains (Nickels et al. 1981). Water which is transported into the pore spaces also provides these micro environments with oxygen. However, in case of the micro environments and in close proximity to the bacteria, the final transport to the microbial cell is governed by diffusion. The microbial reaction is thus dependent on the strength of the concentration gradient between the porewater bulk and the bacterial cell surface and hence on the strength of the flow of porewater advection supplying consistently high oxygen concentrations to this local environment. The oxygen uptake of the sediment depends on the speed at which the porewater advects into the sediment. Microbial reactions in dependence of porewater flow have been studied in the past with flow-through reactors (Rao et al. 2007; Marchant et al. 2014; Ahmerkamp et al. 2017). To comprehensively analyse the oxygen uptake of sediments, both, the difference between diffusion and advection based processes and the influence of the strength of porewater flow rates within the sediment need to be considered.

Advective and diffusive processes differ and so does the expected oxygen distribution and uptake by microbial communities as measured with benthic chambers. The oxygen up-

take measured as a concentration change in the water column is influenced by the microbial oxygen uptake, the phytobenthic oxygen production during the day and the distribution of oxygen as influenced by the diffusive and advective process. The expected difference for the different processes is depicted in Figure 1. For the advective process a stronger measurable oxygen uptake is expected at night and a lower measurable oxygen concentration increase during the day compared to the diffusive process, as most oxygen produced by phytobenthos would be transported and taken up in the sediment. For the diffusive process less oxygen uptake during the night is expected and a resulting higher oxygen concentration increase due to phytobenthos production during the day.

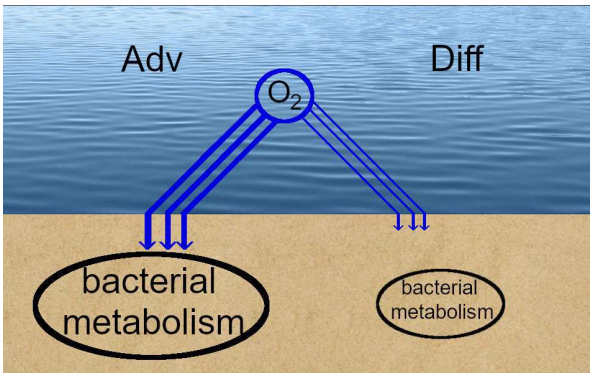

Figure 1: For the advective process the expected higher oxygen supply to the sediment is depicted by thick blue arrows and the resulting increase in oxygen uptake is depicted by a thick black circle. The theoretically smaller transport into the sediment in a diffusive process is depicted by thin blue arrows. The resulting lower bacterial uptake for the diffusive process is depicted by a smaller and thinner black circle.

Factors influencing transport and matter cycling at the sediment water interface are of physical and biological nature. Macrofauna produce mounts and tubes in the sediment which influence the seafloor topography additionally to wave generated ripples. Macrofauna (e.g. polychaetes) additionally induces currents creating advective conditions in their tubes. Kristensen et al. (2012) summarized the process of burrow or sediment flushing (exchange of dissolved substances between the porewater and overlying seawater) and mixing of sediments as bioturbation. If wanting to understand TOU in more detail, the effects of fauna on oxygen uptake, by respiration and transport of oxic water, need to be considered as well. Respiration of macrofauna and other species is influenced by the size of individuals (Seibel 2007; White et al. 2006) and abundance of species. The knowledge on the distribution of macrofauna within the studied area is thus of strong importance as higher abundance may have a stronger effect on oxygen uptake.

For the estimation of in situ effects on TOU one has to calculate the respiration of each occurring macrofaunal species and additionally its influence on bacterial sediment respiration by the increased oxygen supply into the adjacent sediment due to burrow ventilation or sediment flushing. Respiration can be calculated for some species (e.g. polychaeta (Braeckman et al. 2010)), while there are no trustworthy calculations for other species yet (e.g. *M. are-*

naria). In order to understand the TOU, the respiration of each macrofauna population and their indirect effects on oxygen uptake in the adjacent sediment would have to be estimated along with diffusive and advective uptake. The respiration of each species and the influence on bacterial sediment respiration associated with macrofauna, has so far only been calculated for some species under specific conditions (Kristensen et al. 1985; Renz and Forster 2014).

Figure 2: View of the study area (Photo: Dr. Lars Tiepolt).

All processes were studied in an area covered by sandy sediments. The investigated area (Figure 2) was located in the Southern stretch of the German Baltic Sea coast east of Warnemünde (54° 13' N; 12° 9' E). The area is characterized by a protected local fen on the land side (490 ha, Umweltministerium Mecklenburg-Vorpommern 2003) which stretches out into the marine site. The area originated from the Littorina transgression (~8000 years BP) when the fen area was still larger. This area has faced some coastal erosion in the past. This erosion is visible as peat crops out in the shallow part of the marine site. The water depth on the marine site is <10 m and salinity ranges from 10 - 15 (Zettler et al. 2007). Next to rare areas of peat cropping out in the shallow parts, the marine site is characterized by sandy bottom with some occasional hard bottom. The marine site is mainly covered by sand and the area belongs to 20% of the German Baltic Sea where sediments consists of rest sediments (coarse to medium sand) to medium sediments (Al-Hamdani et al. 2007, http://bio-50.io-warnemuende.de/iowbsa/index.php).

Currents influencing the advective transport into the sediments have not been measured

yet in the study area. However, estimations and measurements in areas close by show currents due to inflow events to range up to 0.7 m s^{-1} (Burchard et al. 2005, 2009).

Species diversity and number is lower in this area compared to fully marine waters (Bonsdorff 2006; Zettler et al. 2007, 2014; Vuorinen et al. 2015) as salinity ranges from 10 - 15. Studies defined the benthic community in this area as a *Hydrobiidae*, *Pygospio* and *Cerastoderma glaucum* community based on abundance data. However, based on biomass data the community is defined as *H. diversicolor*, *M. arenaria*, *Hydrobiidae* and *C. glaucum* community (Gogina et al. 2016).

Generally processes in sandy sediments have rarely been studied. We chose a study area where neither the sediments, nor the processes have been studied until now. The investigated area served as a model area in order to gain further knowledge and understanding of the processes controlling the TOU in sandy areas. This includes improved knowledge on the macrofauna respiration and its influence. To gain further understanding on the processes and interaction in sandy sediments, we additionally applied laboratory studies.

The main objectives of this work are to

1. investigate the sediments, its properties and the currents within the study area,
2. investigate the oxygen uptake rate of sediments and the influence of different processes on this parameter ex situ and in situ, and
3. investigate the most influential macrofauna and estimate their respiration rates including the establishment of a reliable approximation for respiration rates for *M. arenaria*.

2 Methods

2.1 Characterization of the study area

The chosen study area was located east of Rostock, Warnemünde at the Baltic Sea coast. Water depth in the area ranged from 0.5 m to 6.5 m (Table A.2, Figure A.1).

Figure 3: Map of the study area including all sampled stations of this study. Three benthic chamber deployments marked in red; the position of the current profiler (AWAC) marked in blue (https://www.flopp-caching.de/; Google Maps).

For a first characterization of the study area, the following parameters were analysed: sediment characteristics, current and wave patterns and macrofauna abundance. Methods used are described in the following subchapters.

Sediment samples were taken for the study area characterization and always again for each in situ deployment or lab incubation. Methods for sediment characterization were always identical and are thus described only once (Chapter 2.1.1).

2.1.1 Sediment characteristics

Sediments were sampled on several occasions (Table A.1) at 15 stations (Figure 3) within the study area (station locations Table A.2). Stations were chosen from a sampling grid used within the project with 50 stations in total (Figure A.1). Stations were located at 50 m, 550 m or 1050 m distance towards the shore. All stations sampled in April were analysed for grain size analysis, porosity, loss on ignition (LOI), chlorophyll a (chl a) content and permeability (k). At each station a minimum of 4 cores (⌀ 36 mm) were taken. All sediment cores were sampled by divers, if not indicated otherwise. Samples for C:N analysis were taken in July and October 2016 in the study area (7 of the 15 stations). Samples were used from either date (July or October) depending on available material (Table A.1).

For grain size distribution in the study area approx. 100 g sediment were weighed and rinsed through sieves with 1000, 500, 250, 125 and 63 µm mesh size. The bottom of the sieves was covered with aluminium foil to retain any grains passing the mesh during the drying process. Sieves were dried (18 h; 60°C) and weighed again to obtain the weight of sediment in relation to each mesh size. Weight of grains <63 µm was estimated through subtraction of the cumulated weight (all size fractions) from the initial dry weight of the sediment used in the analyses. The percentage in weight for each size fraction, the median and sorting degree were calculated according to Folk and Ward (1957).

For analysis of the organic content, water content and porosity, three replicates of a specific volume were used (1, 3 or 5 cm^3). Water content was estimated through wet weight (WW) and dry weight (DW, 18 h; 60°C) and measured in % of total WW. The porosity Φ was calculated from the weight difference before and after drying. Density of water in $g\,cm^{-3}$ was defined according to measured temperature and salinity during the measurement. For the sediment grains, a density of 2.65 $g\,cm^{-3}$ was assumed (quartz sand). The organic content (loss on ignition, LOI) was then calculated using the ash free dry weight (AFDW, 16 h; 500°C). In the Baltic Sea approximately 40% of all organic material (LOI) can be assumed to be organic carbon (Leipe et al. 2011).

Chl a was always measured using a fluorometer (TD 700, Turner Designs). 1 cm^3 of sediment was dissolved in 9 ml acetone, shaken vigorously, extracted overnight in the fridge and centrifuged (4000 g, 2 min). The supernatant was then measured. The supernatant was diluted further, if values were out of calibration range. 125 µl 1 N HCL were added to each sample after the 1^{st} measurement and the supernatant was then measured again to calculate the chl a content without phaeopigments. Chl a content in the study area was always measured as sediment profile/ depth distribution with 0.5 cm steps until 3 cm sediment depth, followed by 1 cm steps until 10 cm sediment depth and 2 cm steps >10 cm sediment depth until the max depth.

The distribution of chl a as an average chl a value at each station was related to a geographical pattern. Differences in chl a values were analysed with regard to distance to the

shore (50 m; 550 m or 1050 m) with a PERMANOVA and a pairwise multilevel comparison in R Studio. In this case, distance was tested for significant influence on chl a content. Distances were then compared using a pairwise multilevel comparison. The influence of water depth on chl a values was tested using a regression analysis. Each chl a value for a specific sampled sediment depth (e.g. 0 - 0.5 cm) at each station was tested against the water depths of the station.

Permeability at each station was measured with the falling head method after Head (1982) using cores with 36 mm in diameter. Permeability was measured for three sediment depths (5, 10 and 15 cm) if enough material was available (if not less depth steps were measured). As the exact depth of 5, 10 or 15 cm was not always possible to be sampled, the exact sampling depth was measured, noted and permeability was calculated according to that specific depth. For simplification reasons permeabilities were depicted in 5 cm steps (Figure 9, Figure 27) and exact core lengths are given in Table A.3.

C:N was analysed using a C:N elemental analyser (NC2500, CE Instruments). For the C:N measurements, either a suspension of 18.15 ± 3.5 g of sediment was filtered through pre-weighed filters or sediment was not filtered. If filtered, filters were analysed and C and N content was recalculated with the original weight accordingly. If not filtered, 92.63 ± 6.61 g of sediment were mortared and subsequently measured in the C:N analyser.

2.1.2 Current patterns

To analyse the wave and current patterns in the study area, an Acoustic Wave and Current Profiler (AWAC, Nortek AS) was placed with divers at 54° 13.422 N and 12° 9.379 E (Figure 3) from 17^{th} of April 2017 until 09^{th} of October 2018. Data were continuously logged. The profiler was removed from the field, cleaned in the lab and data were transferred to a computer every three to five months. Measurement settings were set as follows: Profile interval: 300 s; Number of cells: 24; Cell size: 0.25 m; Average interval: 240 s; Blanking distance: 0.40 m; Number of wave samples: 1024; Wave interval: 1800 s; Wave sampling rate: 2 Hz; Compass update rate: 300 s and Salinity was set to 12.

Velocities were calculated by Nils Karow (unpubl. data) from the wave parameters according to stokes' law third order theory (Stokes 1847).

2.1.3 Macrofauna abundance

For the macrofauna distribution, 3 replicate samples were taken at 5 of the 15 stations: St 3, 13, 23, 33 and 43. Due to the shallow area and the impossibility of using heavy sampling gear (e.g. a Van Veen grab), samples were taken by divers. A plastic ring with a diameter of 20 cm was placed in the sediment and sediment down to 15 cm was shovelled into a canister. The sand was then sieved in the lab through a 1 mm sieve and macrofauna was

fixed in 4% formalin and stored until determination. Most macrofauna specimen were determined until species level, while some were identified to genus or family level (*Cerastoderma* spp., *Marenzelleria* spp., *Gammarus* spp., *Bathyporeia* sp., *Littorina* spp. and *Nemerta* spp., *Hydrobiidae*).

The differences in macrofaunal distribution between the stations was analysed with a simprof and a non-multidimensional scaling analysis in R Studio. Data were fourth-root transformed. As distance analysis the Bray-Curtis index was used.

2.2 Influence of flow on sediments

Influence of advective porewater flow on sediment metabolism was measured with benthic chambers during in situ deployments (at three stations) and in the laboratory (for two different sediment types).

To analyse the influence of advective porewater flow on the metabolism of the sediment, the benthic chamber was calibrated by measuring the actual pressure differences applied on the sediment under varying rotation speeds.

2.2.1 Benthic chamber

For respiration rate measurements in situ and ex situ, benthic chambers were used (Figure 4). A benthic chamber consists of an acrylic glass cylinder (referred to as chamber hereafter, diameter = 19 cm; height = 32 cm) and a lid which closes the cylinder. A disc (diameter = 15 cm, thickness = 1 cm) is attached to a cylindrical plastic shaft which is attached through the lid to a motor. Rotation of the disc can be controlled by the rotation speed of the motor. The height of the rotating disc can be adjusted and thus the distance of the rotating disc to the lid (and the distance to the sediment accordingly) is adaptable. The motor has two principle settings. The disc can rotate in an alternating clock- and anticlockwise manner at short time intervals and slow rotation speed (Figure 4.B). At this setting no pressure gradient is induced and the exchange between sediment and overlaying water occurs only by molecular diffusion without accelerated porewater flow. For an advective setting the disc can rotate in one direction at different speeds (Figure 4.C). The faster rotation speed leads to an increased porewater flow with increased oxygen supply into the sediment. This porewater flow resembles the flow paths under ripples, as the dynamic pressure is high at the outer boundary of the chamber and low in the centre. The motor can be power supplied either through a DC Power Supply (in the lab) or through a battery (in the field). The rotation speed of the disc can only be set prior to the chamber deployment, as the rotation speed needs to be set with an external device.

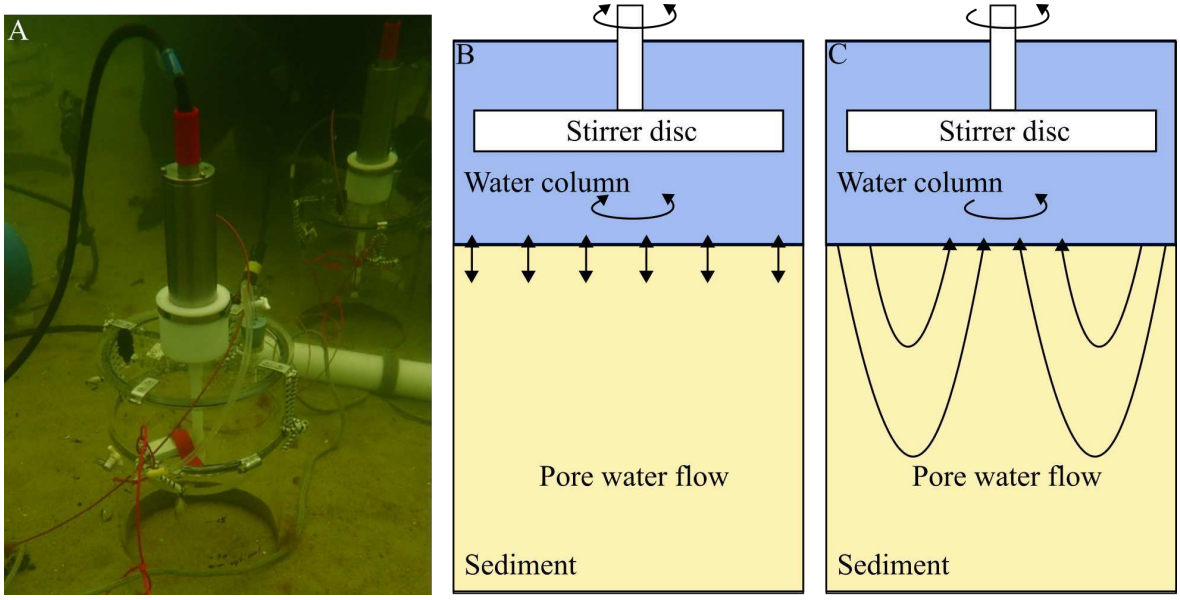

Figure 4: Benthic chamber A) In operation in the field B) Schematic drawing of the chamber under diffusion condition changed after Meysman et al. (2006) C) Schematic drawing of the chamber under advection condition changed after Meysman et al. (2006).

2.2.2 Calibration of the benthic chamber

To estimate the differential pressure (dp) between the centre of the chamber and the chamber wall at the level of the sediment surface at different rotation speed settings, the benthic chamber was calibrated prior usage. We therefore designed a false bottom with 9 holes (Figure 5.A); 4 holes each to the side of the centre with 2.1 cm; 4.2 cm; 6.3 cm and 8.4 cm distance to the centre and one hole at the centre. The false bottom was coated with sand to imitate a bottom roughness. To measure the differential pressure between the centre and each hole to the side, the chamber was filled with water and the lid was closed. The dp between each of the holes on the radius and the center hole at the bottom of the chamber was measured by connecting the outlets of the false bottom to a wet-wet differential pressure sensor as used in Janssen et al. (2005b) (Figure 5.B). Differential pressure was measured with increasing rotation speed (0 - 80 rounds per minute (rpm)) and for 6 cm, 8 cm and 10 cm vertical distance of the rotating disc to the false bottom. Differential pressure increased with decreasing distance of the false bottom to the rotating disc, with increasing rotation speed (Figure 6 and with increasing distance to the centre (Figure 6.A).

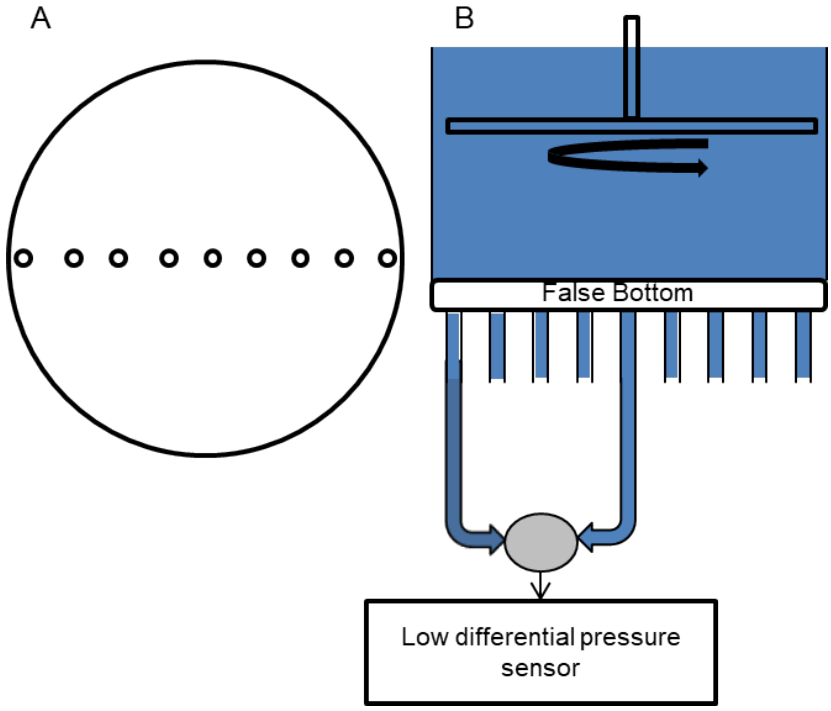

Figure 5: Schematic of the false bottom inserted into a water filled chamber to measure differential pressure between each of the holes on the radius and the centre hole at the bottom of the chamber. A) top view of the bottom disc B) side view of the bottom disc placed in the chamber

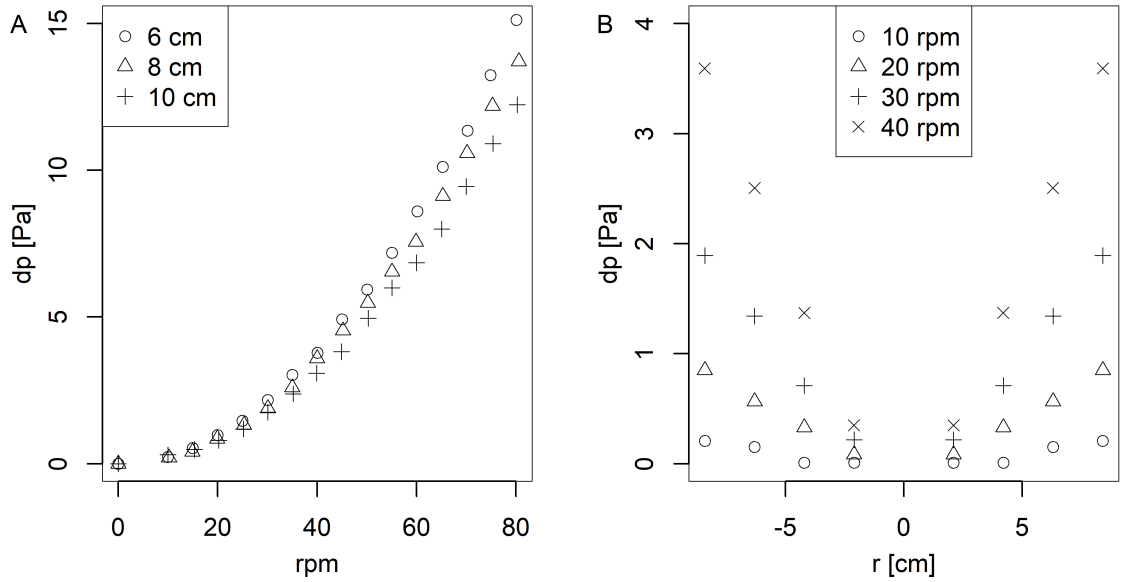

Figure 6: Differential pressure in the benthic chamber. A) Increase in differential pressure (dp) for r = 8.4 cm compared to the centre of the bottom disc with increasing rotation speed (rpm) for 6, 8 and 10 cm distance from the disc to the bottom; B) increase in dp for r = 2.1; 4.2; 6.3 and 8.4 cm distance from centre of the false bottom at 10, 20, 30 and 40 rounds per minute.

The influence of rotation speed on the dp [Pa] was calculated for 8.4 cm distance between the centre and the outermost sampling port. The resulting three equations for 6 cm (Equation 1); 8 cm (Equation 2) and 10 cm (Equation 3) distance of the rotating disc to the bottom of

the chamber were used to calculate the applied dp in the experiments.

$$\mathrm{dp} = 0.0023x^2 + 0.0044 - 0.0263 \tag{1}$$

$$\mathrm{dp} = 0.0021x^2 + 0.006 - 0.0767 \tag{2}$$

$$\mathrm{dp} = 0.0019x^2 + 0.0018 - 0.0121 \tag{3}$$

2.2.3 Laboratory benthic chamber incubations

Sediments were incubated in benthic chambers in the laboratory from Feb to May 2017. Incubations were performed either with sieved sediment (for medium grained sediment) or undisturbed cores taken from the field into the lab (for finer grained sediment).

During the incubations oxygen uptake rates, an oxygen time course at different sediment depths and micro-profiles, to obtain an oxygen penetration depth, were measured. For oxygen uptake rates and an oxygen time course, the oxygen concentration in the overlaying water and the porewater was logged constantly with an Optical Oxygen Meter (FireStingO2, PyroScience). For oxygen uptake measurements, sensor spots were placed on the inside of the lid in two (Warnemünde) or 3 (Langenwerder 1 and 2) chambers. For oxygen time course measurements, sensor spots were additionally placed at certain sediment depths on the inside wall of one chamber (Warnemünde, Langenwerder 2).

For the calibration of the Optical Oxygen meter, the lids were placed in 0% and 100% oxygen saturated fresh water applying a two-point calibration. To gain 100% oxygen saturation water was continuously air supplied, while oxygen depleted water was achieved by the addition of Sodium Dithiosulfate ($Na_2S_2O_4$). Temperature and air pressure were measured by the device itself. Salinity was set in the program and values were recalculated by the system accordingly. To calibrate the sensor spots on the side of a chamber, the chamber was filled with 0% or 100% oxygen saturated water and spots were calibrated accordingly.

For oxygen uptake measurements, the cores were closed off and the depletion of oxygen in the water column was measured over time. Oxygen uptake [mmol O_2 m^{-2} d^{-1}] in the cores was calculated from delta O_2 (Δ O_2 [µmol l^{-1}] with regard to the volume of the overlaying water (V_{H_2O} [l]), the area of the sediment (A_{Sed} [m^2]) and the duration of the measurement.

For the oxygen time course measurement, oxygen concentration was logged constantly at the specific sediment depth by the sensor spots.

Additional to oxygen uptake and the oxygen time course, micro-profiles of oxygen concentration in the sediment column were recorded in the cores for different rotation speeds. Micro-profiles were measured with Clark-type electrodes (O_2 micro sensor; Unisense) down to ~1.5 cm sediment depth or to the maximum oxygen penetration depth. For this measure-

ment, the rotation of the disc was stopped and the lid was removed immediately to quickly run micro-profiles in the chamber (thus resembling the profiles during the specific rotation speed). Typically 17 ± 6 (max. 30) minutes passed between stopping the disc rotation and the termination of the profile measurement. Cores were kept in a temperature controlled aquarium for micro-profile measurements to assure a constant temperature during the measurement.

Medium grained sediment was taken from the shallow shore in Warnemünde in Jan 2017 (54° 10.707 N; 12° 3.419 E, Salinity 10; 4.4°C) (hereafter referred to as Warnemünde). For incubations with medium grained sediment, sediment was sieved through 1 mm and taken into the lab. Here the sediment was placed in 3 cores until the distance of the sediment surface to the rotating disc was 8 cm. The water volume in each core was 6.57 ± 0.04 l. Cores were kept at 10°C in a temperature controlled aquarium.

For oxygen uptake measurements two of the cores were closed off and depletion of oxygen in the water column was measured over time ($\overline{x}$ = 15 h). Oxygen in the water column was constantly (one measurement every 5 min) logged via sensor spots below the chamber lids.

For an oxygen time course at different rotation speeds and sediment depths, 4 sensor spots were placed on the inside of one chamber wall at ~0; 0.5; 1 and 1.5 cm sediment depth and a constant oxygen time course was measured. Oxygen concentration was logged to follow the oxygen concentration at each depth with changing rotation speed. Additionally several micro-profiles were recorded at defined distances to the centre of the chamber (r = 2.1; 4.2; 6.3 and 8.4 cm) at different rotation speeds.

To assess the influence of potentially added organic substrate, 30 ml algae (SA/DTs Premium Blend Live Marine Phytoplankton, coralsands) were added to each core. After three days the overlaying water was replaced by fresh seawater (temperature and salinity kept constant) and oxygen consumption, an oxygen time course and micro-profiles were measured again.

Permeability, chl a and grain size parameters were measured after the experimental run.

Cores for finer grained sediment were taken from in situ at Langenwerder in April and May 2017 (54° 01.517' N; 11° 28.964' E; 13.3 Salinity; 8.2°C in April; 13.5 Salinity, 14.7°C in May) (hereafter referred to as Langenwerder 1 and 2), transferred to the lab and kept at 15°C in a temperature controlled aquarium. Four replicate cores were taken and the oxygen concentration in the overlaying water was constantly (every 5 min) measured in three cores. The height of the rotating disc was adjusted to ensure a distance of approx. 8 cm between sediment surface and rotating disc. The water volume in each core was 6.58 ± 0.9 l. For oxygen uptake rate measurements the cores were closed off and depletion of oxygen was

measured over time via optodes (Langenwerder 1: $\overline{x}$ = 16 h; Langenwerder 1: $\overline{x}$ = 14 h).

For an oxygen time course measurement (as in Warnemünde), sensor spots were glued to the inside of one chamber wall (Langenwerder 2) at 0.8 and 1.3 cm sediment depth. An oxygen time course measurement was not possible for Langenwerder 1 as the sensor spots on the inside wall were destroyed during sampling of the core.

Several micro-profiles were recorded at defined distances to the centre of the chamber (r = 2.1 and 8.4 cm).

Permeability, chl a and grain size parameters were measured after the experimental run. All cores were sacrificed after each experiment and sieved through 1000 μm to extract animals inside the cores. Macrofauna was stored in 4% formalin until analysis.

Oxygen uptake data were tested for outliers with a stem-and-leaf-plot in SPSS (IBM Analytics) and one outlier was excluded from the results.

2.2.4 In situ benthic chamber incubations

Benthic chamber in situ deployments were conducted from July 24 - 31 2017 (St 23 and 41) during a cruise of the research vessel Elisabeth Mann Borgese (EMB 160) and from August 27- 28 2018 (St 13) in a combined mission of the "Klaashahn" (catamaran, IOW) and "Gadus alpha" (zodiac, University Rostock). Temperature during the deployment ranged between ~17°C at St 23, ~16°C at St 41 and ~19°C at St 13.

Background sediment values (grain size, porosity, organic content, carbon content, nitrogen content, chl a, permeability) were assessed in triplicates (36 mm ∅), sampled directly next to the benthic chamber deployments. Additional perforated cores (10 cm ∅) were taken to assess porewater nutrient profiles in the sediment. Porewater was sampled at different sediment depths (0, 1, 2, 3, 4, 5, 6, 8, 10, 12, 14 cm) using specific filter elements (rhizons, Rhizosphere). Using rhizons, samples did not have to be filtered. One additional water sample for the analysis of nutrient concentrations was always taken from the water column and filtered through a 45µm GFF Filter. For nutrient determinations (Phosphate; Nitrate; Nitrite; Ammonium; Silicate) sampled water was kept cool at 5°C until it was analysed with an AutoAnalyser by C. Burmeister (QuAAtro, Seal). At St 13 samples had to be frozen until further analysis. Analytical methods were based on Grasshoff et al. (1999). Methods were adjusted according to the protocoll by Seal and phenol was additionally replaced by sodium salicylate. Detection limits differed between water and porewater samples. Limits for water analysis were: PO_4^{3-}: 0.1; NO_3^-: 0.5; NO_2^-: 0.05; NH_4^+: 0.5 and SiO_2: 1 µmol l^{-1}, while limits for porewater analysis were: PO_4^{3-}: 0.25; NO_3^-: 0.5; NO_2^-: 0.1; NH_4^+: 1.5 and SiO_2: 2 µmol l^{-1}. Limits could slightly vary due to the dependency on the calibration and its resulting setting for the photometer. Porewater samples were sampled in quadruplicates. All replicates could be used at St 13, unfortunately 3/4 of replicates were lost at St 41 and 23.

Chl a was converted into organic carbon in the results to compare values to measured

carbon values assessed with different methods (e.g. LOI). For the conversion a carbon to chlorophyll ratio of 50 was assumed. This ratio is usually subject to variation, however 50 ranges within published literature values (Banse 1982; Riemann et al. 1989; Cloern et al. 1995; Sathyendranath et al. 2009).

In order to measure community O_2 production and uptake, benthic chambers (Figure 4) were deployed by scientific divers in duplicates (2 diffusion chambers; 2 advection chambers) at St 13, St 23 and St 41. The chambers were inserted into the sediment as deep as possible or until the distance between the rotating disc and the sediment was 8 cm (resulting distance between the rotating disc and the sediment surface 8 - 12 cm). Insertion depth was noted in triplicates at three different positions on the outside of the chamber to calculate the water volume in the chamber. The motor of each chamber was connected to a battery placed in a water-tight housing, located next to the chambers. Each lid was equipped with a sampling port where two tubes were inserted into the lid. Upon sampling, the sampled water volume (3 x 80 ml) was taken out of the chamber through one tube while the same amount of water entered passively through the second tube. This prevented porewater entering the chamber through the bottom. The stirring disk rotated at two different settings for advection or diffusion setting. For a diffusion setting (Figure 4.B) the disk rotated in an alternating manner at 10 rpm clock- and anticlockwise to mix the water column above the sediment without inducing advective influence. For the advection setting (Figure 4.C) the disk rotated at 45 rpm to induce advective porewater flow into the sediment. Dp for the advection setting was calculated according to the distance between the rotating disc and the sediment with the equation gained in the chamber calibration (Chapter 2.2.2): St 41: 4.2 Pa; St 13: 3.9 Pa; St 23: 4.4 Pa.

The chambers were placed at St 13 for one day- (D1) and night cycle (N1); at St 23 for one day (D1) and two night cycles (N1, N2) and at St 41 during two consecutive day- (D1, D2) and night cycles (N1, N2). During the night cycles the chambers were covered with a light impermeable foil in order to inhibit photosynthetic O_2 production. Between a day and night cycle, the lid of each chamber was lifted to introduce fresh water into each chamber. The chambers were placed on the same station but at a slightly different location for a second day and night cycle. The incubation treatment covered a day period of roughly 5 h, starting around 09:53 AM (± 6 Min) to 2:53 PM (± 10 Min) and a night period lasting 18 h from 3:46 PM (± 36 Min) to 9:35 AM (± 10 Min)).

For O_2 and nutrient concentration determinations, 3 x 80 ml of chamber water was sampled with a syringe through a valve on top of each chamber.

O_2 concentration in the chambers was determined by Winkler titration (Winkler 1888) at the start and end of each day- / night cycle in triplicates. Two syringes were immediately (max 15 minutes after sampling) emptied into ~30 ml Winkler bottles on board the zodiac (or catamaran) accompanying the divers and fixed with $MnSO_4$ as well as alkaline potassium

iodide solution. Samples were kept dark and transferred to the EMB on-board laboratories or home laboratories where the samples were processed within 24h. Oxygen uptake was then calculated using the O_2 concentration decrease over time. O_2 concentration in the chambers at St 13 was additionally monitored constantly (every 5 Min) with HQD sensors (Hach Lange GmbH).

For nutrient determinations in the overlaying water of the chambers (Phosphate, Nitrate; Nitrite; Ammonium; Silicate), sampled water was filtered through a 45 µm GFF Filter and kept cool at 5°C until it was analysed with an AutoAnalyser by C. Burmeister (QuAAtro, Seal). At St 13 nutrient samples had to be frozen until further analysis. Most concentrations of nitrate and nitrite were below the detection limit and thus nitrate and nitrite were excluded for further consideration.

Oxygen uptake [mmol O_2 m^{-2} d^{-1}] in the cores was calculated from delta O_2 (Δ O_2 [µmol l^{-1}]) with regard to the volume of the overlaying water (V_{H_2O} [l]), the area of the sediment (A_{Sed} [m^2]) and the duration of the measurement.

Oxygen uptake and nutrient fluxes were analysed for difference between the diffusion and advection setting with a t-test and a Wilcoxon Rank Sum test (R Studio) for each station. Additionally oxygen uptake and nutrient fluxes were tested for the differences between stations for day and night cycles separately. Data which were normal distributed (oxygen flux, day- and night cycle; ammonium and phosphate flux, day cycle) were tested with an ANOVA. If not normal distributed data were transformed to achieve normal distribution (Silicate, night flux; ammonium, night flux) and tested with an ANOVA. Data without normal distribution were tested with a kruskal Wallis test (Silicate, day flux; Phosphate, night flux). All data with significant differences between stations had homogeneous variances. To analyse the relationship between oxygen uptake at night and production at day, a regression analysis was performed for each station separately but also for all replicates of all stations where day and night data pairs existed (R Studio).

2.2.5 Microbial volumetric oxygen consumption depending on flow

Microbial volumetric oxygen consumption depending on flow was measured in different flow-through experiments (FTEXP 1 - 4). Experiments differed in sedimentary parameters and in treatments applied (Table 5). Experimental conditions of the 4 flow-through experiments can be found in Table 5 and are described below. Sedimentary parameters were always assessed after and/ or before the experiment (Chapter 2.1.1). Nutrients were always measured during the experiment as background parameters (Table A.9). Nutrients were measured as explained in Chapter 2.2.4.

The basic system for all flow-through experiments was equal. The flow-through adjustion was partly based on the principle after Edme Mariotte (the Mariotte bottle), the final flow-rate was adjusted with little screws on each supplying tube (Construction Figure 7). Each core

was connected to a header tank, which was filled with seawater. Three header tanks were used and 4 - 6 cores were connected to each header tank. The water ran from the header tank through supplying tubes into each core and through those into a catch basin (Figure 7). In the catch basins the water was aerated and pumped back into the header tanks 1- 2 times per day.

Oxygen concentration was measured using self-made flow-through cells equipped with a sensor spot and connected through optical fibres to an Optical Oxygen Meter (FireStingO2, PyroScience)). Oxygen concentration was measured in the outflow of each core and additionally in a separate outflow of the header tanks (for the oxygen concentration in the header). 6 cores could be measured simultaneously. The channels were interchanged several times per day to measure all cores and existing header tanks.

The delta between oxygen concentration in the inflow and oxygen concentration in the outflow was the oxygen consumption of each core (Δ_{O_2} [µmol l^{-1}]). All volumetric oxygen consumption rates (R [µmol l^{-1} h^{-1}]) were then calculated according to Equation 4, with the oxygen consumption rate related to the flow [ml min^{-1}] and the sediment volume (Vol_{Sed} [l]). Plug flow [cm h^{-1}] was calculated according to Equation 5, with the flow related to the sediment area (A_{Sed} [cm^2]) and the porosity of the sediment (Φ).

$$R = \frac{\Delta_{O_2} * \text{flow}}{Vol_{Sed}} * 60 * 1000 \tag{4}$$

$$\text{Plug flow} = \frac{\text{flow}}{A_{Sed} * \Phi} * 60 \tag{5}$$

Sediment cores which were used were of a diameter of 36 mm (FTExp 1 and 2) or 64 mm (FTExp 3 and 4). Water was always taken off Warnemünde and kept in a storage tank in our laboratory prior usage (acclimated to 15°C). All experiments were run at 15°C.

FTExp 1 was conducted with three sediment types (W, Warnemünde; S, Schnaterman and W/S, a mixture of both other types. In FTExp 1 all oxygen consumption rates were measured in dependence of flow (Plug flow = 10 - 60 cm h^{-1}). Flow rates were always adjusted similar for all cores. After measurements of oxygen consumption rates for each sediment type, glucose was added to each header tank. After the addition of glucose oxygen consumption was again measured in dependence of flow. Permeability was measured before and after the experiment to assess any change due to the addition of glucose. Seawater used during this experiment had a salinity of 13 (W), 12 (S) and 11 (W/S).

For determination of the glucose concentration (or the amount of added glucose to the header tanks), 1 ml of seawater samples from the header tanks were centrifuged at 3000 x g for 3 min at room temperature. The supernatant was separated and used for glucose measurements. Glucose concentrations were measured using the phenol-sulfuric acid method

by Masuko et al. (2005). Samples or glucose standards (100 µl) were mixed with 300 µl of concentrated H_2SO_4. Immediately 60 µl of 5% phenol were added. Samples were incubated for 5 min at 90°C and then cooled. Absorbance was measured at 492 nm using a SpectraMax M2 microplate reader (Molecular Devices GmbH, Biberach-an-der-Riß, Germany). Glucose was then calculated according a calibration curve.

Cores in FTExp 2 contained one sediment type (AWAC) and flow rates were adjusted for each header tank separately (slow (Plug flow = 12 – 19 cm h^{-1}), medium (Plug flow = 37 – 46 cm h^{-1}) and fast (Plug flow = 31 – 62 cm h−1)). Basic oxygen consumption rates were measured in dependence of flow. 0.5 ml algae (SA/DTs Premium Blend Live Marine Phytoplankton, coralsands) were then added to each header tank. Oxygen consumption was measured again in dependence of flow (with different flow rates adjusted for each header tank) after the addition of algae. Permeability and C:N values were measured after the experiment. C:N values were measured for 0 - 1 cm sediment depth and 4 - 5 cm sediment depth (to assess the formation of a potential biofilm). Permeability was measured several times on several days to assess the temporal development of permeability after the addition of algae. Water used during this experiment had a salinity of 11 for all header tanks.

In FTExp 3 and in FTExp 4 DOC was added instead of algae. For DOC, frozen macroalgae were ground with a mortar and pestle and a certain amount of this mush was filtered through a 45 µm filter and stored in a -18°C freezer until usage. Macroalgae used were taken from the beach and not further determined. The DOC content of the produced DOC stock could not be measured prior addition, so the amount of addition could only be measured in ml. The DOC stock was reproduced several times and differed in concentration every time it had to be renewed.

In FTExp 3 sediment used was the same as sediment used in FTExp 2 (AWAC). In FTExp 3, 6 cores were supplied by one header. Basic oxygen consumption rates were measured in dependence of flow (Plug flow = 5 – 24 cm h^{-1}). After the measurement of basic oxygen consumption rates, 400 ml of the DOC stock was added to the header (containing 50 l of seawater) and oxygen consumption was measured again in dependence of flow. Seawater used in this experiment had a salinity of 15. For the measurement of DOC concentration (before and after the addition of DOC to the cores), a sample of 20 ml was taken from the header tanks, filtered through a 45 µm filter and stored at -18°C until measurement. DOC concentrations were measured according to the accredited methods of the IOW analytic group according to Lysiak-Pastuszak and Krysell (2004) and HELCOM (2017).

In FTExp 4, sediment used was medium grained sediment off Warnemünde (as in FTExp 1, W sediment). 3 cores were connected to each header tank. Basic oxygen consumption rates were measured in dependence of flow (Plug flow = 4 – 24 cm h^{-1}). After the measurement of basic oxygen consumption rates depending on flow, DOC was added in different amounts to the header tanks. Whilst one header tank was left as a control (C, without ad-

dition of DOC), DOC was added to the second header tank (containing 30 l of seawater) (II, high DOC, 400 ml) and half of the amount of DOC was added to the third header tank (containing 30 l of seawater) (III; DOC, 200 ml). Oxygen consumption rates were measured afterwards in dependence of flow (medium, fast, and slow). Seawater used in this experiment had a salinity of 16. DOC concentrations were measured as in FTExp 3.

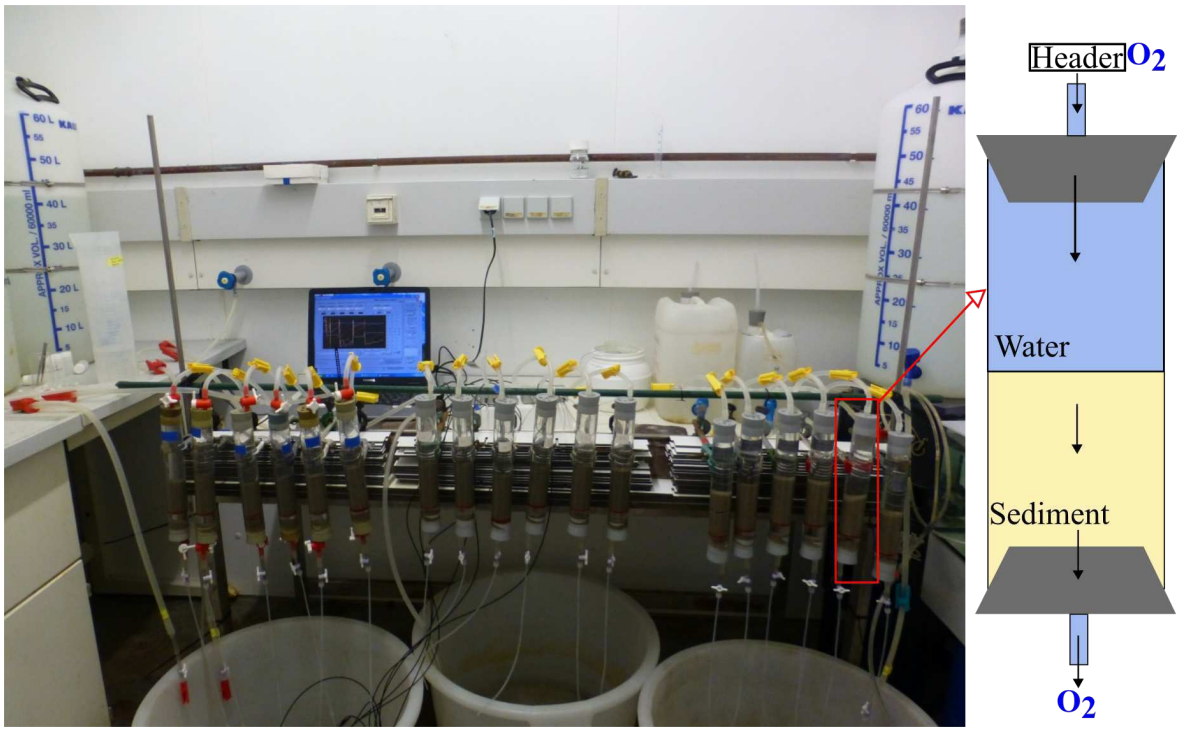

Figure 7: Flow-through cores in the lab, the principle of each core was depicted in the zoomed drawing. Oxygen concentration was measured in the header and in the outflow of each core (indicated by O_2).

2.3 Macrofauna respiration

Individual macrofauna respiration was calculated based on existing, published equations. For some species an individual respiration weight relationship needed to be investigated to calculate respiration rates.

2.3.1 Respiration of *M. arenaria*

For[1] *M.arenaria* a respiration to weight relationship had to be determined prior to the calculation of respiration rates for the community, as no reliable published equations existed. Individuals of *M. arenaria* were sampled at the Schnatermann (a shallow bay of the Warnow river mouth, 54° 10.36500 N; 12° 08.48667 E) in Nov ‘16 to June ‘17 at 40 - 80 cm water

[1]This chapter was changed after Schade et al. (2019). Some paragraphs were taken from the published article, all paragraphs taken from the article are marked with ””

depth. Out of the dense Schnatermann population (250 - 1000 ind. m^{-2} (Forster and Zettler 2004), individuals ranging from 9 to 60 mm were collected for the size dependent respiration measurements. After transportation to the lab, animals were acclimatized in 10 l aquaria in the dark with a temperature of 5 or 15°C (± 1°C) depending on the temperature treatment and at salinity 12 (± 0.6) for a minimum of 3 weeks. Salinity in the sampling area ranged from 8.4 to 10.6 and temperature from 6°C to 17°C during sampling. During acclimation animals were fed 3 times per week (DTs Phytoplankton Premium Reef Blend, Sustainable Aquatics ©).

In total 68 bivalves were measured from May to July '17 subsequently in groups of three (experimental runs), with always one individual per core (60 animals from 1 data set and 8 additional animals included for the 15°C from another data set). Individuals used for the 15°C respiration measurements had a shell-length of 9 - 60 mm and a shell-free dry weight (SFDW) of 2.2 - 1239.8 mg. Individuals for the 5°C experiment had a SFDW of 3.8 - 1134 mg with a shell-length of 10 - 59 mm.

The difference of the weight-length relationship between both temperatures was tested with an ANCOVA (data were normal distributed, for the weight-length relationship only one data set was used).

Respiration rates were measured in four constantly mixed seawater-filled cores (acrylic glass tubes, 10 cm diameter, 18 - 23 cm height), which were placed in a cooling basin, keeping the water temperature inside the cores at 5 and 15°C. All cores were filled with sufficient defaunated sand for animals to burrow, collected in the near shore zone off Warnemünde and overlaying seawater (water volume 687 ml ± 84 ml). The sediment from the sampling area had an average grain size of 217 µm, a habitat suitable for *M. arenaria* as the bivalve occurs generally more frequently in fine and median coarse sand (125-500 µm) (Forster and Zettler 2004). Importantly, the used sediment had a low organic content (0.09% DW ± 0.02%), which assured a low microbial background respiration during the experiment. For a reduction of the amount of organic particles and thus the background respiration, potentially added faeces and pseudofaeces was washed out for each measurement cycle and the sediment was dried before addition to the following core setup.

"One animal was placed in each core and slowly covered with sediment. Three cores were always measured at the same time. A fourth core was kept as a control with sand only. Bivalves were fed one last time and then left to acclimatize at least 17 h prior to start of the measurement. Temperature and salinity were controlled before and after each experimental run (5°C ± 0.45°C; salinity 12 ± 0.31 and 15°C ± 0.9°C; salinity 12 ± 0.64). Oxygen consumption of the cores was measured for at least 28 hours in dark for each experimental run. For this measurement, each core was closed and ensured to be bubble free. Oxygen decrease was continuously logged with an O_2-sensor spot placed inside each chamber and optical fiberglass-cables using the software "FireStingO2" (PyroScience GmbH, Aachen,

Germany). Temperature inside the cooling basin and air pressure were additionally constantly logged with the software."

Wet-weight (WW); shell-free wet weight (SFWW); shell-free dry weight (SFDW, 48h, 60°C) and ash-free dry weight (AFDW 10h, 500°C) were measured for most individuals. AFDW could not be measured for some small individuals and was calculated according to Rumohr et al (1987); the used conversion factor was 19.9% of dry weight (DW).

To calculate a SFDW to weight-specific (SFDW) respiration rate relationship for two different temperatures, data treatment was described in the paragraph below and some examples of individual respiration rates were illustrated in Figure 8.

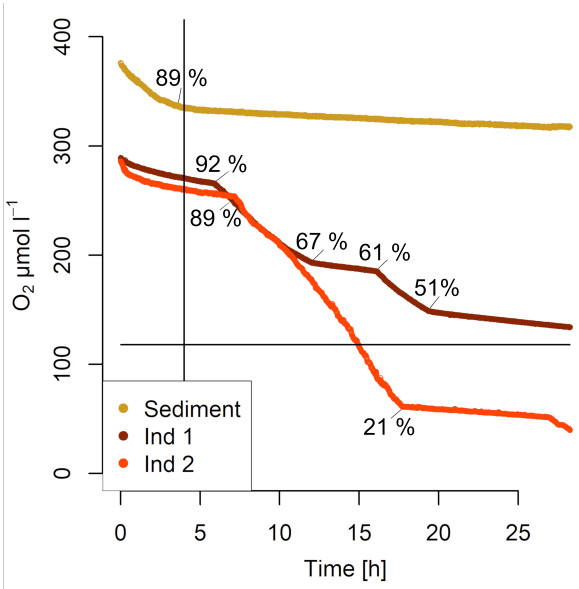

Figure 8: Examples of respiration rate measurements. Sediment is an example of a control sediment respiration at 5°C with a disturbance time of 4 h (indicated by the vertical line). Ind 1 is an example of a concentration decline of one individual at 15°C. Different activity phases were not introduced by a change in oxygen saturation but resemble *M. arenaria* behaviour. Ind 2 is one of eight individuals measured at 15°C where the oxygen saturation level dropped below 30% (indicated by the horizontal line) until the end of the measurement. These individuals were excluded from calculation of weight dependent respiration. This graph was changed after Schade et al. (2019).

The decrease in concentration was inconsistent at the beginning of the experiment (Figure 8) due to potential animal disturbance while placing the lid (Jørgensen and Riisgard 1988) or other inconsistencies. An initial fast signal decline attributed to thermal and mechanical disturbances of the animal and the respiration chamber setup was observed in most measurements. The control sediment curve was an example of a control sediment respiration at 5°C where the disturbance time lasted for 4 h. Even though disturbance time was only approx. 1 hour for most measurements; the initial 4 h were discarded from all measurements to keep the data treatment constant. There was no limitation of oxygen as the oxygen saturation level at this starting point after 4 h was 91.1 ± 3.6% of saturation (value at start: 100% ± 2%) in all measurements used for the respiration rate calculation.

The importance of integrating measurements over 24 h became evident, when looking at Ind 1, which showed the concentration decline of one individual at 15°C. Activity phases were not introduced by a change in oxygen saturation but resembled *M. arenaria* behaviour (change in respiration rate at 92%, 67%, 61% and 51% oxygen saturation).

Generally bivalves change their respiration behaviour if oxygen is limiting (Pedersen 1992). Ind 2, Figure 8 shows one individual (of eight) measured at 15°C where the oxygen saturation level dropped below 30% until the end of the measurement. The respiration rate of this individual was constant down to 21% oxygen saturation, including a change in activity phase observed at 89% oxygen saturation. Respiration rate measurements are often carried out only down to 75 or 70% oxygen saturation (McMahon and Russel-Hunter 1977; Lewis and Cerrato 1997; Lasota et al. 2014), however the measured data agree with Pedersen (1992), who stated respiration rates to be stable down to 25% oxygen saturation. Measurements where oxygen concentration at the end of the experiment fell below 30% of saturation were discarded for the calculation of the weight-respiration rate relationship. Animals showing no respiration over 24 h were additionally excluded from calculation (n=15).

"The oxygen consumption rate was calculated using Equation 6, with C_{tot} as the total consumption, C_{Start} the start oxygen value [µmol l^{-1}], C_{End} the end value [µmol l^{-1}], V_C the core volume [l] and t the measurement duration [h]. C_{Start} and C_{End} were measured with n = 3 individual O_2 measurements with t = 24 h.

$$C_{tot}\ [\mu mol\ h^{-1}] = \frac{(C_{Start} - C_{End}) * V_C}{t} \tag{6}$$

The respiration rate of each bivalve was corrected with the sediment oxygen consumption of control cores ($C_{Control}$ [µmol l^{-1}]) (3.89 ± 2.32 mmol O_2 m^{-2} d^{-1}) (Equation 7).

$$C_{tot}\ [\mu mol\ h^{-1}] = \frac{(C_{Start} - C_{End}) * V_C}{t} - C_{Control} \tag{7}$$

Weight specific oxygen consumption rate [mmol O_2 d^{-1} g^{-1}] was then calculated using the shell-free dry weight of each *M. arenaria*."

As some sampling data only contain shell length data for individual bivalves, it is necessary to calculate weight from shell length enabling a further calculation of weight specific respiration rates. The data was used to calculate a length to SFDW relationship.

"The difference in respiration between the temperatures treatments was tested with a T-Test (program RStudio version 3.4.4)."

2.3.2 Respiration of *Marenzelleria* spp. and *H. diversicolor*

Respiration rates of *Marenzelleria* spp. and *H. diversicolor* were not measured but budgets were calculated. For the calculations, necessary assumptions were made and respiration budgets were calculated according to published literature.

For the respiration of *Marenzelleria* spp. and *H. diversicolor*, the respiration of the worms itself and the increase in bacterial respiration due to burrow wall oxygenation and radial diffusion of O_2 into the sediment needed to be estimated (Karlson et al. 2007). The respiration of the polychaetes *Marenzelleria* spp. and *H. diversicolor* could be estimated with the equation for respiration of the polychaetes published by Mahaut et al. (1995) (Braeckman et al. 2010; Urban-Malinga et al. 2013). The influence of burrows produced by *Marenzelleria* spp. was roughly estimated after Renz and Forster (2014) to be ~80% of the total oxygen uptake (respiration by *Marenzelleria* spp. and influence on bacterial oxygen uptake due to burrows). For the estimation, *Marenzelleria* spp. was assumed to be either *M. viridis* or *M. neglecta* due to the distribution of species where *M. arctia* is only found in the northern part of the Baltic (Renz and Forster 2014). The influence of burrows by *H. diversicolor* could be roughly be estimated assuming the respiration by the polychaete itself to be only ~11% of the total oxygen uptake change due to the occurrence of *H. diversicolor* after Kristensen et al. (1985).

3 Results

3.1 Sediments of the study area

Most of the sediment in the study area consisted of sand. Permeability in the upper 10 cm of the sediment ranged from $1.36{*}10^{-12}$ m^2 to $113{*}10^{-12}$ m^2 (Figure 9) within the study area, with the majority of stations being permeable. As indicated with a black threshold line (Figure 9) only Station 33 was per definition impermeable when measured for 10 cm sediment depth. Grain sizes in the study area ranged from 171 µm to 729 µm (Table 1); defining the sediment in the area as a sandy site with sediment properties ranging from fine to coarse sand (Wentworth 1922). The organic content ranged from 0.1 to 0.2% of DW, so the whole study area showed a low organic content (Table 1). C and N content measured as suspension on filters showed some variation within the study area. C content ranged from 0.5 to 4 mg g^{-1} sediment, N content ranged from 0.1 to 0.3 mg g^{-1} sediment and C:N ratios varied from 5 to 37 (Table A.4).

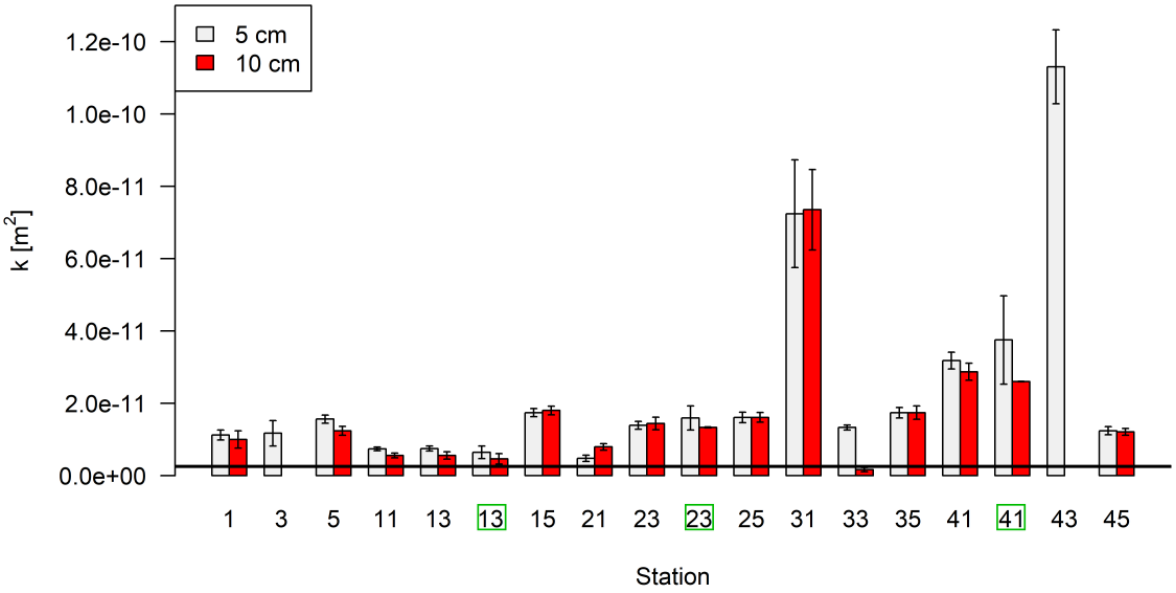

Figure 9: Permeability in the study area with $2.5{*}10^{-12}$ m^2 as permeability threshold marked with a black line. Green boxes mark the deployment stations and permeability's measured again during deployment (described in Chapter 2.2.4).

Chl a was sampled at 15 stations within the study area with different distances to the shore (data in Table A.5, Table A.6 and Table A.7). Chl a concentrations ranged from 0.15 to 11.41 µg ml^{-1} with the highest values in the upper centimetres of the sediment and the lower values in deeper sediment. Related to a geographical pattern, chl a values were analysed with regard to distance to the shore (50 m; 550 m or 1050 m; Figure 10). Distance had a significant influence on the chl a content ($p < 0.05$), with 50 m being significantly different to

Table 1: Summarized grain size analysis data for the study area. Grain size, porosity, permeability for 5 and 10 cm sediment depth and organic content at each station measured in the study area.

Station	Grain Size [µm]	Porosity	Perm (5 cm) k [m^2] $*10^{-12}$	Perm (10 cm) k [m^2] $*10^{-12}$	Corg [%DW]
1	182.9	0.36	11.2 ± 1.4	10 ± 2.4	0.13 ± 0.01
3	186.5	0.37	11.7 ± 3.5	NA	0.13 ± 0.02
5	312.5	0.34	15.6 ± 1.1	12.4 ± 1.2	NA
11	279.8	0.34	7.6 ± 0.5	5.6 ± 0.7	0.12 ± 0.01
13	170.9	0.41	7.5 ± 0.7	5.6 ± 1	0.18 ± 0.01
15	318.6	0.34	17.4 ± 1.1	18.0 ± 1.2	0.15 ± 0.0
21	180.5	0.37	4.75 ± 0.9	7.9 ± 0.9	0.16 ± 0.01
23	251.1	0.38	13.9 ± 1.1	14.4 ± 1.8	0.13 ± 0.01
25	222.2	0.36	16.1 ± 1.5	16.1 ± 1.3	0.10 ± 0.0
31	188.3	0.37	72.4 ± 14.9	73.5 ± 11.1	0.09 ± 0.0
33	185.7	0.37	13.3 ± 0.7	1.6 ±0.6	0.17 ± 0.02
35	410.2	0.39	17.4 ± 1.4	17.4 ± 1.8	0.09 ± 0.01
41	363.7	0.36	31.8 ± 2.3	28.7 ± 2.3	0.18 ± 0.01
43	728.6	0.36	113 ± 10.2	NA	0.2 ± 0.04
45	176.9	0.4	12.4 ± 1.1	12.1 ± 0.9	0.11 ± 0.01

550 m. Generally stations with 50 m distance to the shore were shallower compared to 550 m and 1050 m (Figure 10). Chl a values at the deeper stations were ~twice as high as at the shallower stations.

To test for the influence of water depth (Table A.2) on the chl a content; a regression analysis was performed in which the chl a content of each sediment depth (Table A.5, Table A.6 and Table A.7) of each station was correlated with the respective water depth at the stations. Water depth had a significant influence on the chl a content for all sediment depths (Table 2), however R^2 ranged from 0.22 to 0.56 explaining less then half of the variation in chl a content.

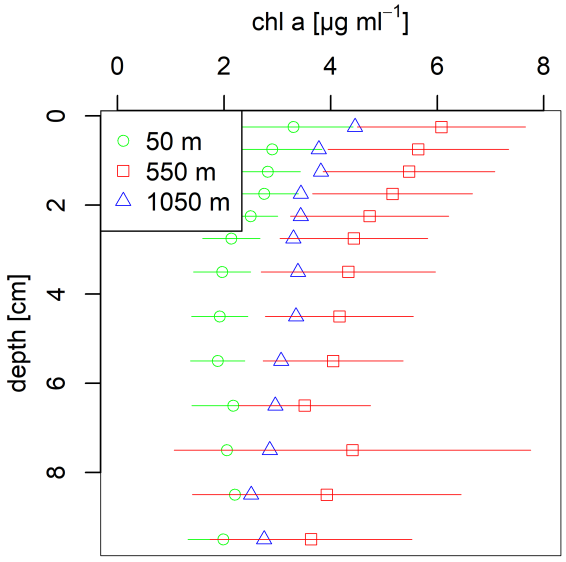

Figure 10: Distribution of chl a in the study area at 50 m, 550 m and 1050 m distance of the sampled stations to the shore.

Table 2: R^2 for each the regression of each sediment sampling depth compared to water depth at the sampled station. All regressions were significant.

Sediment depth [cm]	p-value	R^2
0.25	0.00	0.42
0.75	0.01	0.27
1.25	0.00	0.39
1.75	0.00	0.36
2.25	0.00	0.38
2.75	0.00	0.42
3.5	0.00	0.41
4.5	0.00	0.54
5.5	0.00	0.56
6.5	0.00	0.48
7.5	0.02	0.25
8.5	0.03	0.22
9.5	0.01	0.31

3.2 Wind and currents in the study area

Waves in the study area were constantly monitored for over a year. Figure 11 summarizes wave heights and frequencies at the monitored station. Waves measured during the deployment were as high as 1.7 m and longest waves lasted up to 14 h. Smaller waves <0.5 m occurred frequently and also for longer periods of time up to ~13 hours. Larger waves <1 m also occurred less frequent and with shorter durations. Generally shorter durations of wave periods were much more frequent than longer lasting waves of the same wave height.

Boundary layer flow velocities under waves in the field ranged from 0 - 0.5 m s^{-1} (12). Frequency of occurring velocities decreased with increasing velocity. Velocities <0.14 m s^{-1} were most frequent and constituted >70% of frequencies.

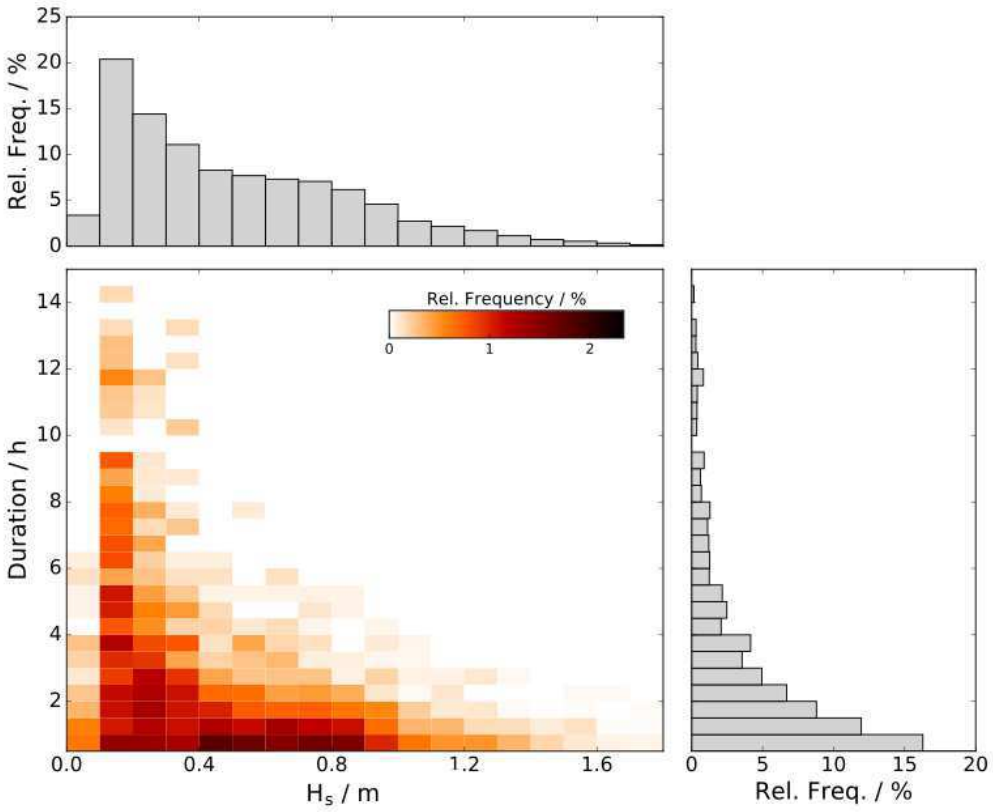

Figure 11: Frequency, duration and height of waves in the study area from April 2017 to October 2018 (Figure by Xaver Lange).

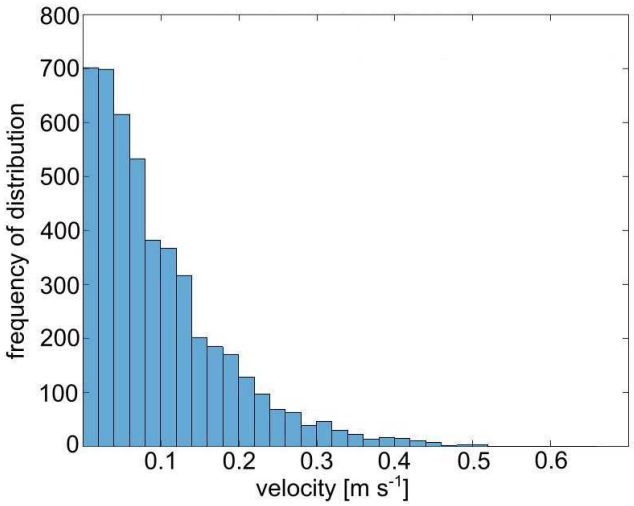

Figure 12: Frequency distribution of velocities within one meter above the sea bed from April 2017 to July 2017 (Figure by Nils Karow).

3.3 Oxygen uptake of coastal sediments

Oxygen uptake was measured in the laboratory with natural sediments piled up in chambers, sediment cores taken from the field into the laboratory and in situ measurements. Oxygen uptake was additionally measured as a function of flow and food enrichment in flow-through cores with different sediment types.

3.3.1 Laboratory benthic chamber incubations

Measurements in the laboratory were conducted with medium and fine grained sediment cores respectively to gain insight on the oxygen dynamics in different sediment types. Micro-profiles were always measured at a specific distance to the centre (0, 2.1, 4.2, 6.3 and 8.4 cm), they are referred to in the next paragraph with the rounded cm value only.

Permeability of the medium grained sediment was $\sim 2.4 * 10^{-11}$ m^2; grain size was ~300 µm and the organic content was ~0.09% DW.

The addition of algae to the overlaying water had no influence on the oxygen uptake (Figure 6). Oxygen uptake data were thus pooled and an average oxygen uptake value was calculated for medium grained sediment. Micro-profiles for medium grain size were presented exemplarily in Figure 14. The addition of algae had no effect on the oxygen penetration depth.

Oxygen uptake in the chambers with medium grained sediment (n= 2) was 3.9 ± 1.5 mmol O_2 m^{-2} d^{-1} at a temperature of 8°C (Figure 15). Oxygen uptake was constant despite the change in differential pressure from 0.2 Pa (lowest value) to 2.4 Pa (maximum dp). For an

oxygen time course, oxygen was logged constantly at 4 different sediment depths within the chamber. With increasing differential pressure the oxygen concentration inside the sediment increased. Respectively, with decreasing differential pressure, the oxygen concentration in the sediment decreased (Figure 13). Oxygen continuously decreased with increasing sediment depth. Oxygen concentration changes occurred parallel for all measured depths.

Micro-profiles measured for 10 and 45 rpm are shown here in Figure 14. At low dp the oxygen penetration depth varied between 10 mm and 15 mm for measured profiles at the centre, 2, 4 and 6 cm (Figure 14). For 8 cm, the penetration depth of oxygen increased to >1.5 cm already at 0.2 Pa dp. With increasing dp, the oxygen penetration depth increased for the profiles more distant to the centre of the chamber, while it decreased at the centre. For 0 and 2 cm, the oxygen penetration depth was only 4 mm at a dp of 2.4 Pa. For 4, 6 and 8 cm, the oxygen penetration depth was clearly >1.5 cm at a dp of 2.4 Pa. The oxygen micro-profiles clearly fit to the constant time course at the side of the chamber with increasing oxygen concentrations in the sediment with increasing dp.

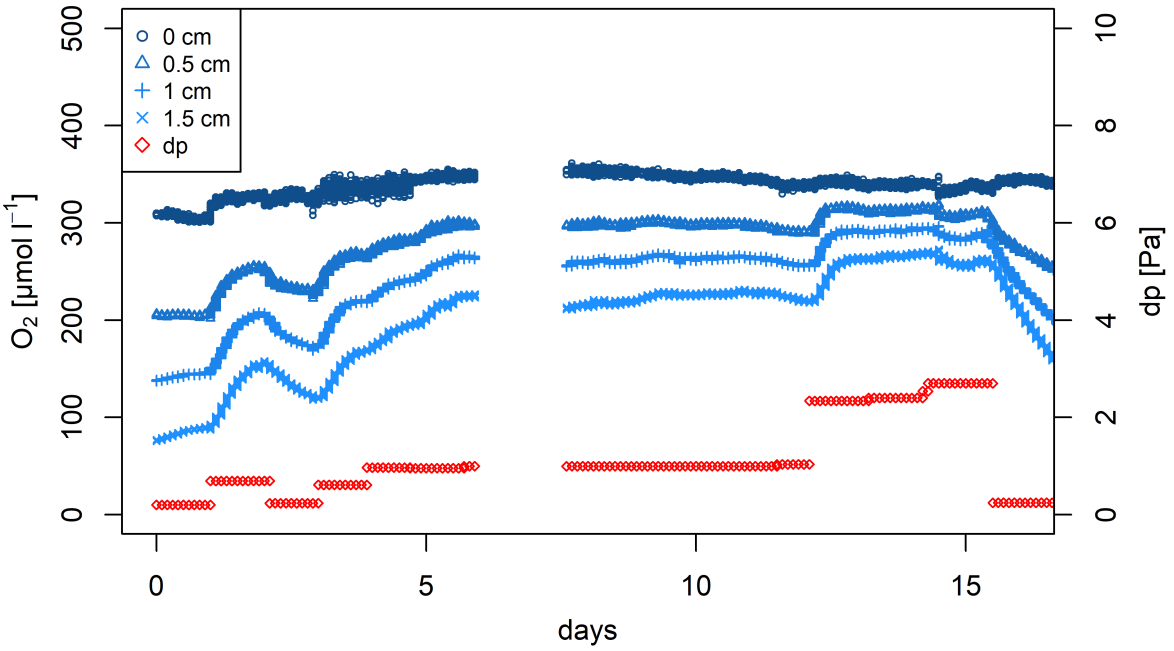

Figure 13: Oxygen level measured at the side of the benthic chamber with medium grained sediment. Blue points show oxygen values at different sediment depths; Red diamonds show the differential pressure applied to the benthic chamber.

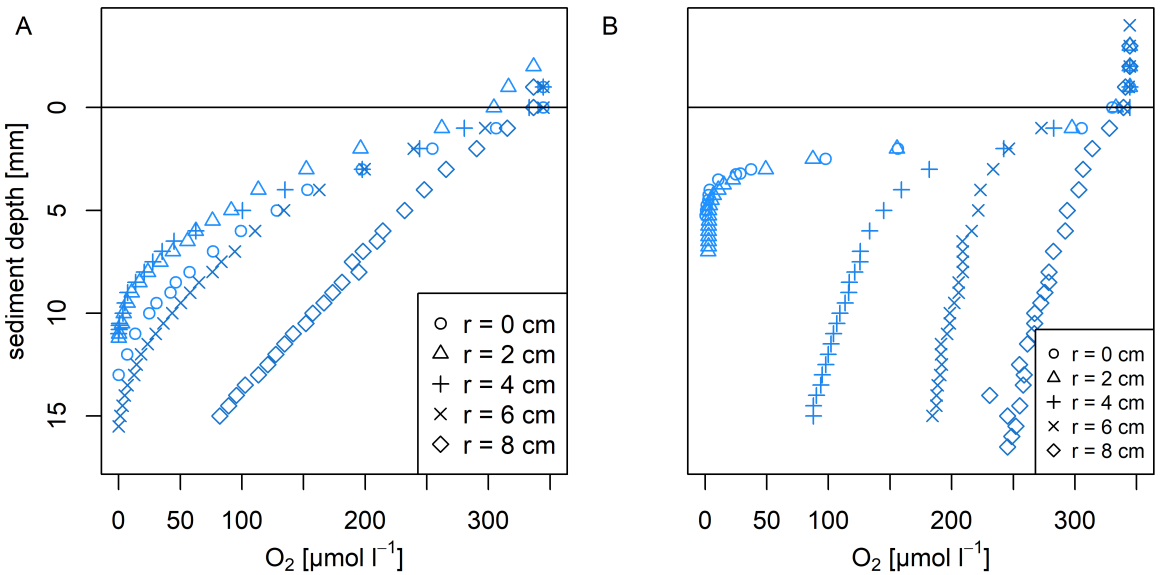

Figure 14: Oxygen micro-profiles measured in the benthic chamber with medium grained sediment. A) oxygen micro-profiles measured at 0.2 Pa dp (or 10 rounds per minute stirring speed) B) oxygen micro-profiles measured at 2.4 Pa dp (or 32 rounds per minute stirring speed).

For the fine grained sediment, two runs (Langenwerder 1, n = 3 and Langenwerder 2, n = 3) were measured at 16°C. Grain size for the first trial was ~217 µm and for the second ~182 µm. The organic content was ~0.17% DW for both trials and the permeability was ~$7.5{*}10^{-12}$ m^2. For both trials oxygen uptake was independent of differential pressure. The first run showed an oxygen uptake of 30.6 ± 2.6 mmol O_2 m^{-2} d^{-1} compared to the lower oxygen uptake of 15.9 ± 3.6 mmol O_2 m^{-2} d^{-1} of the second run (Figure 15).

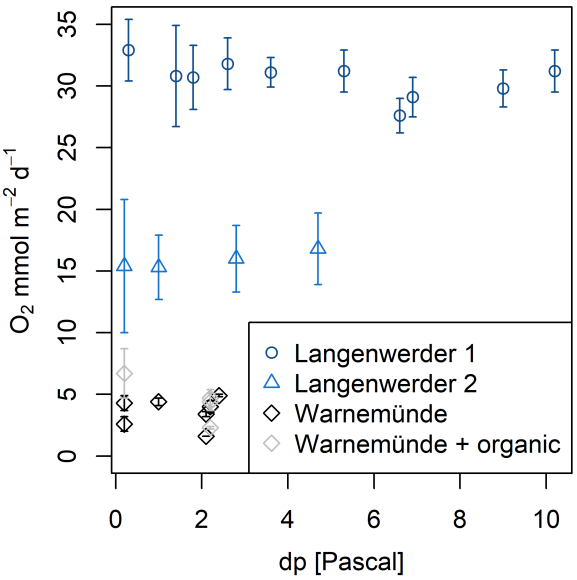

Figure 15: Oxygen uptake of Langenwerder 1 in light blue; of Langenwerder 2 in dark blue and of Warnemünde in grey/ black.

No visible change in oxygen uptake was observed when varying dp. Additionally the

oxygen concentration in the sediment was unchanged. Figure 16 shows the oxygen concentration at 0.8 cm and 1.3 cm sediment depth with increasing dp. The oxygen concentration stayed constantly at ~0 µmol l^{-1} independent of increasing differential pressure. The oxygen micro-profiles agreed with this observation. The oxygen penetration depth varied from 6 to 8 mm for 0 and 8 cm at a high differential pressure of 4.7 Pa (Figure 16). In contrast to the medium grained sediment, there was no visible change in the oxygen penetration depth, not with increasing dp, nor with increasing distance of the measured profile to the centre.

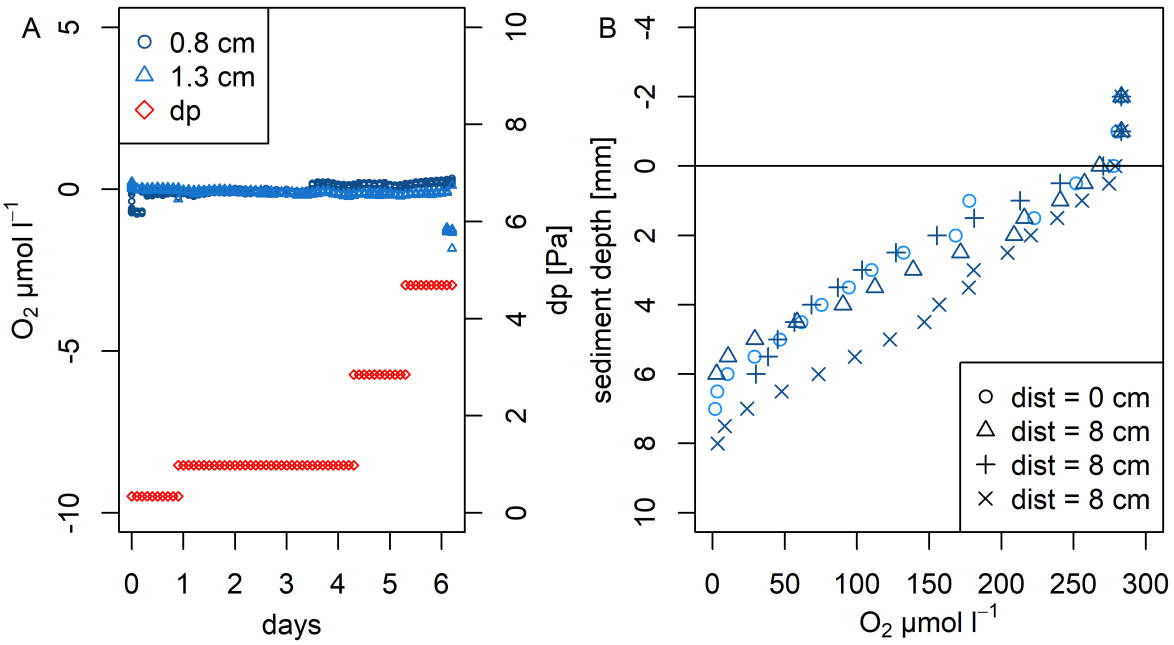

Figure 16: Oxygen profile and micro-profiles inside the benthic chamber with fine grained sediment (from Langenwerder). A) Blue points show the oxygen concentration at different sediment depths (oxygen concentration at 0.8 and 1.3 cm sediment depth were constantly 0); Red diamonds show the differential pressure applied to the benthic chamber. B) Oxygen micro-profiles were measured for Langenwerder 2 at 4.7 Pa dp.

TOU for Langenwerder 1 was observed to be twice as high as for Langenwerder 2. In both trials the macrofaunal biomass was measured. The biomass of polychaetes was 10 times higher for Langenwerder 1 (6.2 g m^{-2} ± 0.6 AFDW) compared to the Langenwerder 2 (0.9 g m^{-2} ± 1.5 AFDW). Biomass of bivalves (only *M. arenaria*) was 3 times higher in cores of Langenwerder 1 (1.8 g m^{-2} ± 0.5 AFDW) compared to Langenwerder 2 (0.6 g m^{-2} ± 0.7 AFDW).

The calculated oxygen uptake due to the influence of the polychaetes was based on literature values (Chapter 2.3.2), oxygen uptake was 12.5 ± 0.9 mmol O_2 m^{-2} d^{-1}, while the oxygen uptake during the second run for the polychaetes was lower with 2.4 ± 3.3 mmol O_2 m^{-2} d^{-1}. The apparent calculated difference of ~10 mmol O_2 m^{-2} d^{-1} is similar to the difference between those two runs (14.7 mmol O_2 m^{-2} d^{-1}) and might indicate that macrofauna influence in TOU accounts for most of the difference. The respiration of *M. arenaria* could not be calculated as only the DW and the AFDW were taken while SFDW would be needed

for the calculation.

3.3.2 In situ benthic chamber incubations

Benthic chambers were deployed at three stations in the field in July 2017 and August 2018. Comparing the sediment characteristics with sampling data in 2016, the sediment characteristics were still similar (Figure 9). Permeability was lowest at St 13, ~twice as high at St 23 and highest at St 41 (~5 times as high as St 13).

Regarding the C and N contents, C and N at St 41 were higher compared to contents at St 23 and St 13. St 41 was quite different compared to St 23, as C content increased constantly with depth (2.9 mg g^{-1} for 0-1 cm depth, 9.1 mg g^{-1} for 9 - 10 cm depth, Table 3), while N content stayed constant. N content was constantly ~twice as high at St 41 compared to St 23. Regarding only the top cm, the C content at St 41 was 2.9 mg g^{-1} compared to 2 mg g^{-1} at St 23 or 2.16 mg g^{-1} at St 13, thus the content at St 41 was ~1.5 times higher (Table 4).

While the organic content of St 13 and St 23 was comparable, it was considerably higher at St 41. Organic carbon calculated due to measured chl a at the stations, showed a different trend towards higher organic content at St 13 compared to St 23 and St 41 however, the variation was quite high.

Table 3: C and N content at St 23 and 41 in depth profiles; SD for N values at St 23 was 0.0 for all samples.

	Station 23		Station 41	
Sediment depth [cm]	C [mg g^{-1}]	N [mg g^{-1}]	C [mg g^{-1}]	N [mg g^{-1}]
0 - 1	2.03 ± 0.13	0.09	2.92 ± 0.35	0.2 ± 0.16
1 - 2	1.15 ± 0.1	0.07	4.41 ± 1.28	0.21 ± 0.01
2 - 3	1.6 ± 0.13	0.06	5.01 ± 2.41	0.19 ± 0.01
3 - 4	2.23 ± 0.28	0.06	4.27 ± 0.25	0.20 ± 0.01
4 - 5	1.75 ± 0.21	0.06	4.65 ± 0.72	0.20 ± 0.00
5 - 6	1.95 ± 0.19	0.05	5.78 ± 0.52	0.21 ± 0.00
6 - 7	1.73 ± 0.06	0.05	6.21 ± 0.6	0.21 ± 0.01
7 - 8	NA	NA	5.75 ± 0.18	0.23 ± 0.01
8 - 9	NA	NA	6.46 ± 0.45	0.21 ± 0.01
9 - 10	NA	NA	9.08 ± 0.99	0.19 ± 0.01

Additionally porewater nutrient profiles were measured (n = 4, Figure 17). Porewater profiles showed a high variability between profiles at the same station. The high variation measured at station 13 probably also existed at St 23 and St 41; however, at these stations 3 out of the 4 replicates ran dry before sampling and could thus not be used for porewater profiling. All profiles were nevertheless similar between stations with a tendency of higher nutrient values at the most impermeable station (St 13).

Table 4: Sediment parameters as background values at St 13, 23 and 41. For permeability, Corg (LOI) and Corg (chl a) measurements, n = 3. Station 13 was impermeable when measured over 15 cm sediment depth; Corg from C:N analysis was based on the average value for St 41 and 23 (0-10 cm). Carbon increased with depth at station 41 (Table 3) resulting in the high standard deviation when averaged; Corg calculated from chl a values was calculated for the top centimetre only.

Station	Grain size [µm]	k (5 cm) [m^2] *10^{-12}	k (10 cm) [m^2] *10^{-12}	Corg [mg m^{-2}] (C:N analyser)	Corg [mg m^{-2}] (LOI)	Corg [mg m^{-2}] (chl a)
St 13	166	6.43 ± 1.71	4.63 ± 1.46	3393 ± 131	2195 ± 254	509 ± 106
St 23	213	15.9 ± 3.34	11.0 ± 0.13	3191 ± 675	2304 ± 61	431 ± 116
St 41	543	37.5 ± 12.2	31.0 ± 0.097	8609 ± 2950	5887 ± 2601	357 ± 35

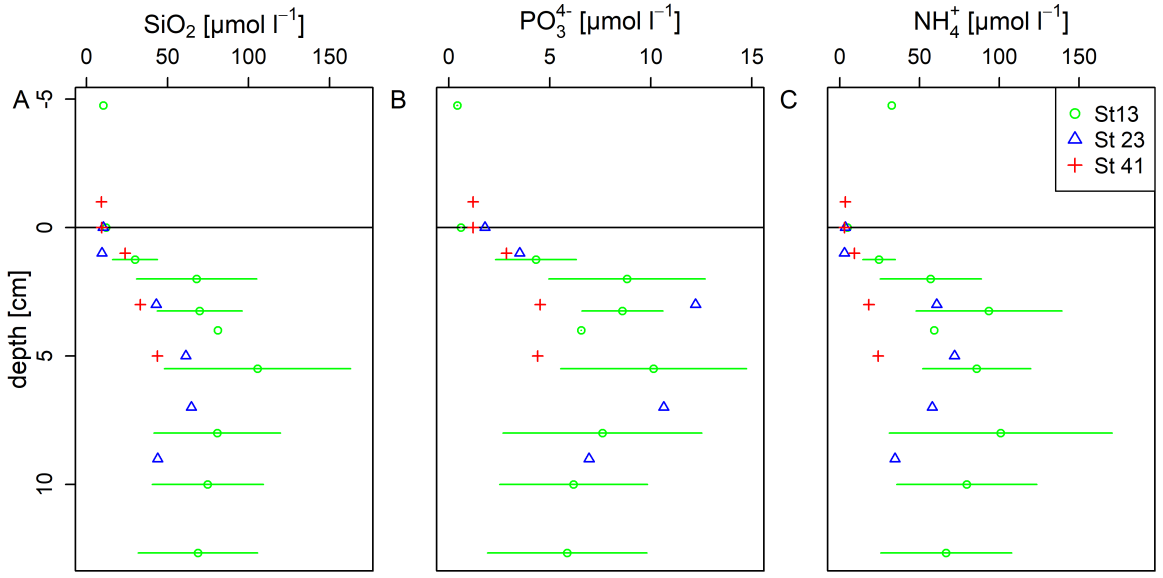

Figure 17: Nutrient porewater profiles at St 13, St 23 and St 41 with the standard deviation obtained at St 13 (n = 4).

TOU was measured at all stations for day and night cycles. In July 2017, the night (sunset until sunrise) was 9 hours and the day was 15 hours, while in August 2018 the night was 10 hours and the day was about 14 hours. TOU measurements took place during manually adjusted day and night cycles and were calculated to either TOU per day (24 h, in the results) or per separate day/ night cycle (9 (10) hours and 15 (14) hours in the discussion). Calculations are presented here per 24 h as a comparison between the stations was more feasible when based on the same duration.

St 13 (n = 2) had the highest oxygen uptake with -27.9 ± 3.8 mmol O_2 m^{-2} d^{-1} for the advection setting and -33 ± 2.1 mmol O_2 m^{-2} d^{-1} for the diffusion setting. Oxygen uptake at St 41 (n = 3) and St 23 (n = 4) was lower with -21.4 ± 7.5 mmol O_2 m^{-2} d^{-1} at St 41 and -12.6 ± 1.4 mmol O_2 m^{-2} d^{-1} at St 23 for the advection setting and -10.4 ± 2.9 mmol O_2 m^{-2} d^{-1} at St 41 and -14.6 ± 7.8 mmol O_2 m^{-2} d^{-1} at St 23 for the diffusion setting.

During daytime net production rates were 7.3 ± 1.7 mmol O_2 m^{-2} d^{-1} at St 13; 11.5 ± 23 mmol O_2 m^{-2} d^{-1} at St 41 and 5.9 ± 8.2 mmol O_2 m^{-2} d^{-1} at St 23 for the advection

setting. Production rates for the diffusion setting were 34.9 ± 13.2 mmol O_2 m^{-2} d^{-1} at St 13, 22.2 ± 8.8 mmol O_2 m^{-2} d^{-1} at St 41 and 1.3 ± 4.6 mmol O_2 m^{-2} d^{-1} at St 23 (Figure 18).

The TOU rates did not differ between the stations, neither for oxygen uptake during the night cycle, nor for oxygen production during the day cycle. Comparing the different sediment parameters it becomes obvious that St 13 differed slightly in oxygen uptake but sediment parameters were quite similar to St 23. Only the permeability was lower at St 13. Chl a values at St 13 were higher compared to St 41. The C and N content at St 41 was three times higher in organic material than at St 23.

For all stations the variation between replicates was quite high. Figure 19 shows single replicates of St 41 indicating the high variation between single measurements.

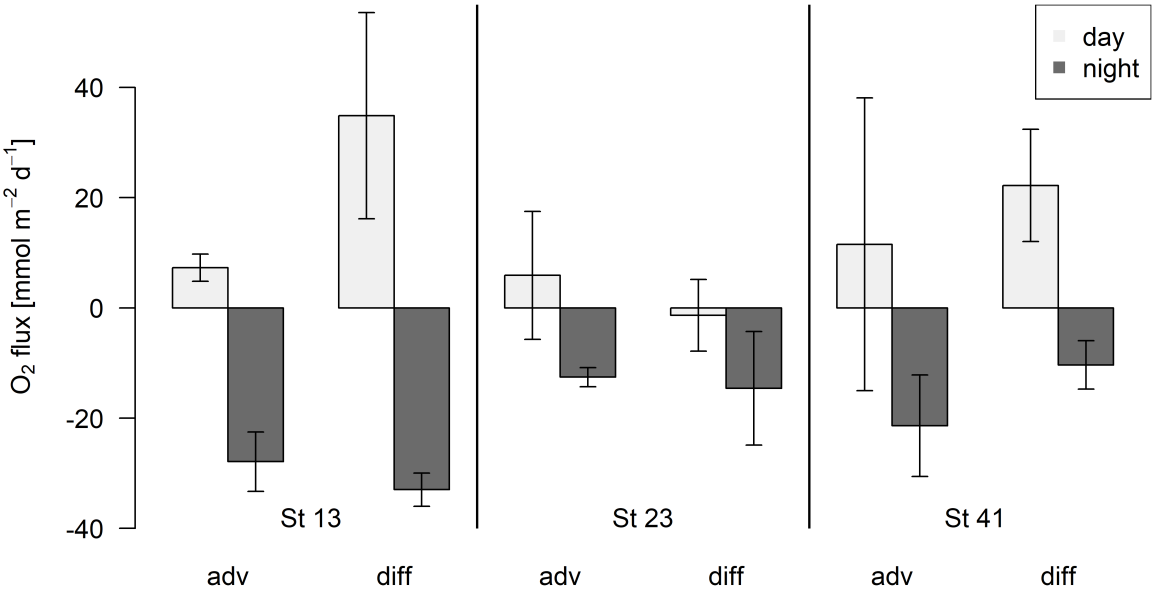

Figure 18: Oxygen uptake at St 13, St 23 and St 41. Oxygen uptake/ production rates were calculated for 24h.

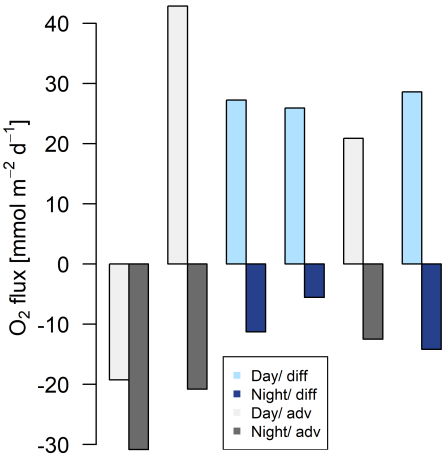

Figure 19: Oxygen uptake at station 41 for each chamber incubation separately. Each day and night measurement plotted next to each other were measured in the same chamber. Oxygen uptake/ production rates were calculated for 24h.

To evaluate if replicates with high oxygen uptake had a lower measurable daily production, examples of day and night oxygen uptake/ production are shown exemplary for each replicate of St 41 in Figure 19. St 41 was the only station for which a difference in oxygen uptake between the two treatments could be observed. No direct relationship between oxygen uptake and daily oxygen production could be observed in this example. Additional to a visual observation, a relationship between oxygen uptake and production was tested. The regression between daily production and night oxygen uptake was insignificant when testing each station and additionally when testing all replicate pairs of all stations.

Nutrient fluxes were measured for each replicate chamber. NH_4^+, SiO_2, PO_4^{3-} fluxes are shown in Figure 20 for the three in situ stations. Fluxes of nitrate and nitrite were often below detection limit and were thus not evaluated. As already observed for TOU, nutrient fluxes were quite variable. In comparison with the oxygen, nutrient fluxes showed an even higher variation between the stations. Especially St 23 showed rather low ammonium fluxes compared to the other two stations. Nutrient fluxes were mostly not significantly different between stations. Fluxes which were statistically different were daily fluxes of phosphate and ammonium which differed statistically between St 13 and St 41. Nutrient fluxes were not statistically different between advection and diffusion setting.

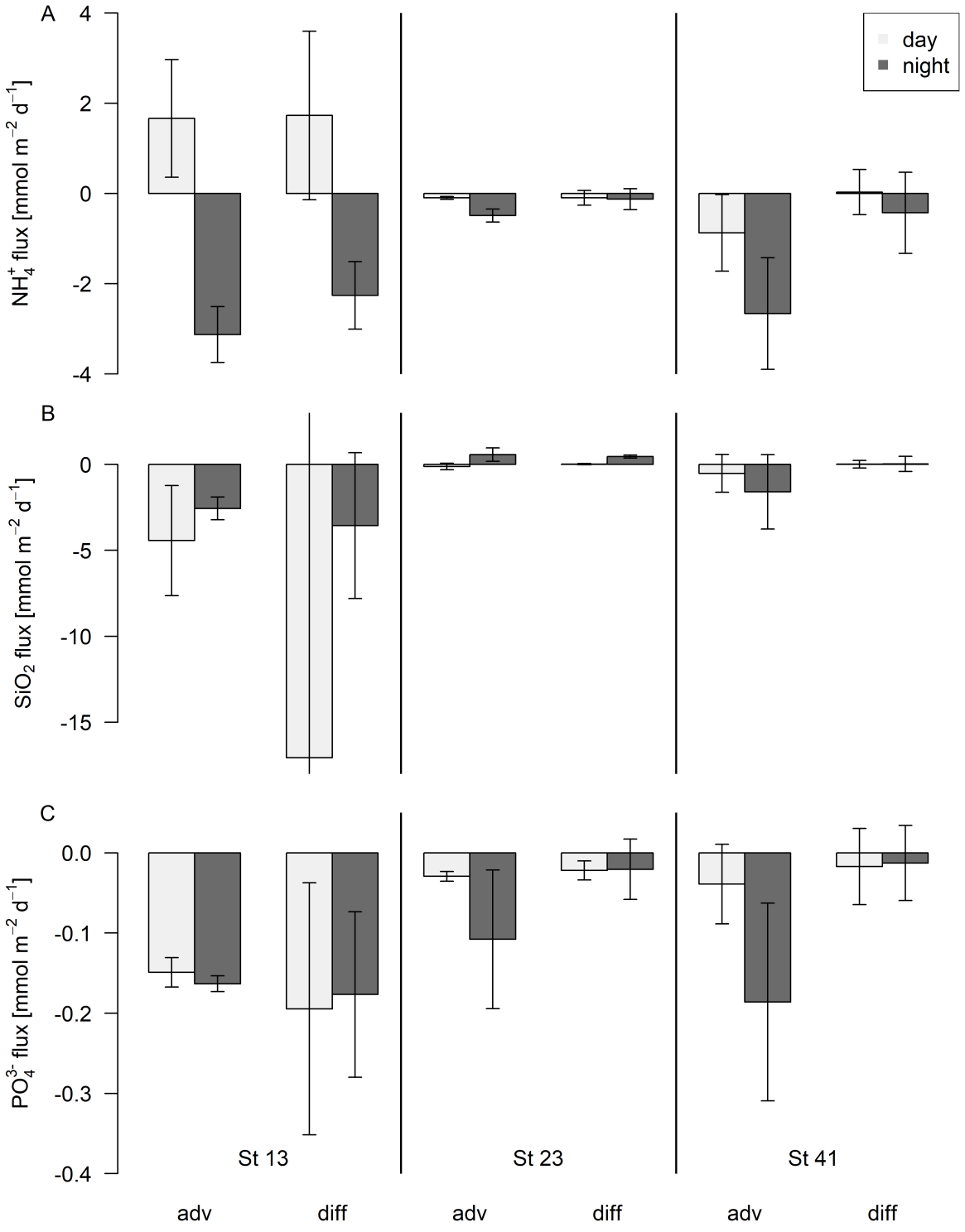

Figure 20: Nutrient flux at St 13, St 23 and St 41. Fluxes calculated for 24 h as day and night flux for each station, error bars show the standard deviation. A) Ammonium flux B) Silicate flux, as the standard deviation for the diffusive day flux at station 13 was rather large, the whole range was omitted. C) Phosphate flux.

3.3.3 Microbial volumetric oxygen consumption depending on porewater flow

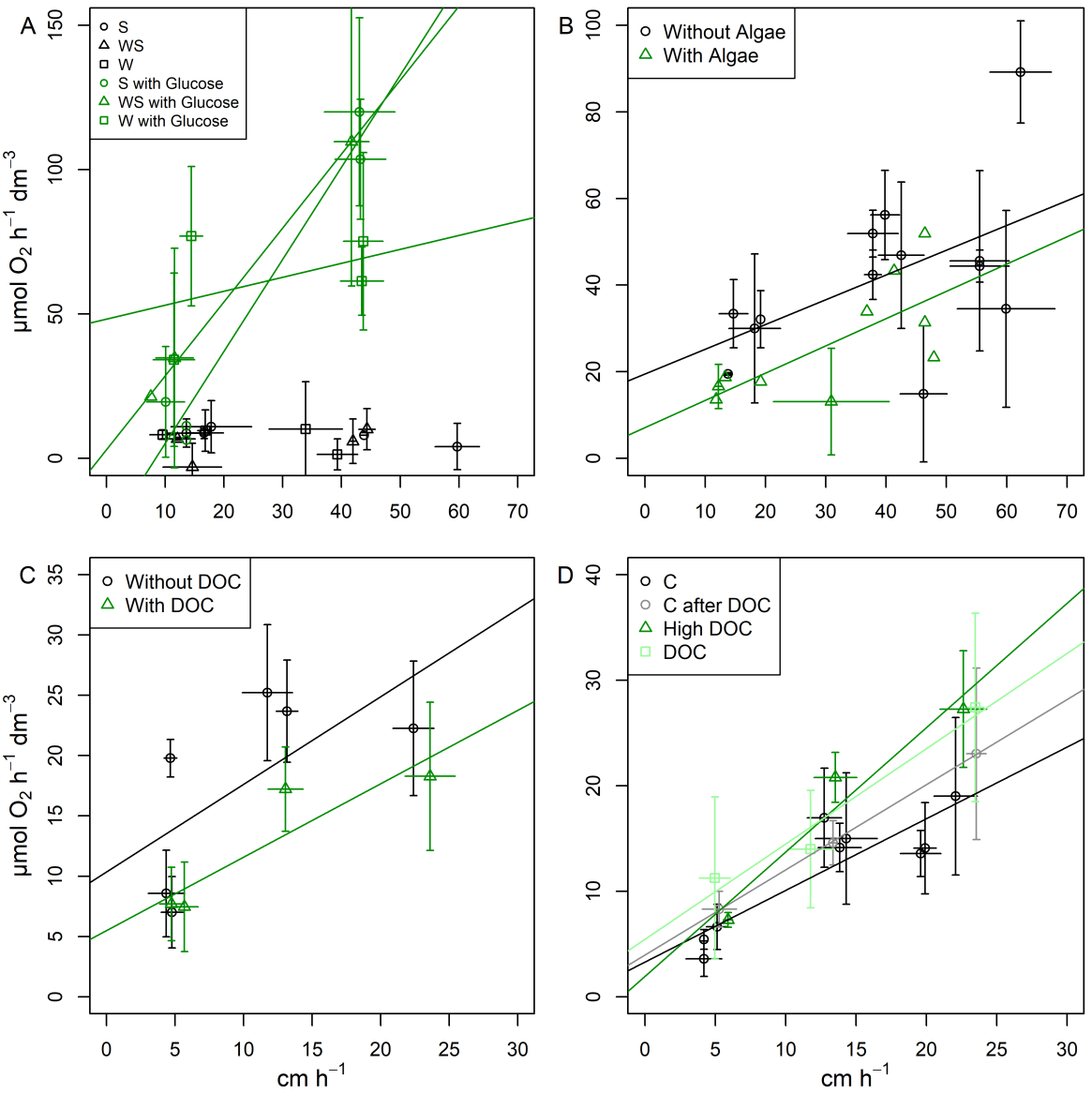

Figure 21: Volumetric oxygen consumption in dependence of flow before and after the addition of A) glucose for three different sediment types (W, S, W/S), B) algae to one sediment type (AWAC), C) DOC to one sediment type (AWAC) and D) two different DOC concentrations to one sediment type (W).

Porewater can flow through sediment at different velocities. An experiment was designed testing the volumetric oxygen consumption of different sediments in dependence of this porewater flow. Plug flow was increased to ~60 cm h^{-1} in the first two experiments (Figure 21.A, B, Table 5) and to ~30 cm h^{-1} in the last two experiments (Figure 21.C, D, Table 5). Additionally seawater flowing through the cores was enriched with glucose, algae or DOC and oxygen consumption of sediments was measured in dependence of the enrichment. Nutrients were variable throughout all experiments and are given as background parameters in Table

Table 5: Conditions for the Flow-through Experiments.

Experiment	Sediment	Replicates [n]	Flow [cm h^{-1}]	Treatment	Salinity
I	Warnemünde (W)	6	10 - 60	Glucose	13
I	Schnatermann (S)	6	10 - 60	Glucose	12
I	Mix W/S	6	10 - 60	Glucose	11
II	AWAC	6	12 - 19	Algae	11
II	AWAC	6	37 - 46	Algae	11
II	AWAC	6	31 - 62	Algae	11
III	AWAC	6	5 - 24	DOC	15
IV	W	3	4 - 24	No	16
IV	W	3	4 - 24	DOC	16
IV	W	3	4 - 24	High DOC	16

A.9.

Oxygen consumption was measured in different experimental set-ups with the differing treatments (Table 5). In total 4 different kinds of sediments were used. Sediment parameters were assessed prior to the experiment (Table 6, 7, and 8); permeability was additionally assessed at the end in most of the experiments. Nutrients were measured as additional parameter in the header tanks 2 - 4 times during each experimental run (Table A.9). Nutrient concentrations in each supplying header tank were measured separately on each date.

FTExp 1 was performed with and without glucose addition to 3 sediment types (W, W/S, S, n = 6 each). Sediment parameters prior the experiments are listed in Table 6. Sediment type W (Warnemünde) consisted of medium grained sediment; Sediment type S (Schnatermann) consisted of fine grained sediment and the sediment type W/S consisted of a mixture of both other types. Sediment S had the lowest permeability, the smallest grain size and the highest organic content. Sediment W had the highest permeability, the largest grain size and the lowest organic content. Sediment W/S was a mixture of the other two sediments and its values thus ranged in the middle of the other two.

FTExp 1 showed no dependence of oxygen consumption on flow rate for none of the sediment types, before the addition of glucose (Figure 21.A). Before any addition, volumetric oxygen consumption was low (average volumetric oxygen consumption ~6 µmol l^{-1} h^{-1}) for all sediments independent of sediment type or flow rate. Slopes varied from -0.52 µmol l^{-1} h^{-1}/ (cm h^{-1}) (W) to 0.2 µmol l^{-1} h^{-1}/ (cm h^{-1}) (W/S). Glucose was increased from ~0.3 mmol to ~0.9 mmol in all treatments.

After the addition of glucose, volumetric oxygen consumption increased in all cores with increasing flow. Highest volumetric oxygen consumption rates were found for sediment S and W/S, while the increase in volumetric oxygen consumption for the sediment W was only ~half of the increase found for sediment S and W/S. Nevertheless, the increase in volumetric oxygen consumption due to the increase in glucose was very pronounced in all cores. Furthermore, after the addition of glucose a clear dependence of volumetric oxygen consumption on flow could be observed for sediment S and W/S. Sediment W showed a different reaction.

The decrease in volumetric oxygen consumption with a decrease in flow rate could also be observed, however, not as pronounced as for the other two sediments. Slopes varied accordingly from 0.48 µmol l^{-1} h^{-1}/ (cm h^{-1}) for W sediment to 2.56 µmol l^{-1} h^{-1}/ (cm h^{-1}) for W/S sediment and 3.19 µmol l^{-1} h^{-1}/ (cm h^{-1}) for S sediment after the addition of glucose.

Table 6: Sediment parameters for the FTExp 1.

Sediment	k *10^{-12} [m^2]	k (end) *10^{-12} [m^2]	Grain size [µm]	Corg [% DW]	C end [mg g^{-1}]	N end [mg g^{-1}]
W	24.7 ± 0.28	2.08 ± 1.08	290	0.1	2.43 ± 0.1	0.04 ± 0.0
W/S	18.3 ± 0.22	1.28	229	0.13	1.88 ± 0.7	0.07 ± 0.0
S	13.2 ± 0.14	7.56	214	0.14	1.28 ± 0.9	0.07 ± 0.0

As glucose is not a natural food source occurring in the field, the next experiment (FTExp 2) consisted of addition of algae to the flow-through cores, as we tried to mimic the effect observed due to glucose input with a natural food source.

Sediment used for FTExp 2 was sediment taken from the actual study area to mimic more realistic field conditions. In this experiment, volumetric oxygen consumption rate was dependent on flow (Figure 21.B). With increasing flow, the volumetric oxygen consumption increased, the resulting slope before the addition of algae was 0.57 µmol l^{-1} h^{-1}/ (cm h^{-1}).

An addition of algae to the suppling water did not change the volumetric oxygen consumption rate in this experiment. The volumetric oxygen consumption rate still increased with increasing flow and the slope differed from before the addition only slightly with 0.63 µmol l^{-1} h^{-1}/ (cm h^{-1}).

The effect of the addition of algae could nevertheless be seen in the development of a visible biofilm on the cores. The existence of a biofilm after the experiment could also be measured in the C and N content as the C and the N content was higher in all cores in the upper sediment layer (0-1 cm) compared to the lower sediment layer (4-5 cm) (Table 7). The development of a biofilm additionally led to a reduction in the permeability (Table 7).

As flow was set for each header separately, the development of permeability differed between treatments. Permeability was measured on day 2 and day 3 after the addition of algae. Permeability of the cores experiencing faster flow (U1 and U2 cores) decreased faster compared to the control cores (C, slow flow). Permeability on day 2 was lowest for the core experiencing the fastest flow and highest for the core for the control group (Table 7) respectively. At day 3 all cores were impermeable.

Independent of the clear effects of the addition of algae on permeability, a change in volumetric oxygen consumption could not be observed. Instead of adding algae, DOC was used in the following two experiments as DOC was supposedly easier digestible for the bacteria in the sediment.

Table 7: Sediment parameters for the FTExp 2. Permeability before the experiment (23.04.18) was 15.2 ± $1.25*10^{-12}$ m^2 for the AWAC sediment. Permeability before the addition of algae (04.05.18) was 5.26 ± $1.37*10^{-12}$ m^2. C and N content was measured after the experiment. Grain size measured for this sediment was 192 µm and Corg was 0.16 ± 0.01% DW.

Sample	C:N (0-1 cm)	C [mg g^{-1}] (0-1 cm)	N [mg g^{-1}] (0-1 cm)	C:N(4-5 cm)	C [mg g^{-1}] (4-5 cm)	N [mg g^{-1}] (4-5 cm)	k $*10^{-12}$ [m^2] Day 2	k $*10^{-12}$ [m^2] Day 3
C	25.15	3.143	0.14	33.21	2.1	0.07	7.2	0.2
U1	24.51	2.82	0.13	30.23	1.98	0.08	2.08	0.16
U2	27.67	3.52	0.15	33.12	2.01	0.07	0.28	0.43

A test trial was run with only 3 cores without parallel control. The sediment used was the W sediment from FTExp 1. During this test, DOC was added instead of algae. The volumetric oxygen consumption before the addition of DOC was as low as in the FTExp 1 (~2 µmol l^{-1} h^{-1}). After the addition of DOC (200 ml DOC stock into 25 l of seawater in the header tank), the volumetric oxygen consumption increased ~20 times to ~40 µmol l^{-1} h^{-1}. The measured DOC content revealed the DOC to have been increased 3 times compared to pre-addition levels (~0.55 to ~1.72 mmol l^{-1}).

As the effect of DOC was quite pronounced in the test trail, DOC was used in the following two experiments.

For the first DOC experiment (FTExp 3), sediment from the field was used. Here we used the same sediment as used for the algae addition (FTExp 2). Figure 21.C shows the volumetric oxygen consumption in dependence of flow before and after the addition of DOC. Volumetric oxygen consumption increased with increasing flow from ~10 µmol l^{-1} h^{-1} to 25 µmol l^{-1} h^{-1} resulting in a slope of 0.73 µmol l^{-1} h^{-1}/ (cm h^{-1}). Volumetric oxygen consumption did not seem to change with the addition of DOC. Volumetric oxygen consumption rate differed only slightly to the volumetric consumption rate before the addition of DOC and the observed volumetric oxygen consumption values ranged from ~5 µmol l^{-1} h^{-1} to 20 µmol l^{-1} h^{-1} with a slope of 0.61 µmol l^{-1} h^{-1}/ (cm h^{-1}).

The determination of the DOC content revealed that the DOC was only slightly increased with the addition of fresh DOC (0.48 mmol l^{-1} to 0.50 mmol l^{-1}). This slight increase did not have an influence on the volumetric oxygen consumption of the sediment. Additionally the permeability measured after the experiment indicated that permeability stayed constant during the experiment. The permeability prior the experiment was measured for the algae experiments as sediments used were the same. The permeability changed from $15.2*10^{-12}$ m^2 with the addition of DOC to 14.8 ± $0.87*10^{-12}$ m^2. Thus no change in permeability could be observed due to any increase in DOC concentration.

For the second DOC experiment (FTExp 4) the W sediment was used again (see glucose experiment). In this experiment the volumetric oxygen consumption increased with increasing flow from ~5 μmol l^{-1} h^{-1} to 18 μmol l^{-1} h^{-1} with a slope of 0.68 μmol l^{-1} h^{-1}/ (cm h^{-1}).

In this experiment, the addition of DOC was supplied in two levels, one treatment with a high amount of DOC and one treatment with less DOC (Table 8). One of three header tanks was kept as a control. The volumetric oxygen consumption seemed to change slightly with the addition of DOC. The volumetric oxygen consumption was highest for the treatment with the highest DOC value and lowest for the control (without DOC addition) (Figure 21.D). However, none of these trends was significant. The slope increased for all treatments after the addition of DOC with the highest DOC addition resulting in the steepest slope: 0.81 μmol l^{-1} h^{-1}/ (cm h^{-1}) (for the control), 0.9 μmol l^{-1} h^{-1}/ (cm h^{-1}) (for the treatment with less DOC addition) and 1.18 μmol l^{-1} h^{-1}/ (cm h^{-1}) (for the treatment with the highest addition of DOC).

The DOC measurement indicated a doubling of the DOC in the highest treatment to 1.04 mmol l^{-1} compared to 0.5 mmol l^{-1}, while the DOC in the lower treatment was only slightly higher (0.8 mmol l^{-1} compared to 0.5 mmol l^{-1}, Table 8). DOC again decreased with duration of the experiment. The DOC addition could be seen in a slight reduction in permeability (highest permeability measured in the control and lowest permeability in the highest treatment) and in the C values in the sediment (maximum in the highest treatment and lowest in the control). This shows the addition of DOC to have an effect (as was also observed in the test trial), however the doubling of DOC content did not lead to a significant increase in volumetric oxygen consumption.

Table 8: Sediment parameters for the FTExp 4. Initial and subsequent concentration of DOC/ DN before (03.07.18) and after addition of DOC (10.07, 11.07 and 13.07.18); Permeability carbon values of each core after the experiment (13.07.18).

Sample	DOC/ DN [mmol l^{-1}] 03.07.18	DOC/ DN [mmol l^{-1}] 10.07.18	DOC/ DN [mmol l^{-1}] 11.07.18	DOC/ DN [mmol l^{-1}] 13.07.18	$k*10^{-12}$ m^2 [m^2]	C upper layer [mg g^{-1}]	C lower layer [mg g^{-1}]
C	0.55/ 0.17	0.52/ 0.17	0.52/ 0.17	0.52/ 0.17	27.5	2.17	1.92
Low	0.49/ 0.17	0.8/ 0.21	0.53/ 0.16	0.57/ 0.18	24.5	2.55	2.58
High	0.49/ 0.17	1.04/ 0.22	0.65/ 0.18	0.58/ 0.17	19.8	2.82	2.70

3.4 Macrofauna abundance and respiration in the study area

Macrofauna[2] abundance was sampled on one occasion at 5 stations within the study area. These were the 5 stations with 550 m distance to the shore. The distribution of macrofauna in the study area was quite variable between the stations (Figure 22). In total a number of

[2]Some of the data was published in Schade et al. (2019).

22 different taxa were found. The most abundant taxon was *Mytilus* spp. (max. abundance 6051 ± 4291 ind m^{-2}), followed by *Hydrobiidae* (max. abundance 1412 ± 1663 ind m^{-2}) and *M. arenaria* (max. abundance 265 ± 131 ind m^{-2}). However, while *Mytilus* spp. and *Hydrobiidae* were found at all stations, the distribution pattern of *M. arenaria* differed quite strongly between stations and this species was absent on two of the five stations sampled (Figure 22, Figure 24). *Mytilus* spp. was often found in clumps on the sediment with associated fauna. Regarding all species resulted in rather variable benthic communities, with *Mytilus* spp. being the most abundant species at most stations.

Nevertheless, with regard to the biomass, *Mytilus* spp., *M. arenaria* and *Cerastoderma* spp. covered most of the biomass with >95% at all stations sampled. The analysis of the abundance and biomass data with an NMDS plot (non-multidimensional scaling) showed a high variation at St 3. Regardless of the variation, all stations were rather similar (Figure A.2). Regarding biomass, no difference could be observed between stations (apart from replicates of St 3 being rather variable again). However, a simprof analysis revealed three clusters when analysing all abundance data with replicate 3 and replicate 1 of St 3 being a cluster each and all other replicates clustering together (Figure A.3). Analysing the data for biomass reveals a similar result with replicate 3 at St 3 being different to the rest. In terms of biomass (AFDW), *Mytilus* spp. was the most abundant species (max. 486.9 g m^{-2}), with *M. arenaria* constituting the second most of the biomass (max. 236.7 g m^{-2}). The main constituting polychaetes (as average over all stations) were *H. diversicolor* (max. 0.25 g m^{-2}) and *Marenzelleria* spp. (max. 0.26 g m^{-2}).

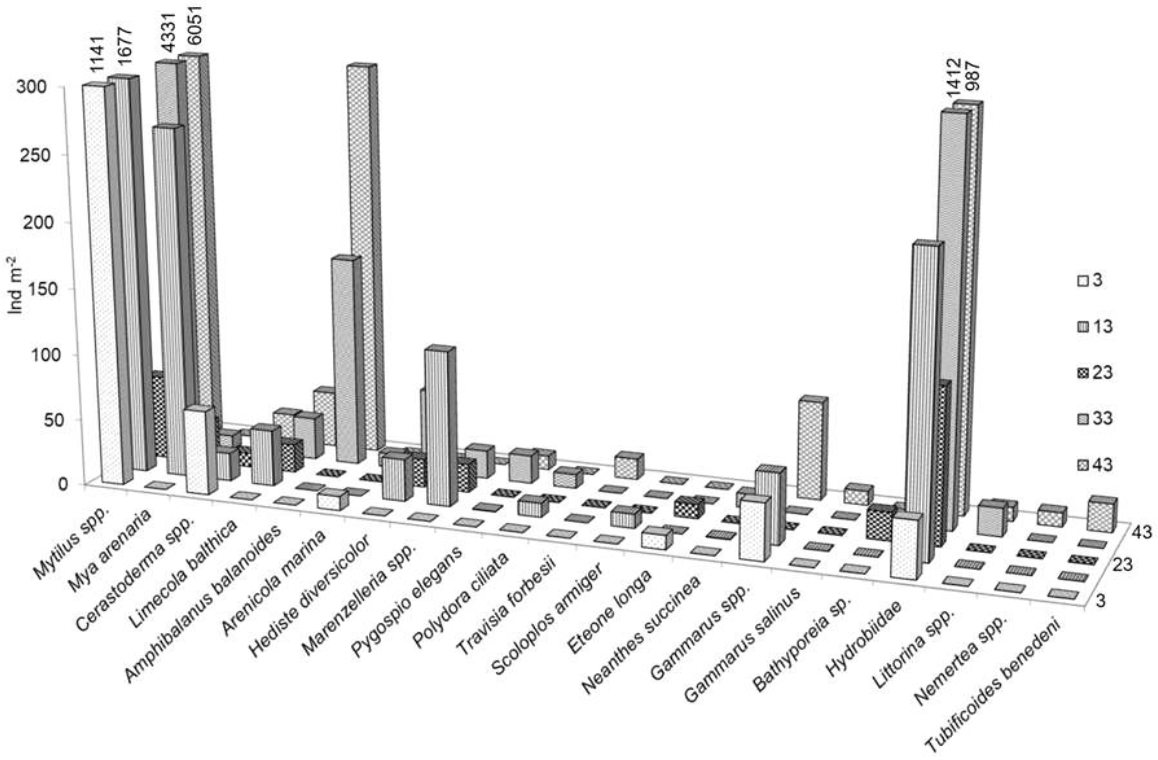

Figure 22: Abundance of macrofauna species at 5 stations in the study area.

To be able to estimate the different shares of total oxygen uptake, we need to be able to calculate the oxygen uptake rate for the different macrofaunal species. Oxygen uptake of some species can be calculated using literature values (e.g. *Marenzelleria* spp. and *H. diversicolor*), while respiration rate for other species has only been defined unsatisfactory (e.g. *M. arenaria*). As *M. arenaria* was the most dominant sediment dwelling species (by biomass), its respiration rate calculation was of some importance for this study.

To estimate the respiration rate of *M. arenaria*, respiration rate was calculated in dependence of individual dry weight (raw data in Table A.8). To estimate the respiration rate depending on shell length, a dependency of individual SFDW of *M. arenaria* on size (x = length [mm]) was calculated for 5°C (Equation 8, $r^2 = 0.972$) and 15°C (Equation 9, $r^2 = 0.991$) separately.

$$\text{SFDW [mg]} = 0.0036x^{3.1079} \tag{8}$$

$$\text{SFDW [mg]} = 0.0029x^{3.1699} \tag{9}$$

SFDW increased with increasing shell length slightly different for the two temperatures. The difference of the weight-length relationship between both temperatures was tested

with an ANCOVA. Neither the slope differed, nor had the temperature an effect (p = 0.58, p = 0.59). Both equations were used nevertheless, as these were the original data and belong to two different experimental treatments.

The dependency of respiration rate on SFDW was shown in Figure 23. The functions were calculated for 5°C (Equation 10, r^2 = 0.772) and 15°C (Equation 11, r^2 = 0.569). Independent of temperature smaller individuals had a higher mass specific respiration rate compared to larger/ heavier ones. The correlation between SFDW and weight-specific respiration rate (rr) was described with a power function for both temperatures (Equation 10 and 11). Bivalves respired significantly more in 15°C compared to 5°C (p = 0.04).

$$\text{rr [mmol d}^{-1}\ \text{g}^{-1}_{\text{SFDW}}\text{]} = 2.2211 * \text{SFDW [mg]}^{-0.729} \tag{10}$$

$$\text{rr [mmol d}^{-1}\ \text{g}^{-1}_{\text{SFDW}}\text{]} = 2.807 * \text{SFDW [mg]}^{-0.55} \tag{11}$$

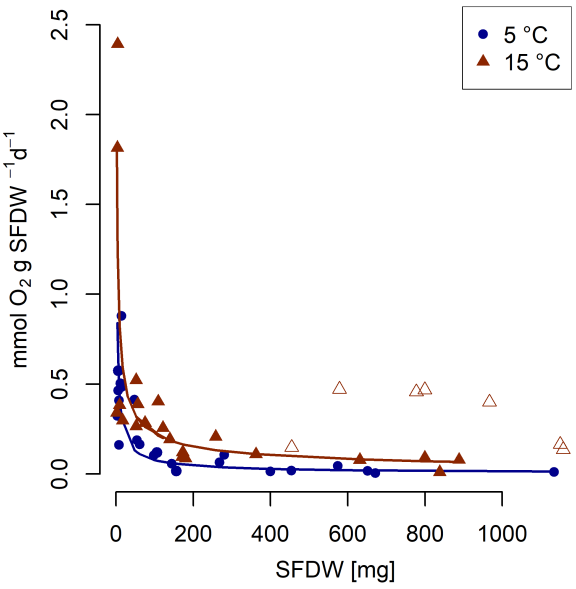

Figure 23: Respiration rate of *M. arenaria* in dependence of SFDW [mg]. Blue points show values for 5°C; red triangles show values for 15°C. Open red triangle show values for 15°C, where O_2 concentration fell below 30%; these values were not used for the respiration rate function. This figure was changed after Schade et al. (2019).

The respiration rate function was then used to calculate the respiration rate of *M. arenaria* within the study area. Respiration was calculated for 15°C, as deployments with the benthic chambers took place in warm water (July and August). The calculated respiration differed strongly between stations (Figure 24). However due to a different size distribution at the stations, the respiration by *M. arenaria* did not necessarily differ in a fixed relation to their abundance. While St 23 had only 12% of the abundance at St 13, the respiration calculated for St 23 was 38% of that calculated for St 13 (1.8 mmol O_2 m^{-2} d^{-1} vs. 4.8 mmol O_2 m^{-2}

d^{-1}). This was due to larger individuals at St 23.

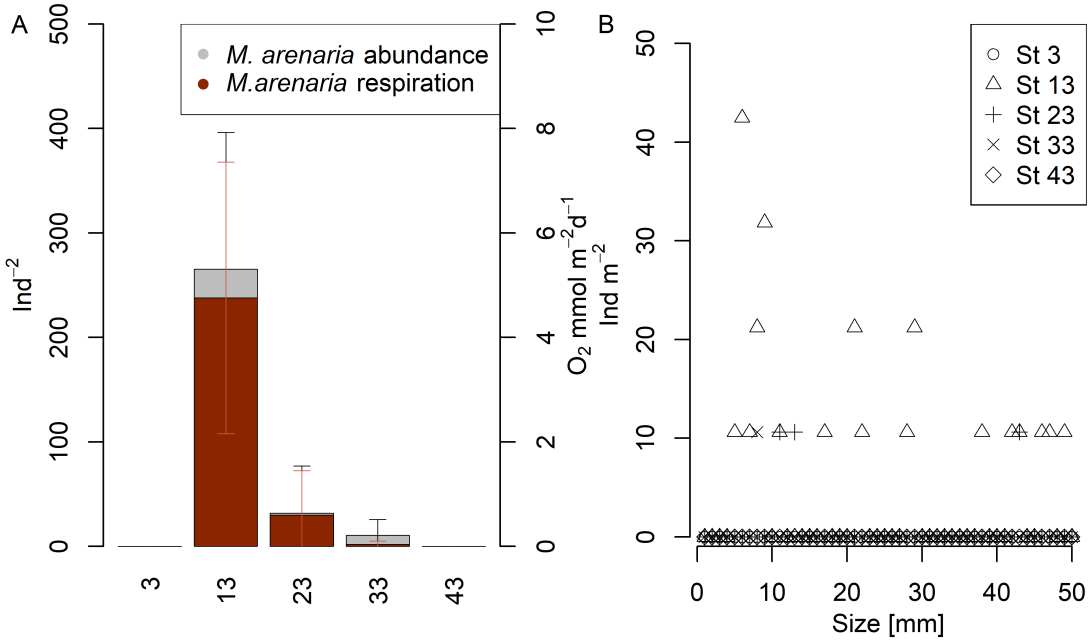

Figure 24: *M. arenaria* abundance, respiration and size distribution. A) Abundance and calculated respiration at 5 stations in the study area. B) Size distribution of *M. arenaria* at 5 stations in the study area.

Respiration could be calculated for *M. arenaria* with the published equation (Schade et al. 2019), while the respiration for the most abundant polychaetes (*Marenzelleria* spp. and *H. diversicolor*) could be calculated with literature data (Kristensen et al. 1985; Braeckman et al. 2010; Renz and Forster 2013). Oxygen uptake for the polychaetes in our calculation was the summed uptake of respiration for the polychaetes itself and the increase in microbial respiration due to building of burrows, while we solely calculated the respiration for *M. arenaria*. The oxygen uptake was calculated for those three species and related to TOU at St 13 and 23 (Figure 25). Both stations differed in macrofaunal abundance and thus the oxygen uptake differed. At St 13, the TOU was 30 mmol O_2 m^{-2} d^{-1} while TOU at St 23 was 14 mmol O_2 m^{-2} d^{-1}. Calculated oxygen uptake due to macrofauna at station 13 was 6 mmol O_2 m^{-2} d^{-1}, while it was 1 mmol O_2 m^{-2} d^{-1} at St 23. Calculated respiration of *M. arenaria* was 4.8 mmol O_2 m^{-2} d^{-1} at St 13 and 0.6 mmol O_2 m^{-2} d^{-1} at St 23. *Marenzelleria* spp. and *H. diversicolor* were calculated to have an oxygen uptake of 0.8/ 0.3 mmol O_2 m^{-2} d^{-1} at St 13 and 0.03/ 0.07 mmol O_2 m^{-2} d^{-1} at St 23.

The calculated change in TOU due to the macrofauna can thus not solely explain the difference between both stations.

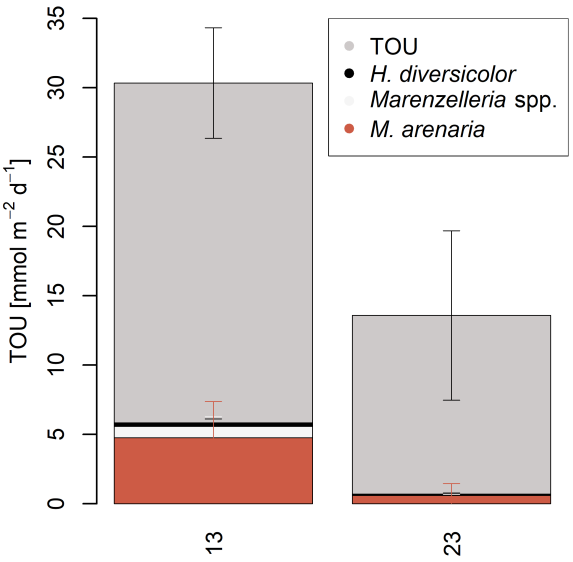

Figure 25: TOU compared to respiratory contribution by different fauna at St 13 and 23.

4 Discussion

4.1 Evaluation of methods

In situ measurements are always subject to stronger uncertainties compared to laboratory investigations. According to the calculated error propagation by Gauss, all values measured in our in situ incubations were subject to 35% variability. For an assumed oxygen uptake of 20 mmol O_2 m^{-2} d^{-1} this corresponds to an uncertainty of 7 mmol O_2 m^{-2} d^{-1}. The measured variability between replicates in the field can nevertheless be even higher within one station.

We applied different methods to improve the accuracy of our in situ measurements. One uncertainty which had to be considered was the enclosed volume of water in the chamber. We measured sediment surface to chamber lid distance at 3 spots and calculated the enclosed chamber volume. With an uncertainty of 0.5 cm in the distance determination, the variation for the volume calculation was 2.5%. One option to improve this variability was tested during our incubations.

The addition of bromide as a non-bioactive tracer is an additional method used in the field (Forster et al. 1999; Tengberg et al. 1995) for different purposes. One purpose is the volume determination within the chambers. In our field experiments a defined concentration of bromide was added to each chamber. Due to the then measured diluted concentration in the overlying water in the closed chamber, an enclosed water volume was calculated. However, the volume calculated based on bromide concentrations did not show less variation compared to volumes determined from the sediment surface-lid distance (see also Andersson et al. 2006). Volume in the core was thus calculated due to sediment-surface-lid distance and volume calculation due to bromide concentration was discarded.

An additional purpose of bromide addition should have been its use as a tracer indicating water penetration depth into the sediment. Measured bromide profiles in the sediment, or alternatively the loss of bromide from the chamber water and a calculated transport of bromide into the pore spaces, can give insight into the water penetration depth due to advection or diffusion in the in situ chambers (Tengberg et al. 1995). Transport of bromide into the pore spaces could be calculated based on the loss of bromide in the overlaying water from start to end of each chamber incubation. The calculated bromide transportation reached down to a sediment depth of 10 – 30 cm. The calculated transportation depths were higher in the advective treatment compared to the diffusive treatment if regarding the average for each treatment. However, the variation between the replicates was very high and the transportation depth for the advection treatment was not always higher compared to the diffusion treatment when considering single replicates. Thus the calculated transportation into the pore spaces did not show any reliable difference between advection and diffusion treatments.

Bromide profiles in the sediment as a measure of the transportation depth should alternatively be directly measurable in sediment cores. However, bromide profiles were often lost due to different reasons. To sample bromide profiles, subcores with prepared holes for porewater sampling had to be taken from each chamber. Before taking the subcores, the lids of the chambers had to be opened resulting in the loss of bromide in the overlaying water. Bromide concentration in the overlaying water was thus reduced to background bromide values. Subcores had to be taken to the ship before porewater sampling could take place. As a results bromide concentrations in the sediment were then often equilibrated to background concentration by the time of sampling on the ship. In conclusion the time between sampling from the core and sampling of the porewater profile was too long. Some bromide profiles had no low values indicating dilution with background values and thus seemed to be reliable. Nevertheless they showed inconsistent results and no consistent difference between diffusion or advection treatment. In addition profiles could only be measured until a max. sediment depth of 12 cm which was much less than the calculated transportation depths of up to 30 cm.

The use of bromide is generally known as a good method to estimate the penetration depths for finer grained sediments (Forster et al. 1999). When sampling at stations with such a long transportation time as in our study a different chamber would need to be designed from where direct bromide porewater samples could be taken (instead of having to open the lid). Alternatively sampling of the complete chamber with overlaying water would probably lead to more reliable bromide values. Unfortunately with the size of the chamber in use, it is impossible to sample the whole chamber with divers without disturbing the porewater.

Bromide did thus not lead to reliable values for transportation depths with none of the tested methods. It was thus rejected for the analysis as non-reliable method and not included into the results.

TOU in situ was measured with the Winkler titration method for St 23 and 41, while an additional system (a continuous measurement with oxygen sensors) was applied at St 13. Daily oxygen production calculated with the Winkler method could be compared to the continuous measurement (every 5 minutes) at St 13. Both methods resulted in similar rates if calculated with one average start and one average end value and the change in concentration over time (Winkler: 35 mmol O_2 m^{-2} d^{-1}; oxygen sensors: 34 mmol O_2 m^{-2} d^{-1}). Calculating the production via a start and an end value assumes a linear increase in oxygen concentration in the chamber. The additional continuous measurement at St 13 shows a slope from which oxygen production could be calculated. The continuous measurement showed the slope not to be linear during the day but to slowly increase from the moment the dark cover was removed. Calculating the production rate from the steepest slope measured during the day led to higher production rates (45 mmol O_2 m^{-2} d^{-1}) compared to production rates calculated with the Winkler method. The calculated production was 1.4 times higher

if calculated with the steepest slope during the day. As light was strongest when the sun was highest and weaker during evening and morning it is quite realistic for the production rates to be generally lower in the morning and the evening and higher during noon (where we found the steepest slope). Nevertheless, the higher production rate calculated with the steepest slope would disregard the slowly increasing/ decreasing production rates at start and end of the day. We assumed the Winkler titration rates to be quite reliable as the slope assumed one average daily production. Oxygen production rates calculated with the steepest slope would possibly overestimate production rates.

TOU during the night was similar for both measurements, as the slope did not change during the night (Winkler: 33 mmol O_2 m^{-2} d^{-1}; Hach Lange: 34.6 mmol O_2 m^{-2} d^{-1}). This was in agreement with the lack of strongly rate-changing processes, such as light-dependant photosynthesis during night.

Generally shallow sediments in the Baltic Sea are quite poor in organic content (Premuzic et al. 1982). Assuming a C:N ratio of ~6.6 (or often 7.5 - 10 as found by Lipka et al. (2018)) N values would be rather low if the C values are low (for example assuming a Redfield Ratio of 6.6; the N content would be 0.15 mg g^{-1} for a C content of 1 mg g^{-1}). N contents in the sediments would thus be expected to be even below detection limits. In the analysis of sediment C and N contents, we thus aimed at measuring larger volumes of sediment to obtain higher signals which were then above detection limit. Most carbon and nitrogen was expected to adsorb on the fine particles (Rusch et al. 2000). Separating the fine sediment, filtering it onto a GFC filter and measuring the filter, was thus a reliable method to analyse larger volumes of sediments. In contrast to pure sediment, N values were always above detection limits, when being measured in the filter. All values were then related to the original sediment weight. N content measured on the filter (example St 45; 0.31 mg g^{-1}) was higher compared to N content measured in pure sediment (example St 45; 0.05 mg g^{-1}), but was considered to be more reliable. C and N content of the field samples was thus always analysed on a filter.

4.2 Oxygen uptake rates and affecting processes

One of the main objectives of this study was to investigate the oxygen uptake rate of sediments and the influence of different processes on this parameter (Objective 2). These processes could then be related to the investigation of the field parameters (discussed in section 4.3) which is why another main aim was to investigate the sediments, its properties and the currents within study area (Objective 1).

Oxygen uptake of sandy sediments is influenced by several processes and parameters (e.g. permeability, currents, advective flow, organic content, and activity of macrofauna community). These processes and parameters interact in the field. When measuring TOU in the

field, some processes could be separated (e.g. advection and diffusion) but all other parameters and processes would interact resulting in one TOU measurement. For this reason processes/ parameters in our study were investigated ex situ and separately in situ as an integrated TOU signal. Ex situ, parameters can be simplified (e.g. excluding macrofauna from the sediment) and thus the influence of different parameters can be analysed separately.

Lab measurements

Oxygen uptake rates for different processes and under different conditions were studied in the laboratory for sediments without macrofauna or with a known abundance of macrofauna. For this purpose coarse and fine sediment was incubated in cores. The permeability for these two sediment types was above the defined threshold of $\sim 2.5 * 10^{-12}$ m^2 and both sediment types were assumed to be permeable. Coarse sediments showed low oxygen uptake rates (3.2 ± 1.9 mmol O_2 m^{-2} d^{-1}) and high oxygen penetration depths of 10 - 15 mm (<15 mm for most parts in the chamber, >15 mm on the outer radius of the chamber). These sediments showed no change in oxygen uptake rates, but rather increasing oxygen penetration depths with increased differential pressure. In these sediments the organic carbon content was low and as microbial activity is dependent on labile organic carbon, no increased metabolic activity could be observed with increased oxygen penetration depth.

The oxygen penetration depth of <8 mm in the fine grained sediment was considerably lower compared to the coarser grained sediment. Neither penetration depth nor oxygen uptake increased with increasing differential pressure. The oxygen penetration depth in the fine grained sediment did not change, thus the sediment was clearly not subject to advective processes. The original assumption of both sediments (fine and coarse) to be permeable and possibly subject to advective influence had to be rejected. These results can be compared to a study by Forster et al. (1996). In their study flow had an impact on the oxygen uptake rate of coarse sand (permeability $5 * 10^{-11}$ m^2), while no impact could be seen on the fine grained sediment (permeability $5 * 10^{-12}$ m^2). In the coarse sand an increase in flow rate from 3 to 14 cm s^{-1} increased the oxygen uptake by 91%. Even though the less permeable sediment was thought to be permeable in both studies (our study and the study by Forster et al. (1996)), no impact on oxygen uptake could be detected and the permeability threshold seemingly has to be debated.

Regarding results of our study, we would suggest to increase the permeability threshold to at least $0.75 * 10^{-12}$ m^2. This threshold will be reconsidered with the results from the lab and the in situ explorations. Extrapolations of oxygen uptake rates for field systems always require the assumption of a certain threshold. Therefore the consequences of a change in threshold and its effects on the assumptions for the study area will be discussed below when discussing the parameters measured in the study area.

Field measurements - oxygen

Laboratory results may generally be more suitable to analyse as there are fewer variables. In situ measurements are nevertheless important to gain natural estimates about TOU in the area.

TOU in the field ranged between -10 mmol O_2 m^{-2} d^{-1} (St 41) and -33 mmol O_2 m^{-2} d^{-1} (St 13) for the stations measured in situ. A change in TOU due to advection could only be observed at St 41, while there was no difference between the treatments at St 13 and St 23.

TOU measured can be compared to published literature oxygen uptake rates. Literature values differ as they applied different methods and were conducted in different areas and seasons. Most published oxygen uptake rates vary between 3 and 30 mmol O_2 m^{-2} d^{-1} (Table 9). Nevertheless the magnitude found in most studies was in a similar range. Regarding studies conducted in the Baltic Sea the variation was quite high ranging from 4 to 36 mmol O_2 m^{-2} d^{-1} (Nilsson et al. 2019, Powilleit, unpubl data). This variation however can also be found in other areas like the North Sea (1 to 37 mmol O_2 m^{-2} d^{-1} in different studies, including stationary and seasonal effects, Table 9). Even within one station the TOU can have a similar extent as the extent in the whole Baltic Sea. For example measurements at one station show TOU to range from 5 mmol O_2 m^{-2} d^{-1} in Feb to 36 mmol O_2 m^{-2} d^{-1} in Sep (Table 9; Powilleit et al unpubl) solely due to seasonal influence. However, rates assessed in our study range within published rates for the Baltic Sea.

One study which was similar to our study was conducted by Janssen et al. (2005a). Their study was conducted as an in situ lander (”Sandy”) study in the North Sea (3 stations; permeabilities of 0.3, 2.6 and $7.5*10^{-11}$ m^2). Sediment parameters were similar to our study area with grain sizes of 160 – 672 µm and TOC content of 0.03 – 0.2% DW. The TOU was also in a similar range (17 - 37 mmol O_2 m^{-2} d^{-1}). The authors found similar increases in oxygen uptake rates with advective influence as found in our area. Comparable to our results they did not find an increase in oxygen uptake rate with advection at their finest station but the highest increase in oxygen uptake rate at the coarsest station with the highest permeability.

It becomes clear that TOU within one relatively small area can vary as much as TOU within a whole sea (e.g. the North Sea or the Baltic Sea). It is obvious from our results and other studies (Table 9), that TOU can be increased with advective influence in some cases, while in other cases no increase was visible despite experimental pressure gradients applied. Increased rates with advective influence could be observed for most studies for sites where permeability was $>2*10^{-11}$ m^2. Sites with a permeability of $5*10^{-12}$ m^2 or less (Forster et al. 1996; Janssen et al. 2005b, our study St 13) showed no increased rates with advective influence, even though sediments with a permeability $>2.5*10^{-12}$ m^2 were assumed to be possibly affected by advective processes in previous studies (Glud et al. 1996; Forster et al.

2003).

A more detailed view on studies on advective influence shows a need to differentiate the advective influence on TOU from a general advective influence on porewater transport. The permeability threshold of $2.5*10^{-12}$ m^2 was based on studies using a dye or bromide as a tracer (Huettel and Gust 1992a; Forster et al. 1996; Glud et al. 1996). The transport of the non-reactive tracer may be sufficient to show the occurence of advective porewater intrusion, but seemingly no sufficient indicator for the influence on oxygen uptake in particular. This is exemplified by the study of Forster et al. (1996), where little dye penetration was observed in the low permeability treatment ($5*10^{-12}$ m^2), while there was no observed change in oxygen uptake with this advective influence.

Oxygen uptake can always be influenced by the available carbon and nitrogen at each station. C and N content within the sediment were highest at St 41 with values being ~1.5 times higher compared to St 13 and 23 if regarding only the top centimetre (Table 4). C and N content was sampled in centimetre steps at St 13 and 41 and the average over the top centimetre would suggest values at St 41 to be ~three times higher than C content at St 23. Taking each centimetre step into account however, it is obvious that C values were increasing continuously with depth at St 41 (2.9 mg g^{-1} for 0-1 cm depth – 9.1 mg g^{-1} for 9-10 cm depth, 3) while they were constant at St 23. N content was constantly ~twice as high at St 41 compared to St 23. Averaging the content over the whole sediment depth would clearly overestimate the difference between the stations and the C and N values. Nevertheless the station with highest k (St 41) and the highest C and N content for bacterial processes was the only station investigated in our work showing an increase in oxygen consumption rate with advective influence.

Field measurements - Nutrients

Oxygen fluxes differed between stations and so did nutrient fluxes. Nutrient fluxes were highest at St 13. Looking at concentrations of nutrients within the porewater, St 41 had the lowest porewater concentrations for ammonium, silicate and phosphate. However, at a comparably low level St 13, 23 and 41 were within the range of concentrations found at a sandy station in close proximity (Lipka et al. 2018). Looking at the N:P ratio of porewater nutrients, we conclude preferential N removal at St 23 and St 41 as N:P ratios were <7 for both stations (measured in the water column or porewater profiles). St 13 was different to the other two stations as, regarding the water column, the ratio was >16 for all values ($\overline{x}$ 20). The ratio in the porewater at St 13 was nevertheless more similar to St 23 and St 41 with N:P ratios <14. Generally we argue high amounts of nitrogen being processed at St 13 as the ratio of N:P changes from the water column to the sediment. Higher fluxes could be possible at St 13 as the N:P ratio was on average higher compared to St 23 and 41. As

Table 9: Benthic oxygen uptake in selected studies. Values of our study were multiplied by -1 to adjust them to published values. The values are separated in in situ benthic chamber or lander deployments (upper values) and values achieved with other methods (lower values).

Publication	Location	k $*10^{-11}$ m^2]	Median Grain size [µm]	Porosity	TOC [% DW]	advective TOU [mmol O_2 m^{-2} d^{-1}]	non-advective TOU [mmol O_2 m^{-2} d^{-1}]
(Janssen et al. 2005a)	North Sea	0.3	163	0.3	0.1	29.2 ± 12.2	28.8 ± 12
(Janssen et al. 2005a)	North Sea	2.63	299	0.3	0.2	37.3 ± 28.5	26.1 ± 81.3
(Janssen et al. 2005a)	North Sea	7.46	672	0.3	0.03	27.7 ± 11.5	17.0 ± 12.8
(Forster et al. 1996)	North Sea	0.5	130	0.4	1.2		30 ± 1.5
(Forster et al. 1996)	Mediterranean Sea	5	270	0.4	0.8	15.5 – 26.7	10 ± 1.5
(Gihring et al. 2010)	Gulf of Mexico	2 - 4.6		0.4	0.1 - 0.6	11.5 ± 0.4	6 ± 1.1
Finke, Bachelor thesis	Baltic Sea		287	0.4	0.3	12.9 ± 0.9	6.4 ± 1.07
Langenwerder 1*	Baltic Sea	0.75	217		0.17		30.6 ± 2.6
Langenwerder 2*	Baltic Sea	0.75	182		0.17		16 ± 3.6
Warnemünde*	Baltic Sea	2.4	300		0.0 - 0.1		3.2 ± 1.9
St 13*	Baltic Sea	0.64	166	0.4	0.1	27.9 ± 5.4	33 ± 3
St 23*	Baltic Sea	1.59	213	0.4	0.1	12.6 ± 1.7	14.6 ± 10.3
St 41*	Baltic Sea	3.75	543	0.3	0.4	21.4 ± 9.2	10.4 ± 4.4
(Fuchsman et al. 2015)	Oregon Shelf						4.3 - 12.5
(Nilsson et al. 2019)	Baltic Sea				0.1 - 6 (POC)		4.25 - 32.8
(McGinnis et al. 2014)	North Sea	0.66		0.43		7	
(McCann-Grosvenor et al. 2014)	Oregon Shelf	1.3 - 4.7			0.1 - 0.4	<30	10
(Devol and Christensen 1993)	Washington Shelf			0.6-0.8			5 - 18
(Reimers et al. 2012)	Oregon Shelf	1.74 - 17.6			0.2 - 0.3		3.2 - 9.8
(Berg et al. 2013)	Estuary, Cape Cod	1.8					29.3 ± 2.8
(Rusch et al. 2006)	Mid Atlantic Shelf Deposits	1	400 - 500	0.37	0.02 - 0.03	40 - 90	15 - 20
(Powilleit, unpubl. data)	Seekanal, Baltic Sea		238		0.1 - 0.2		4.7 - 36.3 (ø 10.5)
(Lipka et al. 2018)	Baltic Sea	0.42		0.4	0.3		3.8 ± 1.7
(Ahmerkamp et al. 2017)	North Sea	<0.1	102-155	0.5	0.15 - 0.4		1-3
(Ahmerkamp et al. 2017)	North Sea	3.1 - 21	207-537	0.4 - 0.5	0.03 - 0.3	8 - 34	

a general finding, St 13 has the highest porewater content of nutrients and was thus seemingly the station with the lowest flushing rate. Combining the porewater content at St 41 and the C and N contents found at this station, we assume St 41 to have the highest flushing rates.

As there were no measurements of microbial or phytoplankton community activities, and no measurement of the oxygen penetration depths within the cores, the reasons for nutrient fluxes remain speculative. Ammonium flux was highest at St 13 and quite low at St 23. At St 41 the ammonium flux differed for the advection and the diffusion treatment. Additionally the ammonium flux seemed to differ between day and night fluxes at St 13 and 41. Ammonium fluxes in our study were mostly negative and directed into the sediment. A release of ammonium was only found for daily fluxes at St 13. Contrarily Janssen et al. (2005a) found a release of ammonium between 1.89 (fine sediment) and 0.04 mmol O_2 m^{-2} d^{-1} (medium sediment) during the night. The nitrogen cycle is comparably complex and there are a few possibilities of flux explanations. As ammonium fluxes differed between day and night in our sediment, most explanations fail. However, there are many processes which might explain at least part of the fluxes. Janssen et al. (2005a) argue their higher release at the station with fine sediment to be due to reduced oxygen penetration depth and thus lower nitrification rates. At St 41 the potentially higher oxygen penetration in the sediment in the advection treatment could have led to higher nitrification of ammonium to nitrate. The ammonium, which is possibly produced in the sediment would not be measured as it would directly be nitrified due to the advective flushing of oxygen into the sediment. Reasons for the negative ammonium flux into the sediment could be the occurrence of heterotrophic phytoplankton taking up nitrogen. Also in anaerobic sediments as for example at St 13, the loss of ammonium could be due to anammox (anaerobic ammonium oxidation) or denitrification, thus the conversion of ammonium to N_2. This would however, not explain the positive daily ammonium flux at St 13. The reversal of fluxes at St 13 could possibly be due to strong ammonium production rates in surface sediments and reduced possibility for denitrification/ anammox which then led to intense day remineralisation close to the sediment surface. A generally higher ammonium flux at St 13 could be due to the high N:P ratio at St 13.

The ammonium flux could additionally be influenced by the presence of bioturbators. Generally, the bacterial abundance and activity can be 10-fold higher in the macrofaunal burrow wall (Bird et al. 2000; Papaspyrou et al. 2005), ammonium production can be increased with higher abundance of macrofauna. Oxygen and ammonium concentrations are higher in macrofaunal burrow walls affecting microbial processes (Laverock et al. 2011). Unfortunately we do not know the biomass of the macrofauna within the cores which were analysed for in situ fluxes. From the background investigation we know the abundance of bioturbators to be ~5-times higher at St 13 compared to St 23, which could explain generally

higher fluxes at St 13 also for ammonia. One macrofaunal species with the highest abundance at St 13 was *Marenzelleria* spp. One explanation for a different ammonium flux during day and night cycles could be a daily activity cycle, which was observed for *Marenzelleria* spp. by Winkler and Debus (Winkler and Debus 1996). However, in their study *Marenzelleria* spp. was active during night hours and during day hours only found below 15 cm sediment depth. This behaviour would contradict the fluxes found at St 13. So even though a day and night migration pattern might be an explanation for fluxes at St 13, the exact cause-effect relation remains a speculation.

Silicate fluxes were highest at St 13, which was the station with the finest sediment. Silicate fluxes were directed into the sediment at St 13 and 41, while they were positive at St 23. Janssen et al. (2005a) only observed stronger silicate fluxes than fluxes measured in our study (1.22 – 2.54 mmol O_2 m^{-2} d^{-1}). Fluxes found in their study were strongest at the fine station which agrees with the strongest flux in our study found at St 13. In contrast to our study however, fluxes observed in the study by Janssen et al. (2005a) were always directed into the water column. One possible reason for the strong negative flux at St 13 could be high biomasses of diatoms taking up silicate for shell growth.

Phosphate fluxes in our study were as average up to twice as high and exclusively into the sediment in contradiction to fluxes observed by Janssen et al. (2005a) (phosphate flux <0.08 mmol O_2 m^{-2} d^{-1}). Unfortunately most explanations also fail. Nevertheless approx. one quarter of the phosphate concentration measured as background value in the study area was taken up during the day. Generally we cannot explain the different nutrient fluxes measured at the different stations but at least the order of magnitude of the nutrient fluxes seemed to be realistic and within the range observed in other sands.

Porewater profiles and nutrient fluxes calculated from in the overlaying water were assessed at the same station, but porewater samples were taken from cores next to benthic chambers, not from the chambers itself. Therefore a direct comparison of the nutrient fluxes to the porewater profiles or a calculation of diffusive fluxes from porewater profiles was not applicable. Regardlessly, porewater profiles at all stations suggest a release from the sediment into the water column. In contrast to the porewater profiles, nutrient fluxes in the overlaying water were mostly observed as fluxes directed into the sediment. One possible reason would be a sink at the sediment water interface. Sinks could be a consumption by organisms as e.g. diatoms taking up silica or algae taking up ammonium (Wilhelm et al. 2006). All fluxes measured by Janssen et al. (2005a) rather correspond to our measured porewater profiles.

Field measurements - implications

Investigations from the field calculate TOU in published literature mostly as rates per 24h (d^{-1}) (Janssen et al. 2005a; Reimers et al. 2012; Fuchsman et al. 2015). We calculated TOU as daily TOU too, but we recalculated TOU as separate day and night TOU in order to be able to estimate net TOU on a daily basis (Figure 26). Obviously these rates can only account for the rates at their measurement dates and would be different for other periods during the year.

Oxygen uptake/ production was calculated dependent on day and night periods at the specific date or during that period of the year. In 2017 we estimated a night period of 9 h and a day period of 15 h, while we estimated 10 and 14 h for 2018 (assumption based on sunset and sunrise). Oxygen uptake/ production calculated accordingly can give further insight into a net TOU. At St 13 and 23 no difference between the diffusive and the advective treatment could be proven. Consequently, one average daily oxygen production rate (12.3 mmol m^{-2} ± 9.8 at St 13 and 1.4 mmol m^{-2} ± 4.7 at St 23) and one average oxygen uptake rate during the night (-12.7 mmol m^{-2} ± 1.7 at St 13 and 5.1 mmol m^{-2} ± 2.3 at St 23) was determined. The resulting net oxygen uptake for a 24h day was -0.4 mmol O_2 m^{-2} d^{-1} at St 13 and -3.7 mmol O_2 m^{-2} d^{-1} at St 23. St 41 was the only station showing a difference between the advection and the diffusion treatment and thus oxygen uptake and production rates and also the resulting net TOU was calculated separately. Daily oxygen production at St 41 was 7.2 mmol m^{-2} ± 14.4 for the advective treatment and 13.9 mmol m^{-2} ± 5.5 for the diffusive treatment. Night oxygen uptake was -8 mmol m^{-2} ± 2.8 for the advective treatment and -3.9 mmol m^{-2} ± 1.1 for the diffusive treatment. This resulted in a net TOU of -0.8 mmol O_2 m^{-2} d^{-1} for the advective treatment and 10 mmol O_2 m^{-2} d^{-1} for the diffusive treatment. In a general assumption (explained in Chapter 1, Figure 1) O_2 produced during the day would be transported relatively deep into the sediment in the advection treatment, while it would only diffuse a few mm into the sediment in the diffusion treatment. This assumed general trend was found for St 41 and resulted in a slightly heterotrophic system in the advection treatment compared to a more autotrophic system in the diffusion treatment. This observed trend might change with season as photosynthesis is light dependent. The system would possibly be more autotrophic with longer lasting light periods, while it would even be more heterotrophic for shorter light days. This trend was not observed at St 13 and 23 as there was no observable difference between diffusive and advective conditions during the night, possibly due to the lower permeability at those two stations. Nevertheless, pronounced differences at those two stations were observed during the day. These differences may be accounted for by spatial differences in microphtobenthos distribution. Advective and diffusive treatments had to be placed on different locations. The colonization with diatoms was probably very heterogeneous leading to locally strong difference in daily production rates.

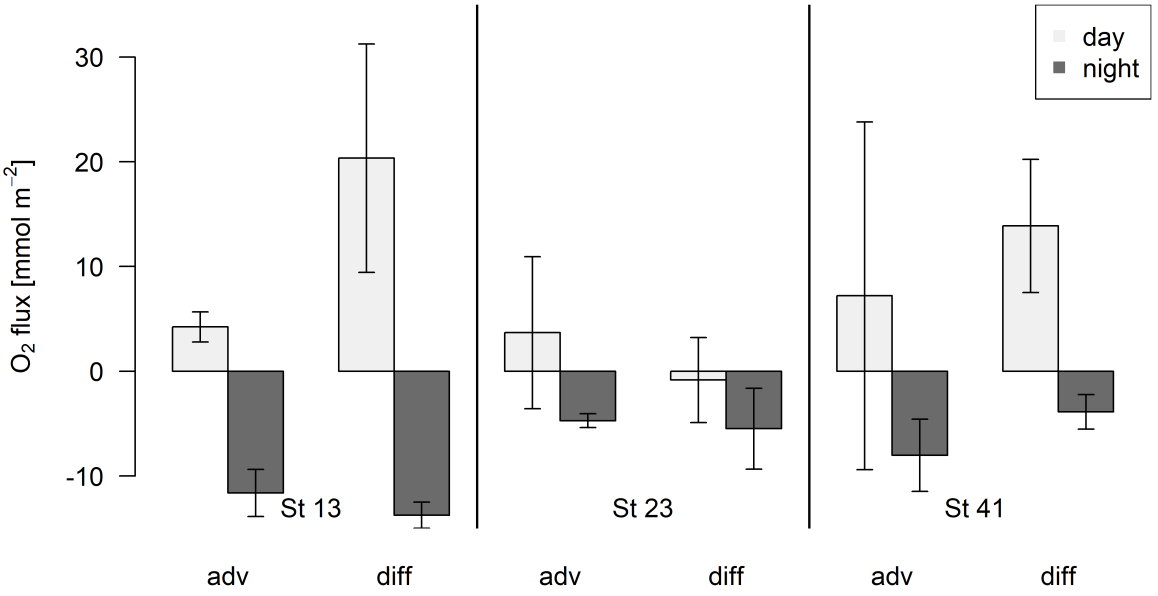

Figure 26: Oxygen uptake at St 13, 23 and 41. Night respiration rates were calculated with a 9 h night period (10 h in 2018) and day production rates were calculated with a 15 h day period (14 h in 2018).

TOU generally relies on the source of carbon. The net TOU may be compared to the carbon stock available in the sediment. We recalculated oxygen uptake/ production as carbon units to estimate the daily net carbon balance at our field stations (Table 10). Carbon units [mg m^{-2}] were calculated by assuming an oxygen to carbon utilization ratio of one. The net carbon balance was then estimated based on the day and night carbon production/ uptake. The calculated carbon units and the resulting net carbon balance was calculated separately for day and night at St 13 and 23, independent of advective and diffusive condition, while we differentiated between the advective and diffusive conditions at St 41. During the day carbon was fixed, while we determined a carbon liberation during night (Table 10). The net carbon balance resulted in a negative balance for St 13, 23 and the advection treatment at St 41, while there was a net carbon gain for the diffusion treatment at St 41.

Comparing the calculated carbon balance to the carbon stored in the sediment (organic carbon measured during the sampling (Table 4), assuming all organic carbon to be labile organic carbon) one can estimate the time it would take until the stored carbon stock is depleted (residence time). For this, the carbon stock was divided by the net carbon balance per station. Carbon balance varied extensively between the stations and also between the different treatments.

The residence time of carbon differed accordingly between the stations. St 13 had a residence time of 473 days compared to 52 days at St 23. At St 41 the carbon balance during the advection treatment was low and the calculated residence time was 604 days, while the carbon balance at the diffusive treatment suggested a net supply of carbon. Except for the diffusive treatment at St 41, we calculated the system to be heterotrophic depending on the supply of organic carbon as nutritious source.

The carbon production during the day usually supplied much carbon (St 13 and 41), so that the net carbon balance was only slightly negative. St 23 is an example station where the supply of carbon during the day was rather low and the net carbon balance was strongly negative. St 23 was thus strongly heterotrophic and would be dependent on external carbon supply already after 1 1/2 month. Results shown here were measured in summer where the light period was long and thus the production during the day was high. The carbon production during the day would be lower during shorter light days and the system would depend on external sources if production during the day decreased during shorter light periods.

Table 10: Carbon production/ uptake for a separate day/ night cycle. Calculated according to day and night periods during sampling time. Rates were calculated as net carbon balance for a daily cycle (24 h) for each station and each treatment using TOU and C units [mg m^{-2}].

Station	Cycle	C production [mg m^{-2}]; Day	C uptake [mg m^{-2}]; Night	Net C balance [mg m^{-2} d^{-1}]
St 13	adv. and diff.	147.5 ± 117	-152.1 ± 20	-4.6
St 23	adv. and diff.	17.1 ± 56.8	-61.1 ± 27.5	-44
St 41	advective	86.5 ± 172.4	-96.2 ± 33.8	-9.8
St 41	diffusive	166.5 ± 66.1	-46.6 ± 16.1	119.9

Without hydrodynamic forcing, no advective flow effects would take place. The benthic chambers only mimic hydrodynamic forcing interacting with ripples by inducing a pressure gradient. Values available from the calibration of the benthic chamber were differential pressures. To estimate a velocity in the field that would roughly generate equivalent dp as applied in the chamber, we referred to a publication by Huettel and Gust (1992b). Huettel and Gust (1992b) measured differential pressure [Pa cm^{-1}] for applied friction velocities at different ripple heights. Thus, we can estimate a friction velocity for a specific ripple height and differential pressure (dp) [Pa cm^{-1}] from their data. Therefore, parameters needed were ripple height and differential pressure. Ripples in the field were 1.96 cm ± 0.24 cm (n = 5) measured on one occasion (24^{th} of July 2018). The measured ripple heights were comparable to ripple heights measured in the Pomeranian Bay (1.7 cm ± 0.25 cm (n = 6), Forster unpublished data). The applied dp during the field deployments was 0.5 Pa cm^{-1}. From Huettel and Gust (1992b) we estimated a friction velocity of 0.4 cm s^{-1} to yield in a differential pressure of 0.5 Pa cm^{-1} for ripples of 2 cm height. The assumption of a conversion factor of ~11 (Precht and Huettel 2003b) for the proportion of friction velocity to current velocity resulted in a calculated current velocity of ~4.4 cm s^{-1}. This is the equivalent velocity in the field leading to the applied dp with the benthic chamber. This calculation was a rough estimate as the real friction coefficient is unknown for the chambers and ripples in the field were not uniform (as mimicked by the benthic chamber). The current velocity of ~4.4 cm s^{-1} mimicked during our in situ chamber experiments ranged on the lower end of current

velocities measured in the field (Figure 12).

The differential pressure in the field was variable depending on ripple height, ripple distance and current velocity. Ripple distance represented with the chamber would had a distance of ~17 cm (r of the chamber 8.5 cm). This distance was quite comparable to ripples measured in the field with a distance of 14.7 cm ± 2.6 cm (as measured on 24^{th} of July 2018). Ripples predicted by Wiberg (Wiberg and Harris 1994) were roughly 1 - 1.5 cm of height with a spacing of ~10 cm at a median grain size of 200 µm in the Oregon area, thus smaller and closer together than ripples measured in our area. Generally length and height of bed forms (also ripples) was supposed to be mainly a function of grain size (Yalin 1985) and we would thus assume ripple form to stay within narrow limits and only change slightly with velocity. The mimicked current velocity would be within the range of the typical velocities occurring in the study area.

Porewater flow

While the differential pressure changed the oxygen distribution in permeable sediments, the flow rate at which porewater flows through the sediment could have an additional effect (Ahmerkamp et al. 2017). Different sediment types were tested with increasing flow rates. While in one experimental set-up no indication for a flow effect was found (Figure 21.A), all other treatments showed an increase in volumetric oxygen consumption rates with increased flow rate. Slopes varied between treatments. Slopes of treatments showing an effect of flow rate on volumetric oxygen consumption varied basically from 0.6 to 0.7 µmol l^{-1} h^{-1}/ (cm h^{-1}). These are considerably lower compared to slopes varying from 0.9 – 1.4 µmol l^{-1} h^{-1}/ (cm h^{-1}) found by Ahmerkamp et al. (2017). Adding nutrition (glucose or DOC) changed the volumetric oxygen consumption rates enormously. An increase of the volumetric consumption rates was not observed in all treatments, but it was obvious when adding glucose and when doubling the DOC. The slopes varied after the addition of nutrition between 0.5 µmol l^{-1} h^{-1}/ (cm h^{-1}) and 3.2 µmol l^{-1} h^{-1}/ (cm h^{-1}) for the addition of glucose and between 0.8 µmol l^{-1} h^{-1}/ (cm h^{-1}) and 1.2 µmol l^{-1} h^{-1}/ (cm h^{-1}) for the addition of DOC. The response to the increased DOC concentrations was very sensible to type and amount of the added DOC. The slopes resulting from the DOC addition, (the more natural treatment) were quite similar to slopes found by Ahmerkamp et al. (2017). Added concentration of high DOC were only half as high as high concentrations found in the field (1.04 mmol l^{-1} compared to 2.18 mmol l^{-1}, Westphal, unpubl. data). The background DOC concentrations (0.5 mmol l^{-1}), however were comparable to lower concentrations found in the field (0.4 mmol l^{-1}, Westphal, unpubl. data). The reaction of benthic volumetric oxygen consumption rates to increased flow rates and/ or increased dissolved organic matter has been found before for other sediments in the Middle Atlantic Bight (Rusch et al. 2006). Comparable with our investigations for the study area in the Baltic Sea, Rusch et al. (2006) argue

rates to be determined by the availability of organic matter (in quality and quantity) and the metabolically active biomass.

Adding nutrition in form of living particles did not achieve any effect on the volumetric oxygen consumption rates. We did however, observe an effect on the permeability of the treated sediment. Obviously even though the applied algae cells do not resemble a useful substrate for nutrition, the addition of algae might have an effect on the sediment in the field. As the permeability decreased with the establishment of a biofilm it might lead to a reduction of oxygen penetration depth. Consequently oxygen would be available for a smaller sediment volume and the TOU would probably decrease with increased undegradable algae material.

Nevertheless, contrasting to the flow-through cores, advective flushing could lead to the removal the algae cells from the uppermost sediment layer in the field. Instead of clogging the pore spaces algae cells would not remain in the uppermost sediment layer and thus the permeability in the field would probably not change if under advective conditions in contrast to the changed permeability in the laboratory treatment. This phenomenon was observed by Huettel et al. (2007) at the Hel Peninsula in the Baltic Sea.

Even though the complex interplay of the different porewater processes which increase TOU is not fully understood and we are still far away from predictions, a general picture can be established in terms of increasing of wave heights. With the up shift of height and length of a wave, the boundary flow velocity is increased. In the interaction with ripples, the dp can rise, leading to an enlargement of the oxic volume in permeable sediments. With an enlarged oxic volume, the TOU can increase if fuelled. Additionally the porewater flow velocity will be faster in some points (Huettel et al. 1998), hence increasing the volumetric oxygen consumption in these parts. The increase of TOU due to the advective influence is thus dependent on the distribution of O_2 in the sediment and the porewater flow velocity induced.

4.3 Field parameters

Wanting to be able to extrapolate the studied processes in situ and ex situ to sediment characteristics found at the field site, we needed to investigate the field parameters (Objective 1). The field site was more heterogeneous in terms of sediment characteristics than suggested by early pre-investigations.

C:N ratios derived from the measurements in our studied area ranged from 7.7 to 16 as sampled in July or October. C:N ratios in the Baltic would generally be expected to be between 8.4 and 9.5 as the main source of organic carbon in the Baltic is primary production (Leipe et al. 2011). Higher C:N ratios suggest input of terrestrial matter or old organic matter

in the system. Contents of organic carbon in our study area ranged from 0.09 - 0.2% DW. These contents were similar to 0.1% DW in the shallow areas of the Baltic Sea observed by Leipe et al. (2011). Premuzic et al. (1982) estimated the organic content in the Baltic to be ~2% DW in a world map which was, however very broad and did not differentiate between areas within the Baltic. The range of TOC in the North Sea was similar with described contents of 0 - 2.8% DW (Neumann et al. 2017b).

Chl a concentration was also similar to values measured previously in the Baltic Sea. Josefson et al. (2012) found values of 0.04 to 8.92 μg cm^{-3} which were within the range of concentrations found in our study area (0.2 - 11.4 μg cm^{-3}). Generally we found the deeper stations to have ~twice as much chl a as the shallower stations. This distribution of chl a was also shown by Sundbäck et al. (1996) at the Swedish West Coast.

From the chl a concentrations, a carbon content was calculated (Table 4) which can then be compared to the total carbon estimated via LOI. Assuming the carbon from chl a concentrations to be fresh organic carbon, we could estimate a percentage of fresh to total carbon in the system. The supply of carbon was very different in quality at the different stations. St 13 had the highest percentage of fresh carbon with 23%, while St 23 had a lower content of fresh carbon with 19%. St 41 had the lowest percentage of fresh carbon with only 6%.

Permeability is an important factor regarding the advective influence on oxygen uptake of sediments. Permeability in the study area ranged over two orders of magnitude from $0.5*10^{-11}$ m^2 – $11.3*10^{-11}$ m^2 for the upper 5 m. Thereby permeability thresholds for porewater flows to occur are controversially discussed. As noted earlier, when wanting to define a permeability threshold we might have to differentiate between advective influence on oxygen uptake and advective influence in general. One estimated threshold was $0.25*10^{-11}$ m^2 (Forster et al. 1996, 2003; Huettel and Gust 1992a; Glud et al. 1996) and based on dye or bromide as a tracer. In his dissertation Ahmerkamp (2016) already discussed this threshold and concluded "for typical pressure gradients of around 2 Pa and bed forms with wavelengths of $\lambda = 0.2$ m and heights of $\eta = 0.02$ m (Janssen et al., 2012) and a typical diffusion coefficient of around 10^{-9} m^2 s^{-1} a permeability of $5*10^{-12}$ m^2 denotes the limit where advection starts to dominate the system" (Ahmerkamp 2016). The critical permeability is thus still debated. Assuming a critical permeability of $0.25*10^{-11}$ m^2, the study area could be defined to be permeable for ~93% of the area (93% of the stations). A porewater exchange due to advective forcing should thus be possible in almost the entire the study area. However, looking at results from the laboratory it becomes clear that permeability cannot be defined by one value. Results from our laboratory experiments could suggest a critical permeability for the advective effect on oxygen uptake of $0.75*10^{-11}$ m^2. If analysing the study area with this redefined threshold of permeability (Figure 27, black line), only 80% could be considered to be permeable. Forster et al. (2003) discussed the permeability of the Southern Baltic Sea

and concluded 82% of calculable area to be permeable (with a permeability of $>2.5*10^{-12}$ m^2). If setting the permeability threshold slightly higher to $7.5*10^{-12}$ m^2 as suggested from our results and reestimating the permeability of the Southern Baltic Sea, less than 48% in the Baltic Sea could be regarded as permeable and subject to advective influence on oxygen uptake. The threshold for measurable permeability effects on the oxygen uptake is thus critical for extrapolations. Janssen et al. (2005a) expected for the German Baltic seafloor only 3% to have the necessary high permeabilities which would be subject to advective influence. Their study was based on oxygen uptake rates.

A few studies investigated the advective influence in dependence of current velocities and sediment characteristics. The advective influence is dependent on the interaction of velocity strength, topography and permeability (Forster et al. 1996; Huettel et al. 1996, 1998; Reimers et al. 2004; Ahmerkamp et al. 2017). Summarizing the onset of effects in different studies, effects can be seen for grain sizes >207 μm and permeability $>2*10^{-11}$ m^2. This fits quite well to the results of our study. The only station where an effect of advection on TOU could be observed in our study had a permeability of $3.2*10^{-11}$ m^2. If taking this critical permeability value above $>2*10^{-11}$ m^2 suggested by the different authors (Forster et al. 1996; Huettel et al. 1996, 1998; Reimers et al. 2004; Ahmerkamp et al. 2017), only 3 out of 15 stations in our study area (20%) could be regarded as permeable (rounded values, Figure 27, dotted black line). Including stations with a permeability of exactly $2*10^{-11}$ - m^2 into the area assumed to be permeable, increased their number to 7 and the permeable area to 47%. Generally a stronger influence could be observed for stations with a higher permeability (Janssen et al. 2005a) and while the threshold might be debatable, it is clearly above $2.5*10^{-12}$ m^2!

A study by Kreuzburg et al. (2018) divided the study area in three grain size areas (divided into A, B and C based on the phi scale). The only station found to be permeable for an advective effect on oxygen uptake in our study, would be within the B category. We thus assumed that the C area and the B area in their study could be counted to the permeable area (with grain sizes roughly fitting to the above mentioned threshold of $2*10^{-11}$ m^2). According to their published map this would amount to 1/3 - 1/2 of the study area, agreeing with the discussed permeable area in our study. The permeable area was found to be mostly in the north of the study area (our study, Kreuzburg et al. 2018).

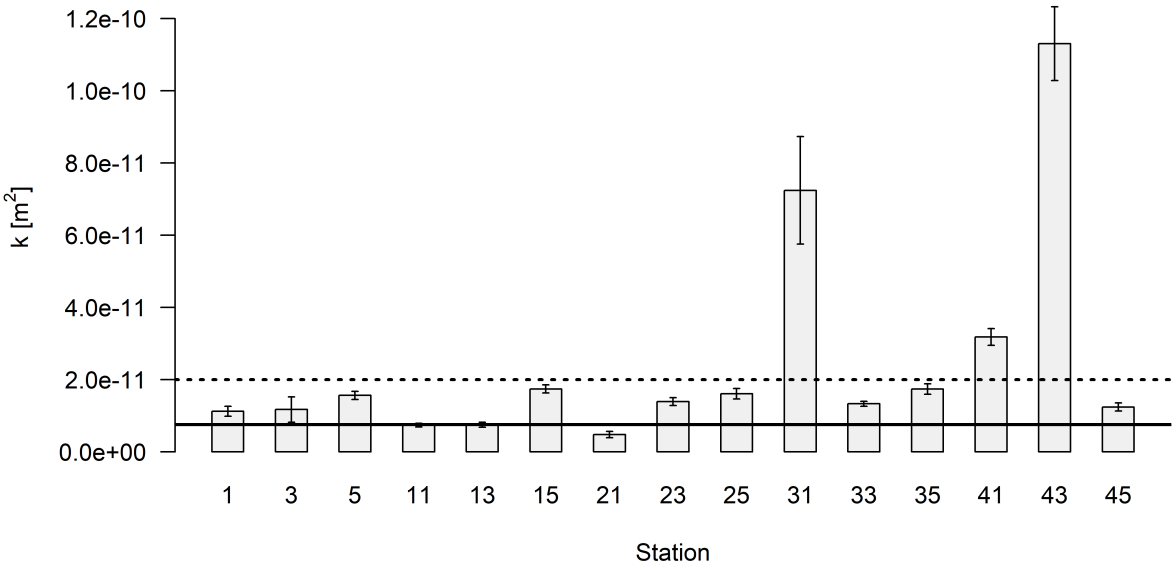

Figure 27: Permeability in the study area with a changed permeability threshold of $7.5*10^{-12}$ m^2 as marked with a black line and a potential threshold of $2*10^{-11}$ m^2 as marked with a dotted black line. Permeability in this graph was measured for the top 5 cm.

Permeable sediments are only subject to advective influence in combination with currents. Currents in the study area were deducted from wave measurements as the Baltic Sea is a micro tidal system and currents are mainly wind driven. Generally wave driven advection would take place in permeable sediments if water depth is <wavelength/2 (Precht and Huettel 2003a). Precht and Huettel (2003b) summarized different regions on the sea floor with respect to waves affecting advective fluxes (according to the basic wave theory). The study area belonged to an area of "episodic wave ripple interaction", meaning the sediment to be episodically reached and affected by waves.

For the investigated area with an approximate water depth of 4.5 m, only wavelength of more than ~9 m would reach the sea floor and and interact with the sediment topography. Regarding the observed wave length ranging from ~3 m to 50 m as measured in the study area (AWAC measurements Apr to July 2017, unpubl. data) ~70% of waves could fulfil this requirement and lead to an advective effect. Waves occurring in the study area were quite variable, with larger waves occurring only for shorter time scales while smaller waves (~0.2 m) occurred frequently also for longer time scales.

The velocities resulting from waves were mostly below 0.2 m s^{-1}. However very slow velocities (0.04 m s^{-1}) were most frequent. These velocities were slower than velocities measured due to inflow events (Burchard et al. 2005, 2009). Nevertheless, also slow velocities would be able to induce advective flow; however the strength of advective input would accordingly be smaller. Generally we can state from literature analysis an influence of currents to be visible already at very slow velocities of ~2 cm s^{-1}, if the sediment is permeable (Forster et al. 1996; Huettel et al. 1996, 1998; Reimers et al. 2004; Ahmerkamp et al. 2017).

Faster velocities could lead to stronger effects. In an example calculation by Precht and Huettel (2003b) (a study on filtering rates), an increased velocity from 0.1 to 0.25 m s^{-1} led to a ~6-fold increased effect. In our study we could observe an increase in metabolic uptake already for a velocities of 0.04 m s^{-1}, however stronger velocity would possibly lead to an even higher oxygen uptake.

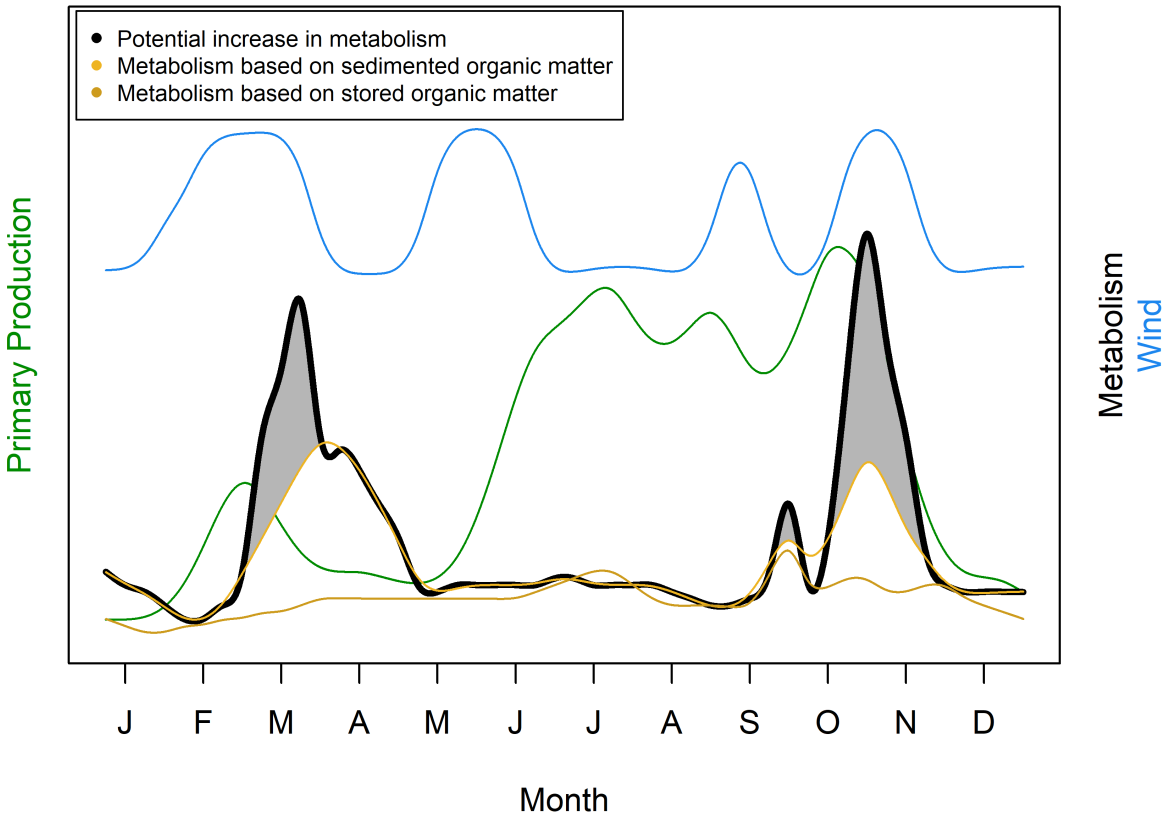

Figure 28: Sketch of different possible states of oxygen uptake and the influence of advection. Wind was plotted only exemplary without any real data; the black line shows the potential increase in metabolism (also depicted as grey areas); the yellow line shows metabolism based on sedimentation; the dark yellow line shows metabolism based on stored organic matter (background metabolism). Background metabolism rates and primary production rates were based on (Graf et al. 1983; Smetacek 1984; Rumohr et al. 1987).

Combining all parameters we can in principle define the states when in permeable sediments advective influence takes place or not (Figure 28). An influence on oxygen uptake is closely coupled to nutritious input and thus in the Baltic Sea mainly linked to primary production. Figure 28 depicts a yearly cycle with spring and autumn bloom (green line) and the resulting sedimentation of organic matter (yellow line). Additionally a basic curve shows the metabolism due to stored organic carbon in the sediment (dark yellow line). The black line shows the potential metabolism which is affected by advective input and dependent on wind and sedimenting organic matter as a yearly cycle. Without primary production, advective forcing due to wind would lead to higher oxygen values in the sediment but without any measurable effect on oxygen uptake (Figure 28, February). Increased oxygen uptake is thus depended on wind forcing or currents in combination with sedimented organic carbon due to

primary production. Only with high advective forcing during a spring or autumn bloom for example, oxygen uptake could be influenced (Figure 28, March, October/ November, grey areas). Regarding a yearly cycle, the increased oxygen uptake would depend on the combination of carbon input, advective influence and permeablility of sediments. Extrapolating TOU as a yearly cycle dependent only on one parameter would always over- or underestimate oxygen uptake in an area.

4.4 Faunal oxygen uptake

When wanting to understand field data on TOU, it is not sufficient to regard only sediment characteristics. For the field investigations it is necessary to include the fauna present in measurement areas (Objective 3). Schade et al. (2019) measured the respiration rates of *M. arenaria* as a function of their dry weight to assess the contribution of this prominent fauna element. Like most sediment organisms, *M. arenaria* induces a direct effect on TOU through its respiration and an indirect effect due to the input of oxygenated water into the sediment. Schade et al. (2019) only estimated its respiration rate. The indirect influence on TOU increase due to increased oxygen input into the sediment by the bivalve has only rarely been studied. The existing studies examining both these effects of *M. arenaria* on sediment respiration differ in their values. Studies examined either the increase in TOU or solely the leakage of water into the sediment due to *M. arenaria* (Forster and Zettler 2004; Michaud et al. 2005, 2006). *M. arenaria* was found to increase the TOU with a factor of 1.2 - 1.6 due to the combined effect of respiration and indirect influence by 6 individuals (Michaud et al. 2005). The leakage of water into the surrounding sediment was estimated to be <1% (Forster and Zettler 2004), and thus rather low. *M. arenaria*'s influence on TOU despite their respiration seems to be rather low. A thesis work by Camillini (2017) however, measured an increased TOU with a factor of ~3.6 due to the occurrence of an *M. arenaria* individual in a core with a dieamter of 9.5 cm. In his study half of the additional oxygen uptake was due to the respiration of *M. arenaria* itself, while half of the increase in oxygen uptake was due to an increased input of oxygen into the sediment. The factor of additional input due to a "leaking" of *M. arenaria* varied extremely. As discussed earlier, the reaction of the sedimentary oxygen uptake is dependent not only on the oxygen input itself but also strongly on the availability of usable substrate. The factor of 3.6 was found by Camillini in sediment used in their experiment, it could be too high for different sediments, like the sediments in our experiments. The increased oxygen uptake due to advective input measured in our study area was rather low (see results) and the organic carbon values were additionally low. Thus, we assumed the increased oxygen input into the sediment by *M. arenaria* to be small and too low to result in pronounced differences in bacterial respiration in our study. Increased TOU due to *M. arenaria* was thus solely assumed to result from the respiration of the bivalve itself.

In this study, calculations of respiration rates by different faunal species focused on *M. arenaria*, *Marenzelleria* spp. and *H. diversicolor*. *Marenzelleria* spp. and *H. diversicolor* showed similar abundances in the studied area. Increases in TOU due to these two polychaete species could be calculated according to published literature. Regarding the polychaetes we calculated both, the respiration by the polychaetes themselves and the increase in TOU due to the increased oxygen input into the sediments by the polychaetes (due to burrowing activities).

For the calculation of the respiration rate we used a formula published by Mahaut et al. (1995) for both species. Respiration of *H. diversicolor* was also estimated based on several studies (Nithart et al. 1999; Braeckman et al. 2010; Gebhardt 2013). Respiration rates calculated with these other publications led to slightly different results than the respiration rate calculated in our study. Nevertheless calculated respiration rates using other publications (0.01 – 0.04 mmol O_2 m^{-2} d^{-1}) were reasonably similar to the respiration calculated in our study (0.01 – 0.07 mmol O_2 m^{-2} d^{-1}). As respiration differed only slightly using formulae from different studies, we assume the calculated rates in our study to be reliable. However, calculated respiration rates for *H. diversicolor* were rather low as the abundance was relatively low in the studied area (the variation in the calculated respiration rate for different calculations was thus naturally low).

The respiration rate for burrowing polychaetes is only a minor part when regarding the total increase in TOU which polychaetes induce. The increased oxygen input into the sediment due to their burrowing activities has a considerably higher influence on the TOU compared to their respiration input (Kristensen et al. 2012; Renz and Forster 2014). Studies on *H. diversicolor* have shown the increase in TOU to be mainly due to the polychaetes' input of oxygen into the sediment due to burrow ventilation (Kristensen et al. 1985; Christensen et al. 2000).

Change in oxygen uptake in sediments due to burrow activities was roughly estimated for both polychaetes using literature. As already discussed for *M. arenaria*, an increase in TOU due to the increased supply of oxygen to the sediment by any species is also dependent on the organic matter in the sediment. As the oxygen input into the sediment by polychaetes is rather high in general compared to *M. arenaria*, we nevertheless assumed this strong influence. As organic content in the sediment was rather low in our study, we have to keep in mind that the calculated additional oxygen uptake due to the abundance of the polychaetes is probably overestimated.

When calculating increases in TOU with single species values, it is important to realize that the additional influence on TOU due to oxygen input into the sediment depends on abundance. The input of each species is dependent on the interaction between different species and interaction between the individuals. Also the individual contribution to TOU decreases

with higher abundance of species or with higher species diversity (Mermillod-Blondin et al. 2005; Duport et al. 2006; Hale et al. 2014). For this reason, calculating the contribution to TOU input of single individuals and species based on simple multiplication of abundance and individual additional oxygen transport, is thus possibly often an overestimation.

When analysing TOU rates at field stations, the partial input on the TOU by the abundant macrofauna is of interest. Macrofauna distribution in the study area was heterogeneous; therefore the increased TOU rates due to macrofauna would be expected to be heterogeneous as well. Increase in TOU by the different macrofauna was calculated for the most abundant species to be able to estimate the contribution of these species and how much of the variation between TOU replicates can be explained by the macrofauna. We have to consider an underestimation of large and deeply burrowed species from our study area macrofauna sampling. Infauna usually inhabits the upper 10 – 50 cm of sediments (Bertics and Ziebis 2009; Aller 2014) and larger animals burry deeper than smaller individuals (Zaklan and Ydenberg 1997). Sediments in our study area were unfortunately only sampled down to 15 cm.

Regarding two TOU measurements during our study in the lab (Langenwerder 1 and 2), an increase in TOU was calculated for *Marenzelleria* spp. At this station the difference in TOU rates between two incubations could almost entirely be explained by the difference in abundance of *Marenzelleria* spp. The calculated increase in TOU due to this polychaete was very close to the difference in TOU rates between those two incubations (31 mmol O_2 m^{-2} d^{-1} with 13 mmol O_2 m^{-2} d^{-1} by *Marenzelleria* spp. and 16 mmol O_2 m^{-2} d^{-1} with 2 mmol O_2 m^{-2} d^{-1} by *Marenzelleria* spp.).

The calculations to our field incubations resolved the difference only partly. Proportion of TOU due to the most abundant macrofauna was calculated for two stations in our study area. The estimated oxygen uptake based on macrofauna abundance showed macrofauna to contribute 20% to TOU at St 13 and 5% to TOU at St 23. *M. arenaria* itself contributed 16% to TOU at St 13 and 4% to TOU at St 23. *M. arenaria* was the species with the highest proportion of TOU at both stations, it can thus explain partly the difference in TOU between those two stations. Of 16 mmol O_2 m^{-2} d^{-1} difference, 4.4 mmol O_2 m^{-2} d^{-1} could be explained by the higher abundance and respiration of *M. arenaria* at St 13 (amounting to 25%).

Also in parallel chambers the difference in respiration of *M. arenaria* could explain the difference in TOU of the chambers to some extent. The calculated respiration of *M. arenaria* at St 13 between different replicates varied from 1.1 to 6.7 mmol O_2 m^{-2} d^{-1} while the difference between TOU measured in these replicates varied from 24 – 35 mmol O_2 m^{-2} d^{-1}. Unfortunately there was no data available on the abundance within each core, so the difference in abundance between each replicate could only be estimated due to the parallel

sampling at the same station. The difference between the calculated respiration was close to the difference between the replicates and could explain up to 50% of variation.

5 Conclusion and Outlook

More than 45% of the inner continental shelf is covered with sands. Sandy sediments were originally thought to be sites of low biogeochemical forcing (Boudreau et al. 2001) as they have low organic contents and lower bacterial abundances compared to muddy sites (Rusch et al. 2003). Nevertheless these sites are nowadays reconsidered as possible sites of comparatively strong mineralization rates due to advective porewater flow and resulting stronger biogeochemical reaction rates than previously thought (Huettel and Webster 2001; Santos et al. 2012; Huettel et al. 2014; Lipka et al. 2018). The role of sediments differ between areas and advective porewater flow does not necessarily lead to increased mineralization rates in all areas. We investigated the advective influence on sediments in a sandy area in the Baltic Sea.

In contrast to expected strong mineralization rates due to advective influence, oxygen uptake rates were less dependent on advective processes than expected and the effect of advection was less pronounced than estimated. Laboratory results showed the increase in advective forcing not to result in a change in oxygen uptake even for possibly permeable sediments. The critical permeability for an advective influence on oxygen uptake needs to be reconsidered as the critical permeability on advective influence using non-biologically active tracers (as dye for example) seems to define a general critical threshold. This general threshold does not seem to hold true for advective influence on TOU. The critical permeability for advection to affect TOU can be redefined to some value between 0.75 and $2*10^{-11}$ m^2, as TOU by sediment with a lower permeability was not affected in our study. Generally we can state from our observations that advection has less impact on oxygen uptake rates than originally thought in our study area.

A dependence of oxygen uptake rates on flow velocity was nevertheless shown for most sediments in through-flow chambers, as well as a dependence on organic carbon input. Applying estimated findings to sediment characteristics showed sediments found in the study area to be permeable for parts of the area. We estimated 47 - 80% of the area to be permeable and possibly subject to advective influence on oxygen uptake. As only approx. 70% of waves would reach the sea floor, the possibility of an advective process to influence TOU would further decrease to 33 - 56%.

Oxygen uptake rates are dependent on primary production and vary seasonally, therefore the measured oxygen uptake rates cannot account for oxygen uptake rates measured at different times. To achieve a more detailed observation of oxygen uptake rates throughout the year and be able to estimate a yearly cycle, benthic chambers would need to be deployed several times throughout the year. Variations in oxygen uptake rates would nevertheless be observed due to a strong heterogeneity of benthic diatoms, fauna and sediment characteris-

tics. A possible solution to deal with less variability in the future could be the deployment of more replicates. However, each chamber is very costly and increasing the amount of chambers might not give less variable rates after all. A study by Janssen et al. (2005a) deployed 5-8 replicates and variation between replicates in their study was very high as well (± up to >100%). Generally strong variations are present in all seas. To extrapolate mineralization rates to larger areas and to a yearly cycle, a more detailed assessment throughout the year would be necessary.

The velocity as mimicked by the benthic chambers was estimated to resemble the flow velocities measured in the study area rather well. Benthic chambers were thus a reliable method for oxygen uptake measurements under increased advective forcing in our study area, despite the strong variation between replicates. Extrapolating results for increased advective flow strength, the influence of advection on oxygen uptake would need to be assessed for varying flow rates. Nevertheless, as a large part of the area did not seem to react with increased oxygen uptake rates on advective forcing, the impermeable part of the area would not need to be assessed.

We established a reliable calculation of respiration rate for *M.arenaria* and estimated its contribution in our study area to be up to 16% of TOU. The most abundant polychaetes were calculated to constitute less to TOU. Generally respiration by macrofauna was lower compared to other areas in the Baltic Sea (compare Powilleit unpubl data St 44/ Seekanal in Schade et al. (2019)). Approximations of macrofaunal oxygen uptake rates are ambiguous as they depend on many factors. Here is a need for further investigations. One main uncertainty is still the increasing oxygen uptake of sediments due to increased oxygen supply into the sediment by indirect effects of macrofauna. This effect has been studied for polychaetes and *M.arenaria* in some studies. Nevertheless as changes in oxygen uptake rates differ between sediments, a detailed study observing the indirect effect is required for different species in different sediments.

References

Ahmerkamp, S. (2016). *Regulation of oxygen dynamics by transport processes and microbial respiration in sandy sediments*. PhD thesis. Universität Bremen, 243.

Ahmerkamp, S., Winter, C., Krämer, K., Beer, D. de, Janssen, F., Friedrich, J., Kuypers, M. M. M., and Holtappels, M. (2017). Regulation of benthic oxygen fluxes in permeable sediments of the coastal ocean. *Limnology and Oceanography* 62.5, 1935–1954.

Aller, R. C., Aller, J. Y., and Kemp, P. F. (2001). Effects of particle and solute transport on rates and extent of remineralization in bioturbated sediments. *Organism-Sediment Interactions*. Vol. 24. 6, 315–333.

Aller, R. C. (2014). *Sedimentary Diagenesis, Depositional Environments, and Benthic Fluxes*. 2nd ed. Vol. 8. Elsevier Ltd., 293–334.

Andersson, J., Middelburg, J. J., and Soetaert, K. (2006). Identifiability and uncertainty analysis of bio-irrigation rates. *Journal of Marine Research* 64, 407–429.

Banse, K. (1982). Mass-Scaled Rates of Respiration and Intrinsic Growth in Very Small Invertebrates. *Marine Ecology Progress Series* 9.1973, 281–297.

Berg, P., Long, M. H., Huettel, M., Rheuban, J. E., McGlathery, K. J., Howarth, R. W., Foreman, K. H., Giblin, A. E., and Marino, R. (2013). Eddy correlation measurements of oxygen fluxes in permeable sediments exposed to varying current flow and light. *Limnology and Oceanography* 58.4, 1329–1343.

Bertics, V. J. and Ziebis, W. (2009). Biodiversity of benthic microbial communities in bioturbated coastal sediments is controlled by geochemical microniches. *ISME Journal* 3.11, 1269–1285.

Bird, F., Boon, P., and Nichols, P. (2000). Physicochemical and microbial properties of burrows of the deposit-feeding thalassinidean ghost shrimp *Biffarius arenosus* (Decapoda: Callianassidae). *Estuarine, Coastal and Shelf Science* 51, 279–291.

Bonsdorff, E. (2006). Zoobenthic diversity-gradients in the Baltic Sea: Continuous post-glacial succession in a stressed ecosystem. *Journal of Experimental Marine Biology and Ecology* 330.1, 383–391.

Boudreau, B. P., Huettel, M., Forster, S., Jahnke, R. A., McLachlan, A., Middelburg, J. J., Nielsen, P., Sansone, F., Taghon, G., Van Raaphorst, W., Webster, I., Weslawski, J. M.,

Wiberg, P., and Sundby, B. (2001). Permeable marine sediments: Overturning an old paradigm. *Eos* 82.11, 133–136.

Braeckman, U., Provoost, P., Gribsholt, B., Van Gansbeke, D., Middelburg, J. J., Soetaert, K., Vincx, M., and Vanaverbeke, J. (2010). Role of macrofauna functional traits and density in biogeochemical fluxes and bioturbation. *Marine Ecology Progress Series* 399, 173–186.

Burchard, H., Janssen, F., Bolding, K., Umlauf, L., and Rennau, H. (2009). Model simulations of dense bottom currents in the Western Baltic Sea. *Continental Shelf Research* 29.1, 205–220.

Burchard, H., Lass, H. U., Mohrholz, V., Umlauf, L., Sellschopp, J., Fiekas, V., Bolding, K., and Arneborg, L. (2005). Dynamics of medium-intensity dense water plumes in the Arkona Basin, Western Baltic Sea. *Ocean Dynamics* 55.5-6, 391–402.

Camillini, N. (2017). *The influence of Mya arenaria on microbial metabolism in marine sediments*. MA thesis. Syddansk Universitet-University of Southern Denmark, 61.

Christensen, B., Vedel, A., and Kristensen, E. (2000). Carbon and nitrogen fluxes in sediment inhabited by suspension-feeding (*Nereis diversicolor*) and non-suspension-feeding (*N. virens*) polychaetes. *Marine Ecology Progress Series* 192, 203–217.

Cloern, J. E., Grenz, C., and Vidergar-Lucas, L. (1995). An empirical model of the phytoplankton chlorophyll : carbon ratio-the conversion factor between productivity and growth rate. *Limnology and Oceanography* 40.7, 1313–1321.

Devol, A. H. and Christensen, J. P. (1993). Benthic fluxes and nitrogen cycling in sediments of the continental margin of the eastern North Pacific. *Journal of Marine Research* 51.2, 345–372.

Doran, P. (1995). *Bioprocess Engineering Principles*. Sydney: Elsevier Science & Technology Books, 430.

Duport, E., Stora, G., Tremblay, P., and Gilbert, F. (2006). Effects of population density on the sediment mixing induced by the gallery-diffusor *Hediste* (*Nereis*) *diversicolor* O.F. Müller, 1776. *Journal of Experimental Marine Biology and Ecology* 336.1, 33–41.

Eyre, B. D. and Ferguson, A. J. P. (2005). Benthic metabolism and nitrogen cycling in a subtropical east Australian estuary (Brunswick): Temporal variability and controlling factors. *Limnology and Oceanography* 50.1, 81–96.

Folk, R. L. and Ward, W. C. (1957). Brazos River bar [Texas]; a study in the significance of grain size parameters. *Journal of Sedimentary Petrology* 27.1, 3–26.

Forster, S., Bobertz, B., and Bohling, B. (2003). Permeability of sands in the coastal areas of the southern Baltic Sea: Mapping a grain-size related sediment property. *Aquatic Geochemistry* 9, 171–190.

Forster, S., Glud, R. N., Gundersen, J. K., and Huettel, M. (1999). In situ study of bromide tracer and oxygen flux in coastal sediments. *Estuarine, Coastal Shelf Science* 49.6, 813–827.

Forster, S., Huettel, M., and Ziebis, W. (1996). Impact of boundary flow velocity on oxygen utilization in coastal sediments. *Marine Ecology Progress Series* 143, 173–185.

Forster, S. and Zettler, M. L. (2004). The capacity of the filter-feeding bivalve *Mya arenaria* L. water transport in sandy beds. *Marine Biology* 144.6, 1183–1189.

Fuchsman, C. A., Devol, A. H., Chase, Z., Reimers, C. E., and Hales, B. (2015). Benthic fluxes on the Oregon shelf. *Estuarine , Coastal and Shelf Science* 163, 156–166.

Gattuso, J. P., Frankignoulle, M., and Wollast, R. (1998). Carbon and Carbonate Metabolism in Coastal Aquatic Ecosystems. *Annual Review of Ecology and Systematics* 29, 405–434.

Gebhardt, C. (2013). *Charakterisierung des Austauschs gelöster Stoffe von Sedimenten der Darß-Zingster Boddenkette unter Berücksichtigung der benthischen Makrofauna*. MA thesis. University of Rostock, 86.

Gihring, T. M., Canion, A., Riggs, A., Huettel, M., and Kostka, J. E. (2010). Denitrification in shallow, sublittoral Gulf of Mexico permeable sediments. *Limnology and Oceanography* 55.1, 43–54.

Glud, R. N. (2008). Oxygen dynamics of marine sediments. *Marine Biology Research* 4.4, 243–289.

Glud, R. N., Berg, P., Stahl, H., Hume, A., Larsen, M., Eyre, B. D., and Cook, P. L. (2016). Benthic Carbon Mineralization and Nutrient Turnover in a Scottish Sea Loch: An Integrative In Situ Study. *Aquatic Geochemistry* 22.5-6, 443–467.

Glud, R. N., Forster, S., and Huettel, M. (1996). Influence of radial pressure gradients on solute exchange in stirred benthic chambers. *Marine Ecology Progress Series* 141, 303–311.

Gogina, M., Nygård, H., Blomqvist, M., Daunys, D., Josefson, A. B., Kotta, J., Maximov, A., Warzocha, J., Yermakov, V., Gräwe, U., and Zettler, M. L. (2016). The Baltic Sea scale inventory of benthic faunal communities. *ICES Journal of Marine Science* 73.4, 1196–1213.

Graf, G., Schulz, R., Peinert, R., and Meyer-Reil, L. A. (1983). Benthic response to sedimentation events during autumn to spring at a shallow-water station in the Western Kiel Bight - I. Analysis of processes on a community level. *Marine Biology* 77, 235–246.

Grasshoff, K., Kremling, K., and Ehrhardt, M. (1999). *Methods of Seawater Analysis*. Weinheim: Wiley-VCH, 632.

Hale, R., Mavrogordato, M. N., Tolhurst, T. J., and Solan, M. (2014). Characterizations of how species mediate ecosystem properties require more comprehensive functional effect descriptors. *Scientific Reports* 4, 1–6.

Hall, S. J. (2002). The continental shelf benthic ecosystem: current status, agents for change and future prospects. *Environmental Conservation* 29.03, 350–374.

Al-Hamdani, Z. K., Reker, J., Leth, J. O., Reijonen, A., Kotilainen, A. T., and Dinesen, G. E. (2007). Development of marine landscape maps for the Baltic Sea and the Kattegat using geophysical and hydrographical parameters. *Geological Survey of Denmark and Greenland Bulletin* 13, 61–64.

Head, K. H. (1982). Volume II: Permeability, shear strength and compessibility tests. *Manual of soil laboratory testing*. Vol. 2. London: Pentech Press, 335–747.

HELCOM (2017). *Manual for Marine Monitoring in the COMBINE Programme of HELCOM*, 361.

Huettel, M. and Gust, G. (1992a). Impact of bioroughness on interfacial solute exchange in permeable sediments. *Marine Ecology Progress Series* 89.2-3, 253–267.

Huettel, M. and Gust, G. (1992b). Solute release mechanisms from confined sediment cores in stirred benthic chambers and flume flows. *Marine Ecology Progress Series* 82, 187–197.

Huettel, M., Ziebis, W., and Forster, S. (1996). Flow-induced uptake of particulate matter in permeable sediments. *Limnology and Oceanography* 41.2, 309–322.

Huettel, M., Ziebis, W., Forster, S., and Luther Iii, G. W. (1998). Advective transport affecting metal and nutrient distributions and interfacial fluxes in permeable sediments. *Geochimica et Cosmochimica Acta* 62.4, 613–631.

Huettel, M., Berg, P., and Kostka, J. E. (2014). Benthic exchange and biogeochemical cycling in permeable sediments. *Annual Review of Marine Science* 6, 23–51.

Huettel, M., Cook, P., Janssen, F., Lavik, G., and Middelburg, J. J. (2007). Transport and degradation of a dinoflagellate bloom in permeable sublittoral sediment. *Marine Ecology Progress Series* 340, 139–153.

Huettel, M. and Webster, I. T. (2001). Porewater flow in permeable sediments. *The benthic boundary layer: Transport processes and biogeochemistry*. New York: Oxford University Press, 144–179.

Jahnke, R. A., Nelson, J. R., Marinelli, R. L., and Eckman, J. E. (2000). Benthic flux of biogenic elements on the Southeastern US continental shelf: Influence of pore water advective transport and benthic microalgae. *Continental Shelf Research* 20.1, 109–127.

Jahnke, R., Richards, M., Nelson, J., Robertson, C., Rao, A., and Jahnke, D. (2005). Organic matter remineralization and porewater exchange rates in permeable South Atlantic Bight continental shelf sediments. *Continental Shelf Research* 25, 1433–1452.

Janssen, F., Faerber, P., Huettel, M., Meyer, V., and Witte, U. (2005a). Pore-water advection and solute fluxes in permeable marine sediments (II): Benthic respiration at three sandy sites with different permeabilities (German Bight, North Sea). *Limnology and Oceanography* 50.3, 779–792.

Janssen, F., Faerber, P., Huettel, M., Meyer, V., and Witte, U. (2005b). Pore-water advection and solute fluxes in permeable marine sediments (I): Calibration and performance of the novel benthic chamber system Sandy. *Limnology and Oceanography* 50.3, 768–778.

Jørgensen, C. B. and Riisgard, H. U. (1988). Gill pump characteristics of the soft clam *Mya arenaria*. *Marine Biology* 99, 107–109.

Josefson, A. B., Norkko, J., and Norkko, A. (2012). Burial and decomposition of plant pigments in surface sediments of the Baltic Sea: Role of oxygen and benthic fauna. *Marine Ecology Progress Series* 455, 33–49.

Karlson, K., Bonsdorff, E., and Rosenberg, R. (2007). The impact of benthic macrofauna for nutrient fluxes from Baltic sea sediments. *Ambio* 36.2, 161–167.

Kreuzburg, M., Ibenthal, M., Janssen, M., Rehder, G., Voss, M., Naumann, M., and Feldens, P. (2018). Sub-marine continuation of peat deposits from a coastal peatland in the Southern Baltic Sea and its holocene development. *Frontiers in Earth Science* 6.103.

Kristensen, E., Ahmed, S. I., and Devol, A. H. (1995). Aerobic and anaerobic decomposition of organic matter in marine sediment : Which is fastest ? *Water* 40.8, 1430–1437.

Kristensen, E., Jensen, M. H., and Andersen, T. K. (1985). The impact of polychaete (*Nereis virens* Sars) burrows on nitrification and nitrate reduction in estuarine sediments. *Journal of Experimental Marine Biology and Ecology* 85, 75–91.

Kristensen, E., Penha-Lopes, G., Delefosse, M., Valdemarsen, T., Quintana, C. O., and Banta, G. T. (2012). What is bioturbation? The need for a precise definition for fauna in aquatic sciences. *Marine Ecology Progress Series* 446, 285–302.

Lasota, R., Pierścieniak, K., Miac, J., and Wołowicz, M. (2014). Comparative study of ecophysiological and biochemical variation between the Baltic and North Sea populations of the invasive soft shell clam *Mya arenaria* (L. 1758). *Oceanological and Hydrobiological Studies* 43.3, 303–311.

Laverock, B., Gilbert, J., Tait, K., Osborn, A., and Widdicombe, S. (2011). Bioturbation: impact on the marine nitrogen cycle. *Biogeochemical Scociety Transactions* 39, 315–320.

Leipe, T., Tauber, F., Vallius, H., Virtasalo, J., Uścinowicz, S., Kowalski, N., Hille, S., Lindgren, S., and Myllyvirta, T. (2011). Particulate organic carbon (POC) in surface sediments of the Baltic Sea. *Geo-Marine Letters* 31.3, 175–188.

Lewis, D. E. and Cerrato, R. M. (1997). Growth uncoupling and the relationship between shell growth and metabolism in the soft shell clam *Mya arenaria*. *Marine Ecology Progress Series* 158, 177–189.

Lipka, M., Woelfel, J., Gogina, M., Kallmeyer, J., Liu, B., Morys, C., Forster, S., and Böttcher, M. E. (2018). Solute reservoirs reflect variability of early diagenetic processes in temperate brackish surface sediments. *Frontiers in Marine Science* 5, 1–20.

Lohrer, A. M., Thrush, S. F., and Gibbs, M. M. (2004). Bioturbators enhance ecosystem function through complex biogeochemical interactions. *Nature* 431.7012, 1092–1095.

Lysiak-Pastuszak, E. and Krysell, M. (2004). Chemical measurements in the Baltic Sea: Guidelines on quality assurance. *ICES techniques in marine environmental sciences*. Vol. 35, 149.

Mahaut, M. L., Sibuet, M., and Shirayama, Y. (1995). Weight-dependent respiration rates in deep-sea organisms. *Deep-Sea Research Part I* 42.9, 1575–1582.

Marchant, H. K., Lavik, G., Holtappels, M., and Kuypers, M. M. (2014). The fate of nitrate in intertidal permeable sediments. *PLoS ONE* 9.8, e104517.

Masuko, T., Minami, A., Iwasaki, N., Majima, T., Nishimura, S. I., and Lee, Y. C. (2005). Carbohydrate analysis by a phenol-sulfuric acid method in microplate format. *Analytical Biochemistry* 339.1, 69–72.

McCann-Grosvenor, K., Reimers, C. E., and Sanders, R. D. (2014). Dynamics of the benthic boundary layer and seafloor contributions to oxygen depletion on the Oregon inner shelf. *Continental Shelf Research* 84, 93–106.

McGinnis, D. F., Sommer, S., Lorke, A., Glud, R. N., and Linke, P. (2014). Quantifying tidally driven benthic oxygen exchange across permeable sediments: An aquatic eddy correlation study. *Journal of Geophysical Research: Oceans* 119, 6918–6932.

McMahon, R. F. and Russel-Hunter, W. (1977). Temperature relations of aerial and aquatic respiration in six littoral snails in relation to their vertical zonation. *Biological Bulletin* 152.2, 182–198.

Mermillod-Blondin, F., François-Carcaillet, F., and Rosenberg, R. (2005). Biodiversity of benthic invertebrates and organic matter processing in shallow marine sediments: An experimental study. *Journal of Experimental Marine Biology and Ecology* 315.2, 187–209.

Meysman, F. J. R., Galaktionov, O. S., Gribsholt, B., and Middelburg, J. J. (2006). Bioirrigation in permeable sediments: Advective pore-water transport induced by burrow ventilation. *Limnology and Oceanography* 51.1, 142–156.

Michaud, E., Desrosiers, G., Mermillod-Blondin, F., Sundby, B., and Stora, G. (2005). The functional group approach to bioturbation: The effects of biodiffusers and gallery-diffusers of the *Macoma balthica* community on sediment oxygen uptake. *Journal of Experimental Marine Biology and Ecology* 326.1, 77–88.

Michaud, E., Desrosiers, G., Mermillod-Blondin, F., Sundby, B., and Stora, G. (2006). The functional group approach to bioturbation: II. The effects of the *Macoma balthica* community on fluxes of nutrients and dissolved organic carbon across the sediment-water interface. *Journal of Experimental Marine Biology and Ecology* 337.2, 178–189.

Miller, D. (1989). Abrasion effects on microbes in sandy sediments. *Marine Ecology Progress Series* 55, 73–82.

Neumann, A., Beusekom, J. E. van, Holtappels, M., and Emeis, K. C. (2017a). Nitrate consumption in sediments of the German Bight (North Sea). *Journal of Sea Research* 127, 26–35.

Neumann, A., Möbius, J., Hass, H. C., Puls, W., and Friedrich, J. (2017b). Empirical model to estimate permeability of surface sediments in the German Bight (North Sea). *Journal of Sea Research* 127, 36–45.

Nickels, J. S., Bobbie, R. J., Martz, R. F., Smith, G. A., White, D. C., and Richards, N. L. (May 1981). Effect of silicate grain shape, structure, and location on the biomass and community structure of colonizing marine microbiota. *Applied and environmental microbiology* 41.5, 1262–8.

Nilsson, M. M., Kononets, M., Ekeroth, N., Viktorsson, L., Hylén, A., Sommer, S., Pfannkuche, O., Almroth-Rosell, E., Atamanchuk, D., Andersson, J. H., Roos, P., Tengberg, A., and Hall, P. O. (2019). Organic carbon recycling in Baltic Sea sediments – An integrated estimate on the system scale based on in situ measurements. *Marine Chemistry* 209, 81–93.

Nithart, M., Alliot, E., and Salen-Picard, C. (1999). Production , respiration and ammonia excretion of two polychaete species in a north Norfolk saltmarsh. *Journal of Marine Biology* 79.1999, 1029–1037.

Papaspyrou, S., Gregersen, T., Cox, R., Thessalou-Legaki, M., and Kristensen, E. (2005). Sediment properties and bacterial community in burrows of the ghost shrimp Pestarella tyrrhena (Decapoda: Thalassinidea). *Aquatic Microbial Ecology* 38, 181–190.

Pedersen, T. F. (Nov. 1992). Temporal variations in heat dissipation and oxygen uptake of the soft shell clam *Mya arenaria* L. (Bivalvia). *Ophelia* 36.3, 203–216.

Precht, E. and Huettel, M. (2003a). Rapid wave-driven advective pore water exchange in a permeable coastal sediment. *Journal of Sea Research* 51, 93–107.

Precht, E., Franke, U., Polerecky, L., and Huettel, M. (2004). Oxygen dynamics in permeable sediments with wave-driven pore water exchange. *Limnology and Oceanography* 49.3, 693–705.

Precht, E. and Huettel, M. (2003b). Advective pore-water exchange driven by surface gravity waves and its ecological implications. *Limnology and Oceanography* 48.4, 1674–1684.

Premuzic, E., Benkovitz, C. M., Gaffney, J. S., and Walsh, J. (1982). The nature and distribution of organic matter in the surface sediments of world oceans and seas. *Organic Geochemistry* 4, 63–77.

Rao, A. M. F., McCarthy, M. J., Gardner, W. S., and Jahnke, R. A. (2007). Respiration and denitrification in permeable continental shelf deposits on the South Atlantic Bight: Rates of carbon and nitrogen cycling from sediment column experiments. *Continental Shelf Research* 27.13, 1801–1819.

Reimers, C. E., Özkan-Haller, H. T., Berg, P., Devol, A., McCann-Grosvenor, K., and Sanders, R. D. (2012). Benthic oxygen consumption rates during hypoxic conditions on the Oregon continental shelf: Evaluation of the eddy correlation method. *Journal of Geophysical Research: Oceans* 117.2.

Reimers, C. E., Stecher, H. A., Taghon, G. L., Fuller, C. M., Huettel, M., Rusch, A., Ryckelynck, N., and Wild, C. (2004). In situ measurements of advective solute transport in permeable shelf sands. *Continental Shelf Research* 24, 183–201.

Renz, J. R. and Forster, S. (2013). Are similar worms different? A comparative tracer study on bioturbation in the three sibling species *Marenzelleria arctia*, *M. viridis*, and *M. neglecta* from the Baltic Sea. *Limnology and Oceanography* 58.6, 2046–2058.

Renz, J. R. and Forster, S. (2014). Effects of bioirrigation by the three sibling species of *Marenzelleria* spp. on solute fluxes and porewater nutrient profiles. *Marine Ecology Progress Series* 505, 145–159.

Riemann, B., Simonsen, P., and Stensgaard, L. (1989). The carbon and chlorophyll content of phytoplankton from various nutrient regimes. *Journal of Plankton Research* 11.5, 1037–1045.

Rumohr, J., Walger, E., and Zeitzschel, B. (1987). *Seawater-Sediment Interactions in Coastal Waters - An Interdisciplinary Approach*. Berlin: Springer, 338.

Rusch, A., Huettel, M., and Forster, S. (2000). Particulate Organic Matter in Permeable Marine Sands—Dynamics in Time and Depth. *Estuarine, Coastal and Shelf Science* 51, 399–414.

Rusch, A., Huettel, M., Reimers, C., Taghon, G. L., and Fuller, C. M. (2003). Activity and distribution of bacterial populations in Middle Atlantic Bight shelf sands. *FEMS Microbiology Ecology* 44, 89–100.

Rusch, A. and Huettel, M. (2000). Advective particle transport into permeable sediments–evidence from experiments in an intertidal sandflat. *Limnology and Oceanography* 45.3, 523–533.

Rusch, A., Huettel, M., Wild, C., and Reimers, C. E. (2006). Benthic oxygen consumption and organic matter turnover in organic-poor, permeable shelf sands. *Aquatic Geochemistry* 12, 1–19.

Santos, I. R., Eyre, B. D., and Huettel, M. (2012). The driving forces of porewater and groundwater flow in permeable coastal sediments: A review. *Estuarine, Coastal and Shelf Science* 98, 1–15.

Sathyendranath, S., Stuart, V., Nair, A., Oka, K., Nakane, T., Bouman, H., Forget, M. H., Maass, H., and Platt, T. (2009). Carbon-to-chlorophyll ratio and growth rate of phytoplankton in the sea. *Marine Ecology Progress Series* 383, 73–84.

Schade, H., Arneth, N., Powilleit, M., and Forster, S. (2019). Sand gapers' breath: Respiration of *Mya arenaria* (L. 1758) and its contribution to total oxygen utilization in sediments. *Marine Environmental Research* 143, 101–110.

Seibel, B. A. (2007). On the depth and scale of metabolic rate variation: scaling of oxygen consumption rates and enzymatic activity in the Class Cephalopoda (Mollusca). *Journal of Experimental Biology* 210, 1–11.

Shum, K. (1993). The Effects of Wave-Induced Pore Water Circulation on the Transport of Reactive Solutes Below a Rippled Sediment Bed. *Journal of Geophysical Research* 98.C6, 289–301.

Smetacek, V. (1984). The Supply of Food to the Benthos. *Flows of Energy and Materials in Marine Ecosystems*. Boston, MA: Springer US, 517–547.

Stokes, G. G. (1847). On the theory of oscillatory waves. *Transactions of the Cambridge Philosophical Society*. Vol. 8, 441–455.

Sundbäck, K., Nilsson, P., Nilsson, C., and Jönsson, B. (1996). Balance between autotrophic and heterotrophic components and processes in microbenthic communities of sandy sediments: A field study. *Estuarine, Coastal and Shelf Science* 43.6, 689–706.

Tengberg, A., Bovee, F. D., Hall, P., Berelson, W., Chadwick, D., Ciceri, G., Crassous, P., Devol, A., Emerson, S., Gage, J., Glud, R., Graziottini, F., Gundersen, J., Hammond, D., Helder, W., Hinga, K., Holby, O., Jahnke, R., Khripounoff, A., Liebermann, S., Nuppenau, V., Pfannkuche, O., Reimers, C., Rowe, G., Sahami, A., Sayles, F., Schurter, M.,

Smallman, D., Wehrli, B., and Wilde, P. D. (1995). Benthic chamber and profiling landers in oceanography—a review of design, technical solutions and functioning. *Progress in Oceanography* 35, 253–294.

Umweltministerium Mecklenburg-Vorpommern, ed. (2003). *Die Naturschutzgebiete in Mecklenburg-Vorpommern*. 1st ed. Schwerin: Demmler Verlag, 730.

Urban-Malinga, B., Warzocha, J., and Zalewski, M. (2013). Effects of the invasive polychaete *Marenzelleria* spp. On benthic processes and meiobenthos of a species-poor brackish system. *Journal of Sea Research* 80, 25–34.

Vuorinen, I., Hänninen, J., Rajasilta, M., Laine, P., Eklund, J., Montesino-Pouzols, F., Corona, F., Junker, K., Meier, H. E., and Dippner, J. W. (2015). Scenario simulations of future salinity and ecological consequences in the Baltic Sea and adjacent North Sea areas-implications for environmental monitoring. *Ecological Indicators* 50, 196–205.

Wentworth, C. K. (1922). A Scale of Grade and Class Terms for Clastic Sediments. *The Journal of Geology* 30.5, 377–392.

White, C. R., Phillips, N. F., and Seymour, R. S. (2006). The scaling and temperature dependence of vertebrate metabolism. *Biology Letters* 2, 125–127.

Wiberg, P. L. and Harris, C. K. (1994). Ripple geometry in wave-dominated environments. *Journal of Geophysical Research* 99.C1, 775–789.

Wilhelm, C., Büchel, C., Fisahn, J., Goss, R., Jakob, T., LaRoche, J., Lavaud, J., Lohr, M., Riebesell, U., Stehfest, K., Valentin, K., and Kroth, P. G. (2006). The Regulation of Carbon and Nutrient Assimilation in Diatoms is Significantly Different from Green Algae. *Protist* 157.2, 91–124.

Winkler, H. M. and Debus, L. (1996). Is the polychaete *Marenzelleria viridis* an important food item for fish? *Proceedings of the 13th Symposium of the Baltic Marine Biologists*, 147–151.

Winkler, L. W. (1888). Die Bestimmung des im Wasser gelösten Sauerstoffes. *Berichte der deutschen chemischen Gesellschaft* 21, 2843–2855.

Winogradow, A. and Pempkowiak, J. (2014). Organic carbon burial rates in the Baltic Sea sediments. *Estuarine, Coastal and Shelf Science* 138, 27–36.

Woulds, C., Cowie, G. L., Levin, L. A., Andersson, J. H., Middelburg, J. J., Vandewiele, S., Lamont, P. A., Larkin, K. E., Gooday, A. J., Schumacher, S., Whitcraft, C., Jeffreys,

R. M., and Schwartz, M. (2007). Oxygen as a control on seafloor biological communities and their roles in sedimentary carbon cycling. *Limnology and Oceanography* 52.4, 1698–1709.

Yalin, M. S. (1985). On the Determination of Ripple Geometry. *Journal of Hydraulic Engineering* 111.8, 1148–1155.

Zaklan, S. D. and Ydenberg, R. (1997). The body size-burial depth relationship in the infaunal clam *Mya arenaria*. *Journal of Experimental Marine Biology and Ecology* 215.1, 1–17.

Zettler, M. L., Karlsson, A., Kontula, T., Gruszka, P., Laine, A. O., Herkül, K., Schiele, K. S., Maximov, A., and Haldin, J. (2014). Biodiversity gradient in the Baltic Sea: A comprehensive inventory of macrozoobenthos data. *Helgoland Marine Research* 68.1, 49–57.

Zettler, M. L., Schiedek, D., and Bobertz, B. (2007). Benthic biodiversity indices versus salinity gradient in the southern Baltic Sea. *Marine Pollution Bulletin* 55.1-6, 258–270.

Ziebis, W., Huettel, M., and Forster, S. (1996). Impact of biogenic sediment topography on oxygen fluxes in permeable seabeds. *Marine Ecology Progress Series* 140, 227–237.

Acknowledgement

Dr. Stefan Forster und Dr. Markus Hüttel for the evaluation of my dissertation and helpful suggestions for future publication.
Stefan Forster for always taking his time also for incomplete/ chaotic manuscripts and for fruitful discussions. Especially I want to thank him for being my mentor during these past 3 ... years.
Gerd Niedzwiedz; Holger Posselt and the rest of the workshop at the IOW to spend time on ships with me, be supportive with good ideas how to optimize work and be patient if things did not work out easily.
Judith always taking her time for discussions, proof reading or just listening to problems that have occurred during the work.
Martin Powilleit and the rest of the working group for the good time I had.
I want to thank Peter Krumm and Martin Riedel for everything they build for me at their workshop.
I want to thank Holger Pielenz for all the support during the experimental set ups and also for explanations on how all technical things work.
Elke Meier for C and N analysis and the general support.
The Marine Biology working group for support and a good work environment.
Thomas Lorenz and FIUM for ship support during the work.
Lenke, Nicole and Annemarie for their work as student helpers during my phd time.
Christian Burmeister for nutrient measurements.
Jenny Jeschek for DOC measurements.
Hauke (especially) and Anne without whom I could not have set the work into a LateX version.
My best friends and Holger for all the complaints about work, bad moods, no time etc they had to listen to.
My family for always being there for me.
And last but not least the Baltic Transcoast Team!

A Appendix

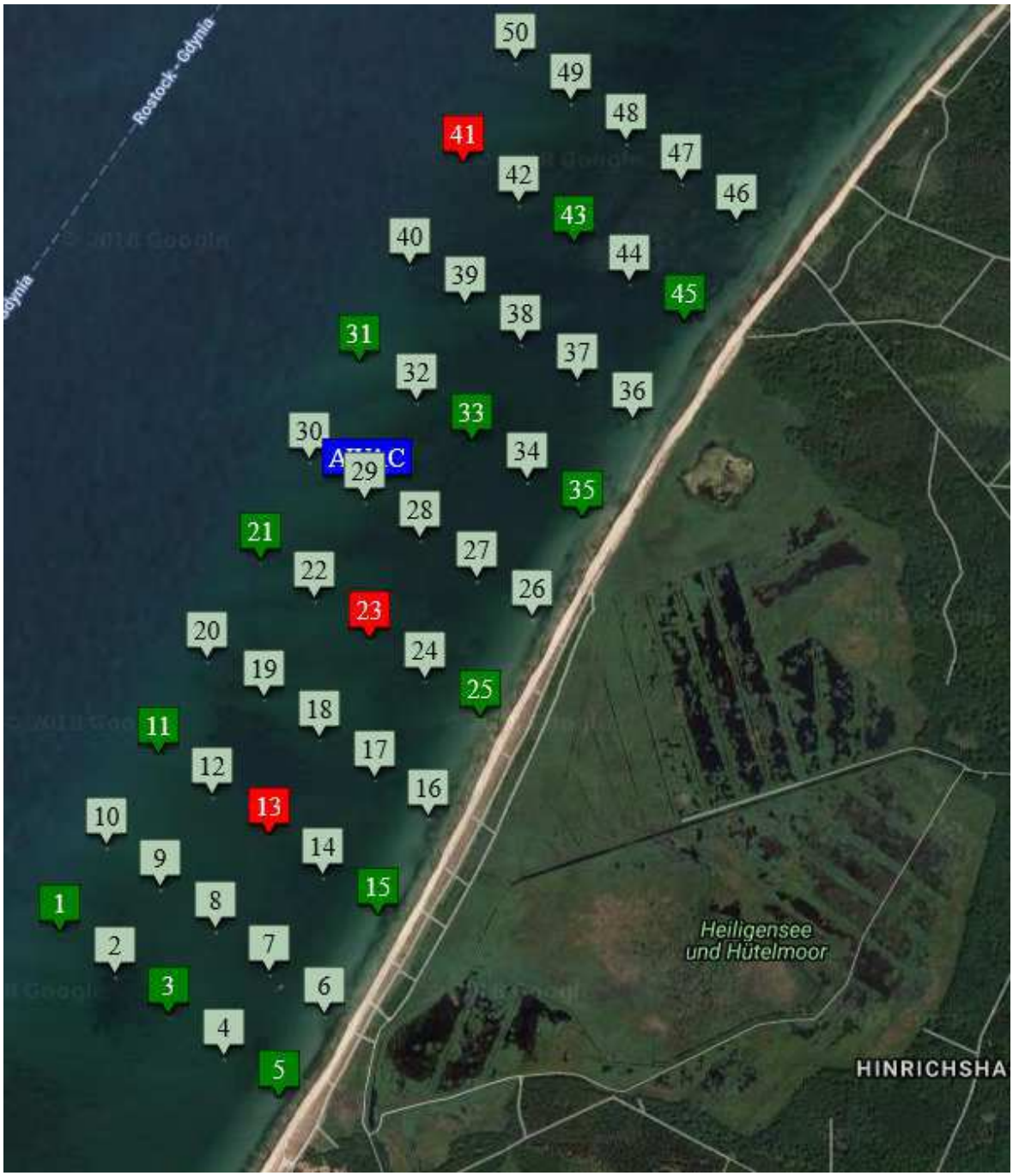

Figure A.1: Map of the study area with all stations. Stations sampled in this study were marked in dark green; stations with benthic chamber deployment are marked in red; the AWAC is marked in blue and all other stations are part of the sampling grid used in the Baltic Transcoast Project but were not sampled in this study (https://www.flopp-caching.de/; Google Maps).

Table A.1: Sampling dates for the characterization of the study area. In situ sampling dates are marked with an asterisk. In cases of fewer stations analysed, analysed stations are denoted in brackets.

Date	Chl a	Permeability	Grain Size Analysis	C and N
April 2016	x	x	x	
July 2016				x (31, 35, 1, 5)
October 2016				x (45, 23, 41)
July 2017 *	x (23, 41)	x (23, 41)	x (23, 41)	x (23, 41)
August 2018 *	x (13)	x (13)	x (13)	x (13)

Table A.2: Coordinates and water depth of all sampled stations.

Station	Water depth [m]	North	East
1	5	54° 12.620094	12° 8.435394 ’
3	3	54° 12.473646 ’	12° 8.772066 ’
5	2.4	54° 12.323994 ’	12° 9.107124 ’
11	4.7	54° 12.93969 ’	12° 8.737302 ’
13	6	54° 12.796272 ’	12° 9.077196 ’
15	2.6	54° 12.650214 ’	12° 9.41451 ’
21	5.6	54° 13.290102 ’	12° 9.051444 ’
23	5.6	54° 13.148592 ’	12° 9.390048 ’
25	3	54° 13.005558 ’	12° 9.729936 ’
31	3.4	54° 13.643856 ’	12° 9.357858 ’
33	6.5	54° 13.50462 ’	12° 9.702258 ’
35	2	54° 13.364622 ’	12° 10.044078 ’
41	6.2	54° 14.002074 ’	12° 9.674574 ’
43	6	54° 13.859844 ’	12° 10.01511 ’
45	4.4	54° 13.716858 ’	12° 10.354356 ’

Table A.3: Permeability at sampled stations in the study area.

Date	Station	k [m^2] $*10^{-12}$	SD [m^2] $*10^{-12}$	Core length [cm]	Samples
160414	1	11.2	1.36	5	1
160414	1	9.99	2.4	10	1
160414	1	7.28	1.66	15.5	1
160414	3	11.7	3.51	3.5	1
160414	3	NA	NA	10	1
160414	3	NA	NA	15	1
160414	5	15.6	1.1	5	1
160414	5	12.4	1.24	9.5	1
160414	5	NA	NA	15	1
160414	11	7.36	0.50	5	1
160414	11	5.56	0.65	10	1
160414	11	5.12	0.62	15	1
160414	13	7.48	0.66	5	1
180830	13	6.43	1.71	5.17	3
180830	13	4.63	1.46	9.17	3
160414	13	5.56	0.99	10	1
180830	13	0	0	13.45	2
160414	13	NA	NA	15	1
160414	13	5.12	0.85	15	1
160414	15	17.4	1.1	5	1
160414	15	18	1.19	8	1
160414	15	NA	NA	15	1
160414	21	4.75	0.88	5	1
160414	21	7.92	0.89	10	1
160414	21	7.75	1.08	15	1
160414	23	13.9	1.08	5	1
170727	23	15.9	3.34	5.17	3
170727	23	13.3	0.13	9.83	3
160414	23	14.4	1.76	10	1
170727	23	13.1	1.4	13.67	3
160414	23	8.53	0.76	15	1
160414	25	16.1	1.45	5	1
160414	25	16.1	1.32	10	1
160414	25	14.7	1.13	15	1
160414	31	72.4	14.9	5	1
160414	31	73.5	11.1	10	1
160414	31	84.3	8.91	15	1
160414	33	13.3	0.67	5	1
160414	33	1.63	0.58	10	1
160414	33	0.21	0.08	13	1
160414	35	17.4	1.44	5	1
160414	35	17.4	1.83	10	1
160414	35	12	0.94	13.5	1
160414	41	31.8	2.34	5	1
170729	41	37.5	12.2	5.67	3
170729	41	26	0.097	9.7	3
160414	41	28.7	2.34	10	1
170729	41	19.6	0.25	12.15	2
160414	41	24.4	1.61	15	1
160414	43	113	10.2	5	1
160414	43	NA	NA	10	1

continued on next page

continued from last page

Date	Station	k [m^2] $*10^{-12}$	SD [m^2] $*10^{-12}$	Core length [cm]	Samples
160414	43	NA	NA	15	1
160414	45	12.4	1.11	5	1
160414	45	12.1	0.94	9	1

Table A.4: C:N ratios and C and N contents as measured in the study area on various stations, C in mg cm^{-3} was calculated using an average content of 1.67 mg sediment cm^{-3} measured in the sampling campaign in April 2016. C contents are given in values measured with filtered sediment.

Station	Sediment depth [cm]	C:N	C [mg g^{-1}]	N [mg g^{-1}]	C [mg cm^{-3}]	n	C (Sed) [mg cm^{-3}]
1	0-1	11.7 ± 0	1.8 ± 0.5	0.2 ± 0.0	2.9	2	
1	4-5	16.6 ± 2.4	1.8 ±1.0	0.1 ± 0.1	2.9	3	
1	9-10	17.8 ± 1.9	2.2 ± 1.1	0.1 ± 0.1	3.7	3	
5	0-1	8.6 ± 0.3	0.5 ± 0.2	0.1 ± 0.0	0.9	3	
5	4-5	16.0 ± 2.4	1.1 ± 0.2	0.1 ± 0.0	1.8	3	
5	9-10	14.3 ± 3.3	1.6 ± 1	0.2 ± 0.1	2.7	3	
23	0-1	16.0	2.7	0.2	4.5	2	2.0 ± 0.1
23	4-5	24.4 ± 5.6	1.8 ± 0.8	0.1 ± 0.0	3.1	3	1.8 ± 0.2
23	9-10	27.6 ± 3.2	2.2 ± 0.6	0.1 ± 0.0	3.6	3	
31	0-1	17.8	3.3 ± 0.2	0.2 ± 0.0	5.5	2	
31	4-5	6.2 ± 0.2	1.1 ± 0.4	0.2 ± 0.1	1.9	3	
31	9-10	8.7 ± 0.6	2.2 ± 0.6	0.3 ± 0.1	3.6	3	
35	0-1	7.7 ± 0.8	2.1 ± 0.2	0.3 ± 0.0	3.5	3	
35	4-5	9.0 ± 0.8	1.9 ± 0.5	0.3 ± 0.1	3.2	3	
35	9-10	7.3 ± 0.3	1.3 ± 0.1	0.2 ± 0.0	2.1	3	
41	0-1	14.2	1.9	0.2	3.1	1	2.9 ± 0.4
41	4-5	24.6 ± 9.8	3.3 ± 1.2	0.2 ± 0.1	5.5	3	4.6 ± 0.7
41	9-10	37.0 ± 6.9	4.0 ± 0.9	0.1 ± 0.1	6.7	3	9.1 ± 1
45	0-1	15.7	3.8	0.3	6.4	2	
45	4-5	5.0	1.3	0.3	2.2	1	1.7
45	6-7	27.3	1.8	0.1	3.0	2	

Table A.5: Chl a values for all samples analysed with a distance to the shore of 50 m. Standard deviation given for all values with >2 replicates.

Sampling date	Station	Sediment depth [cm]	Average [µg ml^{-1}]	SD [µg ml^{-1}]	n
160416	5	0.5-1	1.9	0.2	3
160416	5	0-0.5	2.5	0.2	3
160416	5	1.5-2	2.1	0.0	3
160416	5	1-1.5	2.3	0.0	3
160416	5	2.5-3	2.0	0.1	3
160416	5	2-2.5	2.2	0.1	3
160416	5	3-4	1.8	0.0	3
160416	5	4-5	2.0	NA	1
160416	5	5-6	2.0	NA	1
160416	5	6-7	2.4	NA	1

continued on next page

continued from last page

Sampling date	Station	Sediment depth [cm]	Average [µg ml $^{-1}$]	SD [µg ml $^{-1}$]	n
160416	5	7-8	2.7	NA	1
160416	5	8-9	2.7	NA	1
160416	5	9-10	2.1	NA	1
160728	5	0.5-1	4.8	NA	1
160728	5	0-0.5	5.6	NA	1
160728	5	1.5-2	3.7	NA	1
160728	5	10-12	2.9	NA	1
160728	5	1-1.5	3.8	NA	1
160728	5	12-14	2.4	NA	1
160728	5	14-16	1.9	NA	1
160728	5	2.5-3	3.0	NA	1
160728	5	2-2.5	3.3	NA	1
160728	5	3-4	2.8	NA	1
160728	5	4-5	2.2	NA	1
160728	5	5-6	1.9	NA	1
160728	5	6-7	2.3	NA	1
160728	5	7-8	2.1	NA	1
160728	5	8-9	2.2	NA	1
160728	5	9-10	2.2	NA	1
160416	15	0.5-1	2.5	0.0	3
160416	15	0-0.5	3.3	0.0	3
160416	15	1.5-2	3.0	0.1	3
160416	15	1-1.5	2.9	0.1	3
160416	15	2.5-3	2.1	0.1	3
160416	15	2-2.5	2.4	0.2	3
160416	15	3-4	1.7	0.1	3
160416	15	4-5	1.6	NA	1
160416	25	0.5-1	3.4	0.0	3
160416	25	0-0.5	3.6	0.2	3
160416	25	1.5-2	3.5	0.1	3
160416	25	1-1.5	3.4	0.2	3
160416	25	2.5-3	1.7	0.0	3
160416	25	2-2.5	2.7	0.2	3
160416	25	3-4	1.2	0.0	3
160416	25	4-5	1.3	0.0	3
160416	25	5-6	1.3	NA	1
160416	25	6-7	1.3	NA	1
160416	25	7-8	1.3	NA	1
160416	25	9-10	1.3	NA	1
160416	35	0.5-1	2.2	0.1	3
160416	35	0-0.5	2.3	0.1	3
160416	35	1.5-2	2.0	0.1	3
160416	35	1-1.5	2.1	0.1	3
160416	35	2.5-3	1.7	0.0	3
160416	35	2-2.5	1.7	0.1	3
160416	35	3-4	1.5	0.0	3
160416	35	4-5	1.5	NA	1
160416	35	5-6	1.6	NA	1
160416	35	6-7	1.8	NA	1
160416	35	7-8	1.7	NA	1
160416	35	8-9	1.8	NA	1
160416	35	9-10	1.8	NA	1
160728	35	0.5-1	2.2	NA	1

continued on next page

continued from last page

Sampling date	Station	Sediment depth [cm]	Average [µg ml $^{-1}$]	SD [µg ml $^{-1}$]	n
160728	35	0-0.5	2.1	NA	1
160728	35	1.5-2	2.2	NA	1
160728	35	10-12	1.0	NA	1
160728	35	1-1.5	2.2	NA	1
160728	35	12-14	1.1	NA	1
160728	35	2.5-3	1.5	NA	1
160728	35	2-2.5	2.1	NA	1
160728	35	3-4	1.8	NA	1
160728	35	4-5	1.6	NA	1
160728	35	5-6	1.3	NA	1
160728	35	6-7	1.3	NA	1
160728	35	7-8	1.0	NA	1
160728	35	8-9	1.1	NA	1
160728	35	9-10	1.1	NA	1
160416	45	0.5-1	3.1	0.2	3
160416	45	0-0.5	3.7	0.0	3
160416	45	1.5-2	2.6	0.1	3
160416	45	1-1.5	2.8	0.1	3
160416	45	2.5-3	2.4	0.1	3
160416	45	2-2.5	2.6	0.1	3
160416	45	3-4	2.4	0.1	3
160416	45	4-5	2.9	NA	1
160416	45	5-6	2.7	NA	1
160416	45	6-7	2.8	NA	1
160416	45	7-8	3.1	NA	1
160416	45	8-9	3.0	NA	1
160416	45	9-10	3.1	NA	1
161027	45	0.5-1	3.2	0.1	5
161027	45	0-0.5	3.3	0.2	5
161027	45	1.5-2	2.9	0.5	5
161027	45	10-11	2.8	NA	1
161027	45	1-1.5	3.0	0.3	5
161027	45	2.5-3	2.8	0.6	5
161027	45	2-2.5	2.9	0.4	5
161027	45	3-4	2.5	0.3	5
161027	45	4-5	2.3	0.3	4
161027	45	5-6	2.3	0.1	4
161027	45	6-7	3.4	1.5	4
161027	45	7-8	2.5	NA	2
161027	45	8-9	2.4	NA	2
161027	45	9-10	2.3	NA	1

Table A.6: Chl a values for all samples analysed with a distance to the shore of 550 m. Standard deviation given for all values with >2 replicates.

Sampling date	Station	Sediment depth [cm]	Average [µg ml^{-1}]	SD [µg ml^{-1}]	n
160416	3	0.5-1	7.5	0.2	3
160416	3	0-0.5	5.2	NA	1
160416	3	1.5-2	5.7	0.3	3
160416	3	1-1.5	6.4	0.3	3

continued on next page

continued from last page

Sampling date	Station	Sediment depth [cm]	Average [µg ml $^{-1}$]	SD [µg ml $^{-1}$]	n
160416	3	2.5-3	4.8	0.3	3
160416	3	2-2.5	5.5	0.1	3
160416	3	3-4	4.5	0.1	3
160416	3	4-5	3.3	NA	1
160416	3	5-6	2.7	NA	1
160416	3	6-7	2.5	NA	1
160416	3	7-8	2.0	NA	1
160416	13	0.5-1	6.4	0.1	3
160416	13	0-0.5	6.7	0.2	3
160416	13	1.5-2	6.4	0.2	3
160416	13	1-1.5	6.5	0.1	3
160416	13	2.5-3	5.6	0.1	3
160416	13	2-2.5	5.6	0.5	3
160416	13	3-4	6.4	0.5	3
160416	13	4-5	5.4	NA	1
160416	13	5-6	4.4	NA	1
160416	13	6-7	3.9	NA	1
160416	13	7-8	3.2	NA	1
160416	13	8-9	2.4	NA	1
160416	13	9-10	2.0	NA	1
160416	23	0.5-1	4.5	0.2	3
160416	23	0-0.5	6.2	0.6	3
160416	23	1.5-2	3.7	0.0	3
160416	23	1-1.5	3.5	0.7	3
160416	23	2.5-3	3.0	0.2	3
160416	23	2-2.5	3.2	0.1	3
160416	23	3-4	2.5	0.3	3
160416	23	4-5	3.2	NA	1
160416	23	5-6	4.6	NA	1
160416	23	6-7	3.4	NA	1
160416	23	7-8	11.4	NA	1
160416	23	8-9	8.4	NA	1
160416	23	9-10	6.4	NA	1
161027	23	0.5-1	6.3	1.2	5
161027	23	0-0.5	7.1	1.0	5
161027	23	1.5-2	5.0	0.7	5
161027	23	10-11	2.9	0.5	3
161027	23	1-1.5	5.4	0.6	5
161027	23	11-12	2.7	NA	2
161027	23	2.5-3	4.1	1.0	5
161027	23	2-2.5	3.9	0.4	5
161027	23	3-4	3.5	0.3	5
161027	23	4-5	3.4	0.3	4
161027	23	5-6	3.3	0.4	5
161027	23	6-7	3.2	0.1	4
161027	23	7-8	3.3	0.4	4
161027	23	8-9	3.0	0.2	3
161027	23	9-10	3.2	0.4	3

Table A.7: Chl a values for all samples analysed with a distance to the shore of 1050 m. Standard deviation given for all values with >2 replicates.

Sampling date	Station	Sediment depth [cm]	Average [µg ml^{-1}]	SD [µg ml^{-1}]	n
160416	1	0.5-1	5.4	0.3	3
160416	1	0-0.5	5.4	NA	1
160416	1	1.5-2	3.5	0.1	3
160416	1	1-1.5	4.2	0.1	3
160416	1	2.5-3	3.3	0.1	3
160416	1	2-2.5	3.3	0.2	3
160416	1	3-4	3.6	0.1	3
160416	1	4-5	3.3	NA	1
160416	1	5-6	2.8	NA	1
160728	1	0.5-1	2.1	NA	1
160728	1	0-0.5	2.7	NA	1
160728	1	1.5-2	2.9	NA	1
160728	1	10-12	2.5	NA	1
160728	1	1-1.5	3.8	NA	1
160728	1	12-14	1.0	NA	1
160728	1	14-16	0.3	NA	1
160728	1	16-18	0.2	NA	1
160728	1	2.5-3	1.9	NA	1
160728	1	2-2.5	2.8	NA	1
160728	1	3-4	2.3	NA	1
160728	1	4-5	2.2	NA	1
160728	1	5-6	1.8	NA	1
160728	1	6-7	1.9	NA	1
160728	1	7-8	1.9	NA	1
160728	1	8-9	2.0	NA	1
160728	1	9-10	2.0	NA	1
160416	11	0.5-1	2.8	0.0	3
160416	11	0-0.5	3.0	0.1	3
160416	11	1.5-2	2.9	0.1	3
160416	11	1-1.5	2.9	0.0	3
160416	11	2.5-3	3.1	0.1	3
160416	11	2-2.5	2.9	0.1	3
160416	11	3-4	3.5	0.5	3
160416	11	4-5	3.4	NA	1
160416	11	5-6	3.6	NA	1
160416	11	6-7	4.0	NA	1
160416	11	7-8	4.0	NA	1
160416	11	8-9	3.4	NA	1
160416	11	9-10	4.6	NA	1
160416	21	0.5-1	4.5	0.0	3
160416	21	0-0.5	6.2	0.2	3
160416	21	1.5-2	3.6	0.1	3
160416	21	1-1.5	4.6	0.3	3
160416	21	2.5-3	4.1	0.1	3
160416	21	2-2.5	3.8	0.1	3
160416	21	3-4	4.2	0.3	3
160416	21	4-5	5.2	NA	1
160416	21	5-6	4.5	NA	1
160416	21	6-7	4.3	NA	1
160416	21	7-8	4.0	NA	1

continued on next page

continued from last page

Sampling date	Station	Sediment depth [cm]	Average [µg ml $^{-1}$]	SD [µg ml $^{-1}$]	n
160416	21	8-9	3.9	NA	1
160416	21	9-10	4.1	NA	1
160416	31	0.5-1	1.2	0.0	3
160416	31	0-0.5	1.9	0.2	3
160416	31	1.5-2	1.2	0.1	3
160416	31	1-1.5	1.2	0.0	3
160416	31	2.5-3	1.1	0.0	3
160416	31	2-2.5	1.3	0.1	3
160416	31	3-4	1.2	0.0	3
160416	31	3-4	1.4	NA	1
160416	31	4-5	1.2	0.0	3
160416	31	4-5	1.1	NA	1
160416	31	5-6	1.1	0.0	3
160416	31	5-6	1.1	NA	1
160416	31	6-7	1.2	0.0	3
160416	31	6-7	1.2	NA	1
160416	31	7-8	1.1	0.0	3
160416	31	7-8	1.1	NA	1
160416	31	8-9	1.3	0.1	3
160416	31	8-9	1.3	NA	1
160416	31	9-10	1.2	0.0	3
160728	31	0.5-1	1.6	NA	2
160728	31	0-0.5	1.9	NA	2
160728	31	1.5-2	1.4	NA	2
160728	31	10-12	1.4	NA	2
160728	31	1-1.5	1.6	NA	2
160728	31	12-14	1.4	NA	1
160728	31	14-16	1.4	NA	1
160728	31	16-18	1.5	NA	1
160728	31	18-20	2.0	NA	1
160728	31	2.5-3	1.2	NA	2
160728	31	2-2.5	1.4	NA	2
160728	31	3-4	1.3	NA	2
160728	31	4-5	1.2	NA	2
160728	31	5-6	1.3	NA	2
160728	31	6-7	1.0	NA	2
160728	31	7-8	1.3	NA	2
160728	31	8-9	1.4	NA	2
160728	31	9-10	1.3	NA	2
161027	31	0.5-1	3.2	0.6	3
161027	31	0-0.5	4.3	1.7	3
161027	31	1.5-2	2.7	0.4	3
161027	31	10-11	1.9	NA	1
161027	31	1-1.5	2.9	0.5	3
161027	31	2.5-3	2.6	0.5	3
161027	31	2-2.5	2.8	0.4	3
161027	31	3-4	2.3	0.5	3
161027	31	4-5	2.2	0.2	3
161027	31	5-6	2.2	0.3	3
161027	31	6-7	1.9	0.3	3
161027	31	7-8	1.7	0.1	3
161027	31	8-9	1.6	0.2	3
161027	31	9-10	1.6	0.2	3

continued on next page

continued from last page

Sampling date	Station	Sediment depth [cm]	Average [µg ml $^{-1}$]	SD [µg ml $^{-1}$]	n
160416	41	0.5-1	5.2	0.1	3
160416	41	0-0.5	5.5	0.2	3
160416	41	1.5-2	4.9	0.1	3
160416	41	1-1.5	5.4	NA	2
160416	41	2.5-3	4.2	0.2	3
160416	41	2-2.5	4.8	0.1	3
160416	41	3-4	4.1	0.1	3
160416	41	4-5	4.2	NA	1
160416	41	5-6	3.7	NA	1
160416	41	6-7	3.7	NA	1
160416	41	7-8	3.9	NA	1
160416	41	8-9	3.5	NA	1
160416	41	9-10	4.0	NA	1
161027	41	0.5-1	5.1	0.8	5
161027	41	0-0.5	6.7	1.4	5
161027	41	1.5-2	4.7	0.3	5
161027	41	10-11	4.2	0.2	3
161027	41	1-1.5	4.9	0.4	5
161027	41	11-12	3.6	NA	2
161027	41	12-14	3.4	NA	2
161027	41	14-16	2.4	NA	2
161027	41	16-18	0.7	NA	2
161027	41	18-20	0.1	NA	2
161027	41	2.5-3	4.5	0.5	5
161027	41	2-2.5	4.8	0.4	5
161027	41	3-4	4.3	0.6	5
161027	41	4-5	4.0	0.5	5
161027	41	5-6	4.3	0.3	5
161027	41	6-7	4.1	0.3	5
161027	41	7-8	3.9	0.3	4
161027	41	9-10	4.2	0.2	4
170728	41	0.5-1	6.6	0.2	3
170728	41	0-0.5	7.1	0.7	3
170728	41	1.5-2	6.5	0.3	3
170728	41	1-1.5	6.7	0.2	3
170728	41	2.5-3	7.0	0.8	3
170728	41	2-2.5	6.6	0.3	3
170728	41	3-4	6.9	0.4	3
170728	41	4-5	6.6	0.3	3
170728	41	5-6	5.4	0.9	3
170728	41	6-7	4.6	0.3	3
170728	41	7-8	3.9	NA	1
170728	41	8-9	3.0	NA	1
170728	41	9-10	1.8	NA	1
170724	23	0.5-1	7.5	0.4	3
170724	23	0-0.5	8.6	2.3	3
170724	23	1.5-2	6.5	0.2	3
170724	23	1-1.5	7.2	0.5	3
170724	23	2.5-3	6.1	0.4	3
170724	23	2-2.5	6.2	0.7	3
170724	23	3-4	5.9	0.3	3
170724	23	4-5	5.8	1.0	3
170724	23	5-6	5.8	1.2	3

continued on next page

continued from last page

Sampling date	Station	Sediment depth [cm]	Average [µg ml $^{-1}$]	SD [µg ml $^{-1}$]	n
170724	23	6-7	5.5	0.9	3
170724	23	7-8	5.4	0.3	3
170724	23	8-9	4.9	0.2	3
170724	23	9-10	4.6	0.1	3
160416	33	0.5-1	4.2	0.1	3
160416	33	0-0.5	4.4	0.1	3
160416	33	1.5-2	3.7	0.1	3
160416	33	1-1.5	4.3	0.1	3
160416	33	2.5-3	1.9	0.1	3
160416	33	2-2.5	2.4	0.2	3
160416	33	3-4	1.8	0.0	3
160416	33	4-5	1.9	0.0	3
160416	33	5-6	1.8	0.0	3
160416	33	6-7	1.7	0.0	3
160416	33	7-8	1.5	0.3	3
160416	33	7-8	1.7	0.1	3
160416	33	8-9	1.3	0.2	3
160416	43	0.5-1	3.1	0.2	3
160416	43	0-0.5	4.2	0.2	3
160416	43	1.5-2	3.2	0.4	3
160416	43	1-1.5	3.2	0.2	3
160416	43	2.5-3	4.6	0.1	3
160416	43	2-2.5	4.4	0.1	3
160416	43	3-4	4.4	NA	1
160416	43	4-5	4.8	NA	1
160416	43	5-6	4.9	NA	1

Table A.8: Raw data for the calculation of respiration rate to SFDW relationship. Values marked by [1] are all values excluded from the calculation because oxygen concentration fell below 30% by the end of the measurement period. Values marked by [2] are values added from a different experimental set up, these values were only included into the respiration rate calculations.

Date (2018)	Length [mm]	SFDW [mg]	T [°C]	rr [mmol d^{-1} g_{SFDW} $^{-1}$]	$rr_{Sediment}$ [µmol h^{-1}]
04.07.	9	2.2	15	0.34	0.85
06.07.	9	3.7	15	1.82	0.69
01.07.	11	4.4	15	0	1.27
04.07.	10	4.5	15	2.39	0.85
04.07.	10	5.2	15	0	0.85
01.07.	12	6.1	15	0	1.27
17.06.	14	9.3	15	0.38	0.97
01.07.	13	9.4	15	0	1.27
15.06.	15	17.0	15	0.3	1.47
20.06.	16	21.9	15	0	2.12
17.06.	21	52.3	15	0.27	0.97
15.06.	20	56.2	15	0.39	1.47
20.06.	23	64.5	15	0	2.12
17.06.	25	75.4	15	0.28	0.97
20.06.	25	83.8	15	0	2.12
15.06.	27	139.3	15	0.19	1.47
22.06.	30	171.2	15	0.09	0.69

continued on next page

continued from last page

Date (2018)	Length [mm]	SFDW [mg]	T [°C]	rr [mmol d^{-1} $g_{SFDW}{}^{-1}$]	$rr_{Sediment}$ [µmol h^{-1}]
22.06.	33	172.8	15	0.12	0.69
22.06.	31	180.1	15	0.09	0.69
27.06.	36	258.4	15	0.21	0.97
27.06.	38	362.3	15	0.11	0.97
13.06.	45[1]	454.7[1]	15	0.15[1]	2.56
13.06.	48[1]	578.6[1]	15	0.47[1]	2.56
06.07.	58[1]	777.8[1]	15	0.46[1]	0.69
13.06.	50[1]	799.4[1]	15	0.47[1]	2.56
29.06.	59	838.1	15	0.01	0.89
29.06.	56[1]	967.2[1]	15	0.40[1]	0.89
27.06.	55[1]	1150.1[1]	15	0.17[1]	0.97
29.06.	57[1]	1157.7[1]	15	0.14[1]	0.89
06.07.	60[1]	1239.8[1]	15	0.17[1]	0.69
22.07.	10[2]	30.0[2]	15	4.72[2]	1.31
22.07.	10[2]	35.0[2]	15	0[2]	-
08.08.	24[2]	52.2[2]	15	0.52[2]	1.01
08.08.	27[2]	109.1[2]	15	0.40[2]	1.01
08.08.	31[2]	121.4[2]	15	0.26[2]	1.01
30.07.	50[2]	631.3[2]	15	0.08[2]	1.19
30.07.	56[2]	799.4[2]	15	0.09[2]	1.19
30.07.	57[2]	888.5[2]	15	0.08[2]	1.19
3.06.	10	3.8	5	0.32	0.52
18.07.	11	5.5	5	0.46	0.89
8.06.	13	5.5	5	0.58	0.8
8.06.	11	8.0	5	0.16	0.8
8.06.	14	8.1	5	0.41	0.8
3.06.	15	11.5	5	0.50	0.52
6.06.	16	14.6	5	0.88	0.73
3.06.	14	15.1	5	0.48	0.52
16.05.	15	19.2	5	0	2.64
23.05.	18	32.6	5	0	2.62
6.06.	20	47.7	5	0.41	0.73
1.06.	19	54.2	5	0.19	0.82
1.06.	21	61.4	5	0.16	0.82
23.05.	23	70.8	5	0	2.80
15.07.	26	97.9	5	0.10	0.87
16.05.	24	105.8	5	0.12	0.83
15.07.	27	120.1	5	0	0.87
30.05.	29	144.2	5	0.06	0.58
16.05.	29	155.7	5	0.02	0.95
23.05.	31	187.5	5	0	2.34
30.05.	38	268.1	5	0.06	0.58
15.07.	35	280.3	5	0.11	0.87
23.05.	46	300.7	5	0	2.55
13.07.	41	399.9	5	0.01	0.47
16.05.	47	436.3	5	0	1.99
13.07.	44	454.5	5	0.02	0.47
30.05.	49	574.3	5	0.04	0.58
13.07.	48	651.4	5	0.02	0.47
1.06.	55	671.6	5	0.01	0.82
18.07.	59	1134.0	5	0.01	0.89

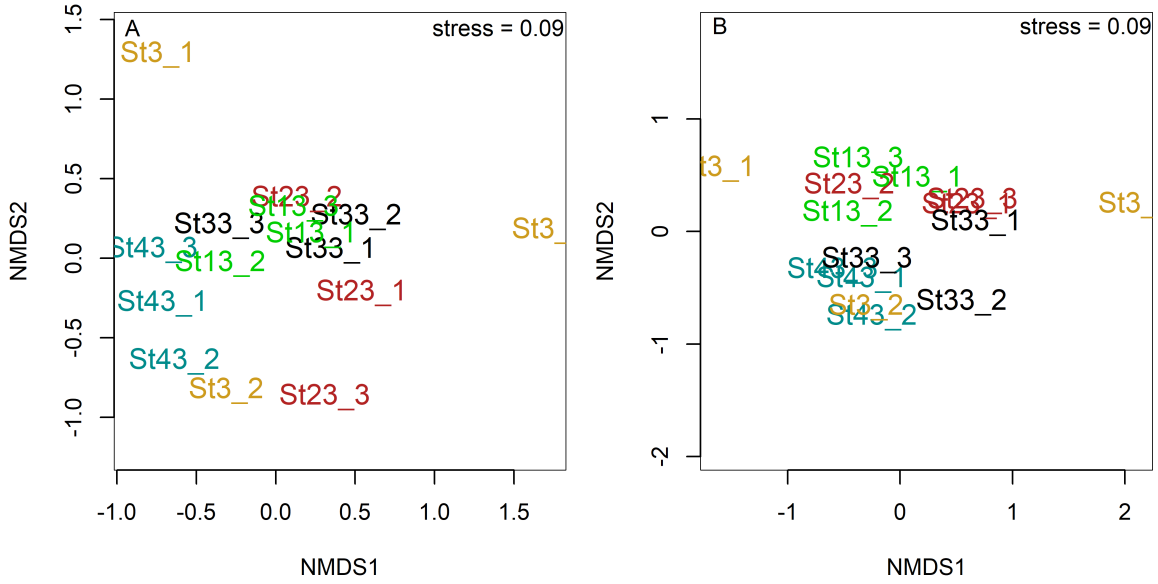

Figure A.2: NMDS plot for abundance (A) and biomass (B) of macrofauna from the study area.

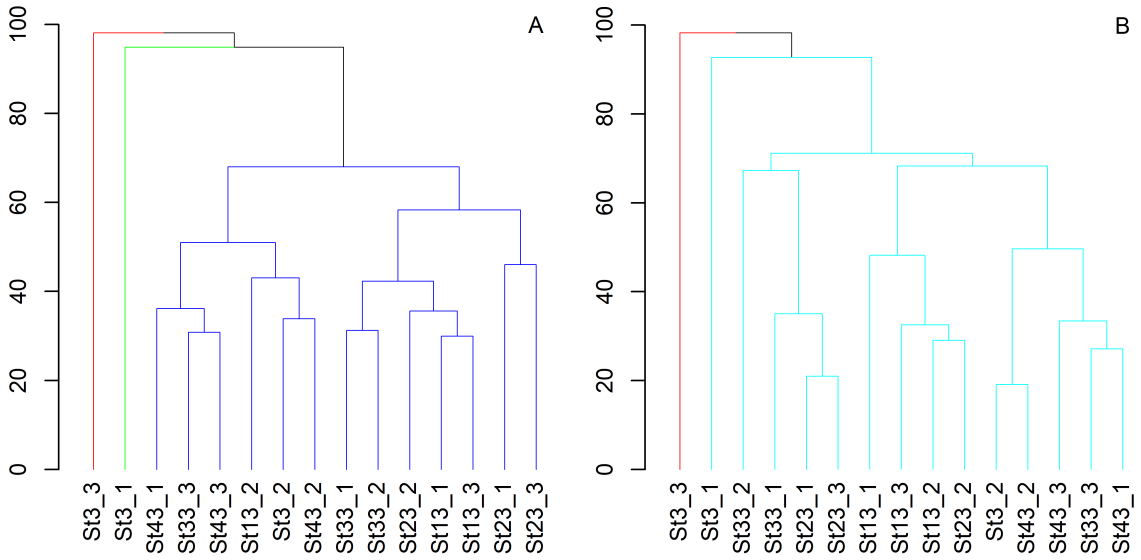

Figure A.3: Dendrogramm analysing all single replicate abundance (A) and biomass (B) macrofauna data.

Table A.9: Nutrient values in the header tanks during the flow-through experiments. Nutrient values for the different experiments measuring volumetric oxygen uptake rates in dependence of flow.

Experiment / Fig 21	Date	Header	PO_4^{3-} [µmol l^{-1}]	NO_3^- [µmol l^{-1}]	NO_2^- [µmol l^{-1}]	NH_4^+ [µmol l^{-1}]	SiO_2 [µmol l^{-1}]
I (Fig 21A)	19-03-18	W	1.5	72.7	0.6	1.5	39.2
I (Fig 21A)	19-03-18	S	0.3	4.0	0.1	<0.5	51.8
I (Fig 21A)	19-03-18	W/S	71.2	31.8	0.4	<0.5	51.3
I (Fig 21A)	05-04-18	W	<0.1	1.7	0.1	<0.5	41.1
I (Fig 21A)	05-04-18	S	<0.1	18.9	1.4	<0.5	60.1
I (Fig 21A)	05-04-18	W/S	<0.1	43.3	0.3	<0.5	60.4
I (Fig 21A)	20-04-18	W	5.0	91.0	0.7	10.7	30.9
I (Fig 21A)	20-04-18	S	2.7	98.5	0.4	6.2	30.3
I (Fig 21A)	20-04-18	W/S	<0.1	81.1	0.6	5.5	30.6
II (Fig 21B)	26-04-18	slow	0.6	81.5	6.0	27.3	28.0
II (Fig 21B)	26-04-18	medium	<0.1	76.2	0.9	53.6	27.1
II (Fig 21B)	26-04-18	fast	0.3	67.7	1.3	47.0	27.0
II (Fig 21B)	07-05-18	slow	<0.1	73.2	23.9	6.6	16.7
II (Fig 21B)	07-05-18	medium	0.5	77.9	9.4	46.5	29.0
II (Fig 21B)	07-05-18	fast	0.6	79.4	2.8	51.8	29.6
III (Fig 21C)	11-06-18		4.3	19.8	10.0	48.8	41.8
III (Fig 21C)	18-06-18		2.0	60.3	0.9	2.0	21.0
IV (Fig 21D)	03-07-18	Control	3.4	100.5	2.3	3.8	25.1
IV (Fig 21D)	03-07-18	DOC	3.6	92.3	4.8	10.4	25.5
IV (Fig 21D)	03-07-18	high DOC	3.2	95.6	3.6	5.7	24.9
IV (Fig 21D)	10-07-18	Control	4.1	72.0	2.5	3.5	21.3
IV (Fig 21D)	10-07-18	DOC	6.3	94.5	11.0	10.5	27.7
IV (Fig 21D)	10-07-18	high DOC	8.0	102.6	4.4	8.4	28.3
IV (Fig 21D)	11-07-18	Control	3.5	100.8	2.3	1.6	28.6
IV (Fig 21D)	11-07-18	DOC	5.2	92.3	12.8	5.0	28.8
IV (Fig 21D)	11-07-18	high DOC	5.1	100.0	4.5	1.0	28.8
IV (Fig 21D)	13-07-18	Control	3.4	102.2	1.5	1.7	28.8
IV (Fig 21D)	13-07-18	DOC	5.4	90.8	15.6	8.2	28.8
IV (Fig 21D)	13-07-18	high DOC	6.0	98.8	5.9	9.2	27.6